A Relative Spectral Measurement of Neutrino Oscillation at Daya Bay

Bryce Littlejohn

University of Cincinnati

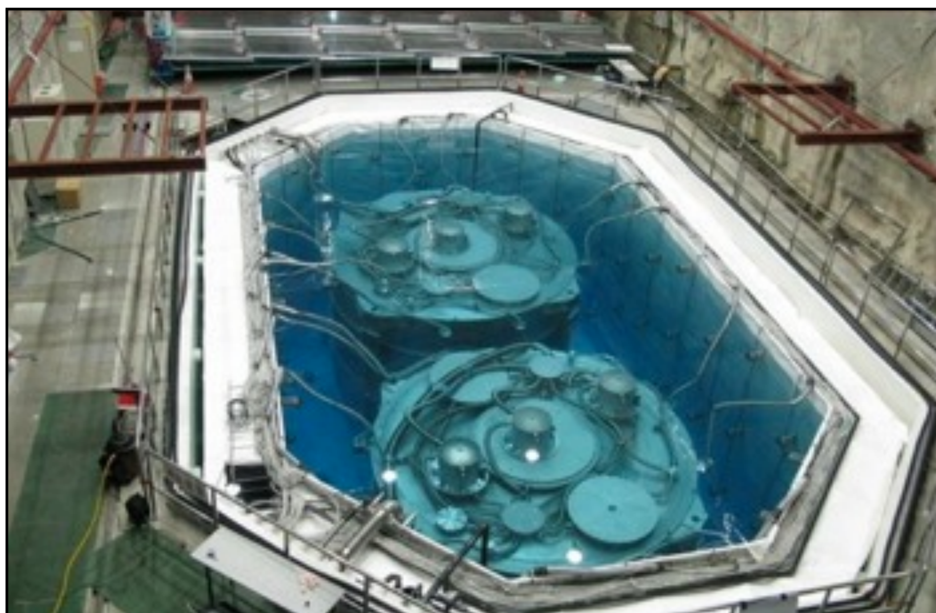

9/6/2013

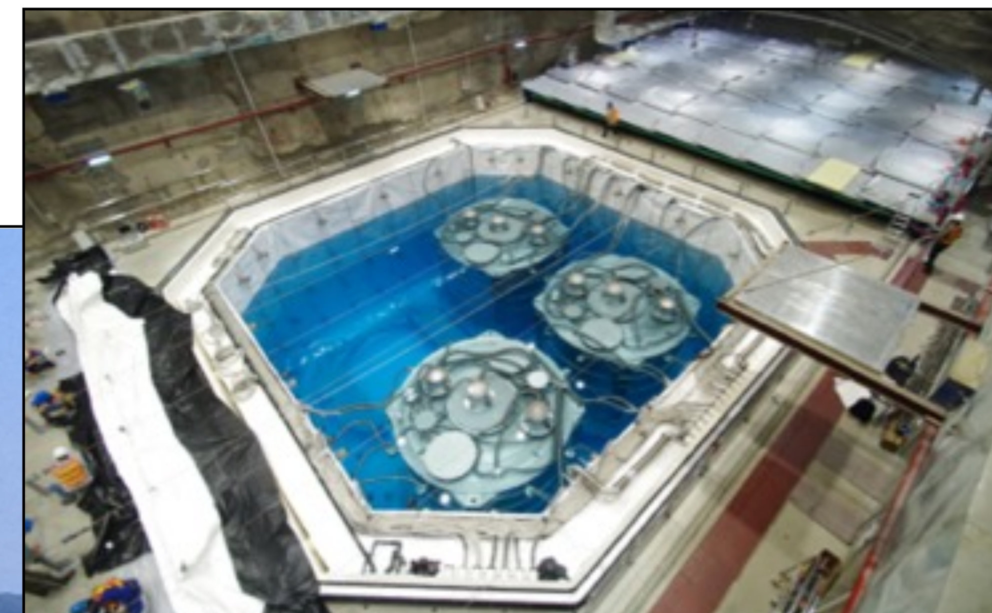

50+ Years of Accelerator Neutrinos

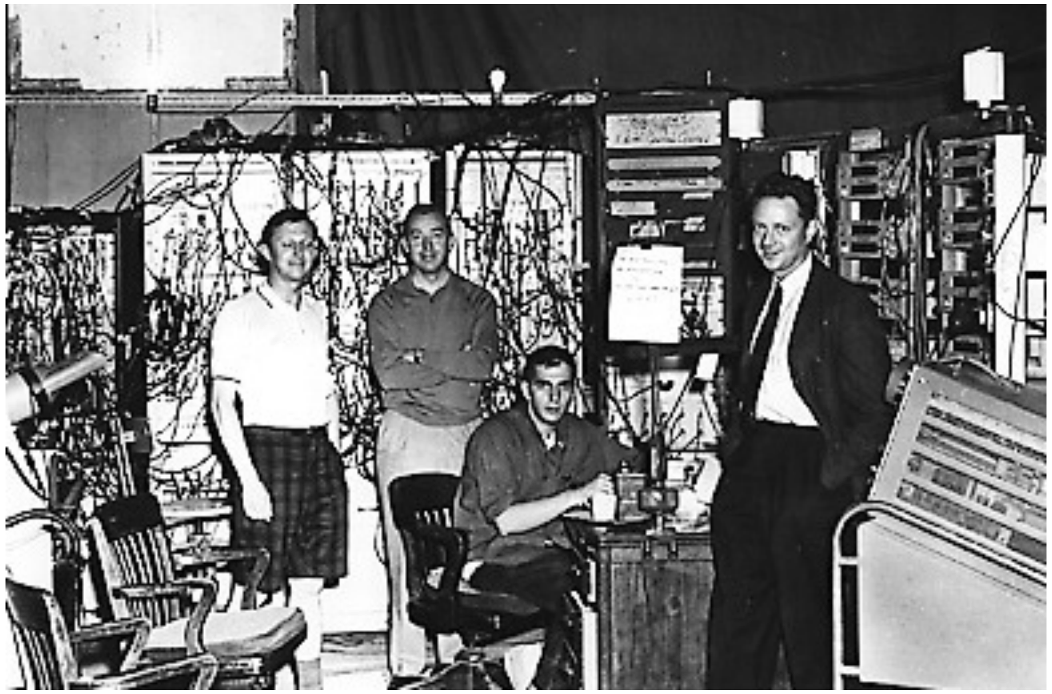

Muon Neutrino Discovery

K2K and MINOS; Atmospheric Mixing... In a Lab!

Off-Axis; Mass Hierarchy: NOvA

Gargamelle and Weak Neutral Currents

Large-Δm^2 Mixing: LSND and MiniBooNE

LAr@Fermilab: MicroBoone, LBNE

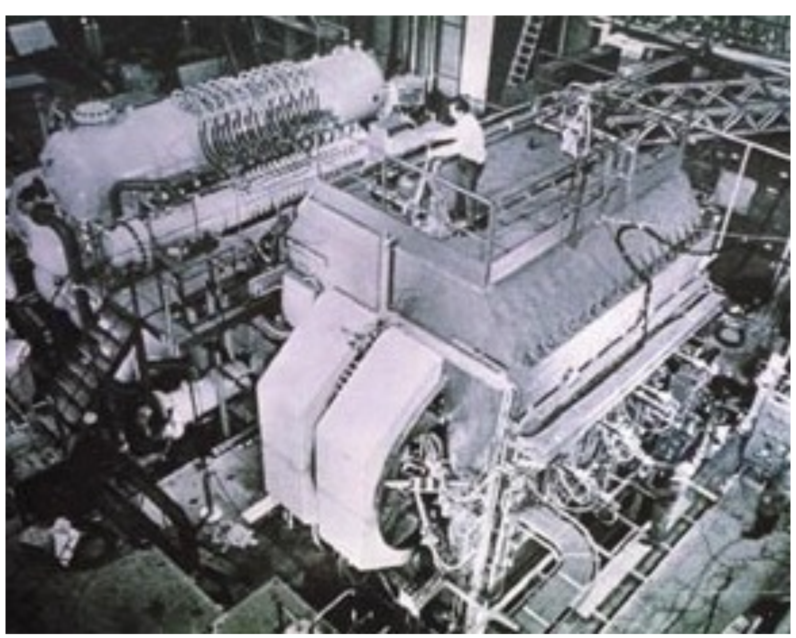

Plus much more...

50+ Years of Non-Accelerator Neutrinos

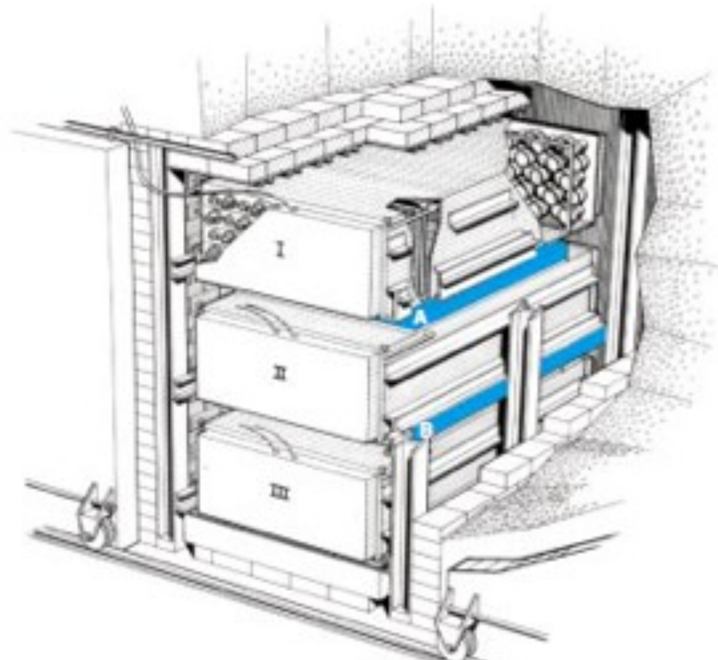

The Savannah River Detector:
First Unambiguous Neutrino Discovery!

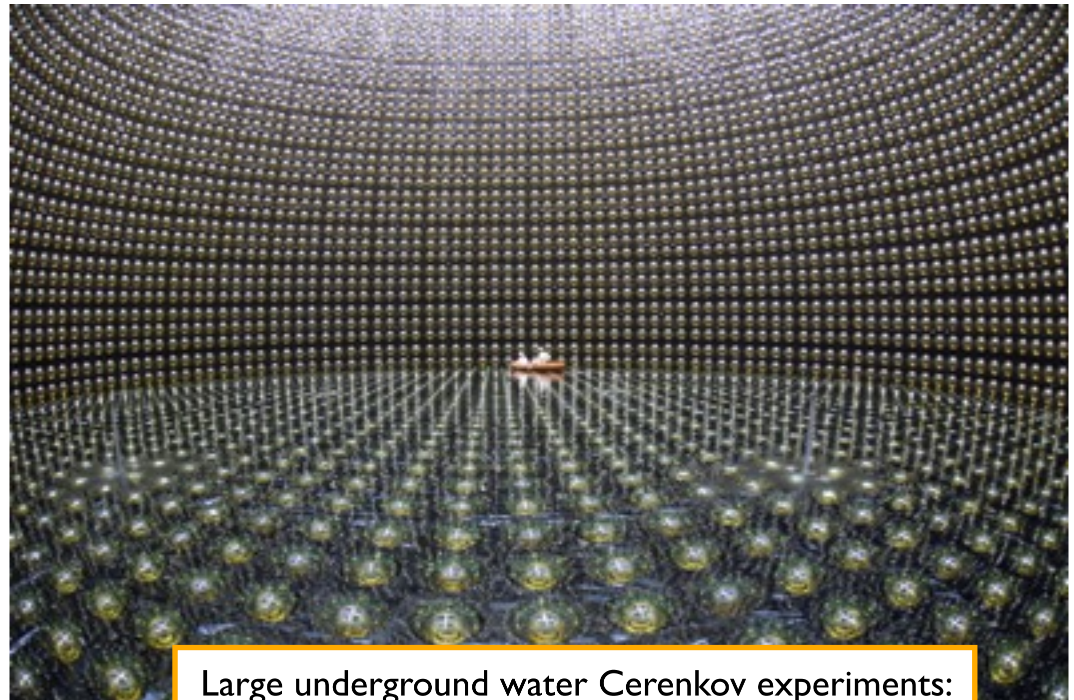

Large underground water Cerenkov experiments:
atmospheric neutrino oscillations and more!

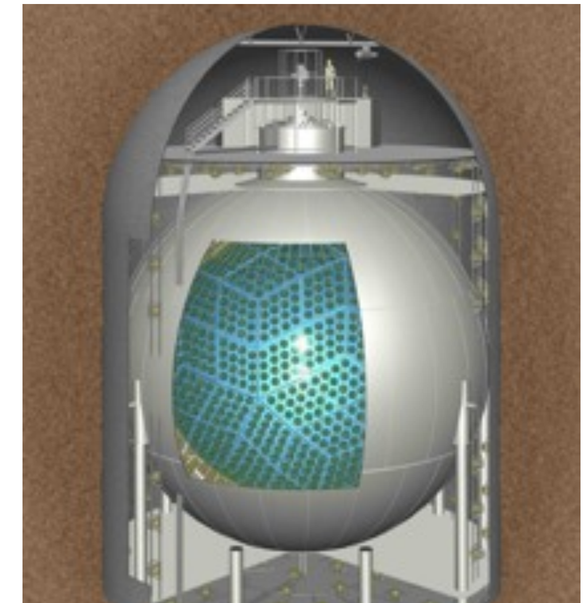

KamLAND: First Reactor
Neutrino Oscillations!

more to come!

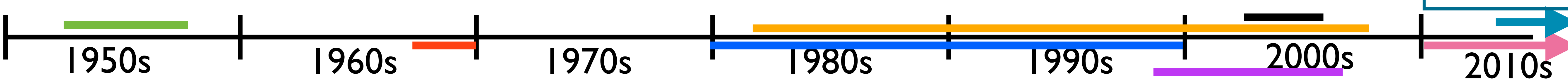

Davis's Homestake Experiment
Inception of Solar Neutrino Problem

Short-baseline reactor experiments, like
CHOOZ, search for oscillation signatures

SNO: Solves solar neutrino problem,
evidence of solar oscillations

The Hunt For θ_{13}:
Daya Bay, RENO,
Double Chooz

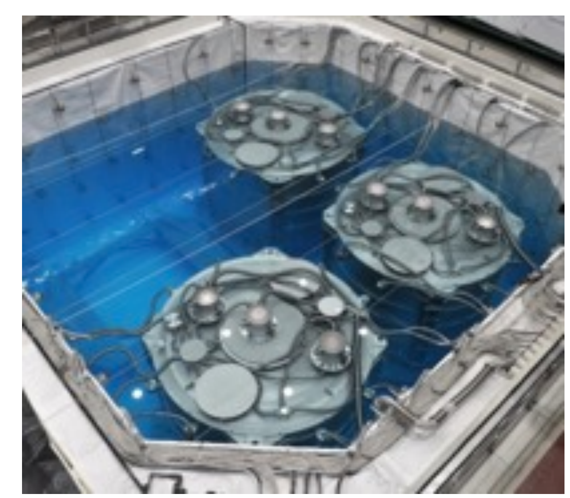

Not even mentioning
neutrinoless double beta decay!

Neutrino Oscillations

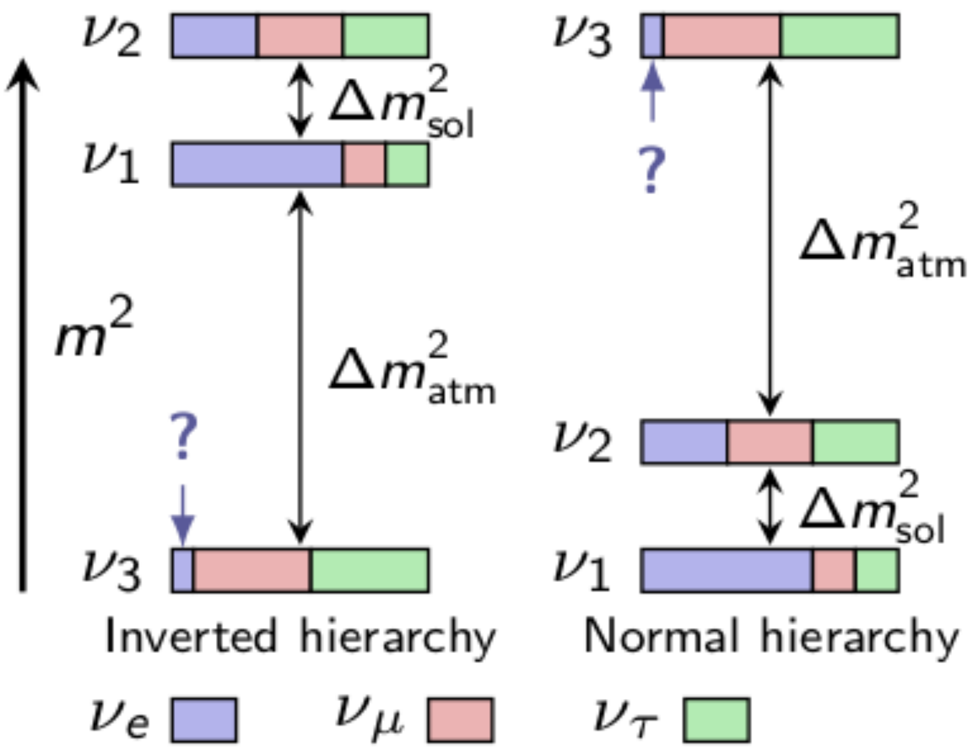

Weak and mass eigenstates need not correspond:

1. How they interact
2. How they propagate

$$|\nu_\alpha\rangle = \sum_{i=1}^{3} U_{\alpha,i} \, |\nu_i\rangle$$

Neutrino flavor changing determined by mixing angles θ and mass splittings Δm^2

$$U = \begin{pmatrix} 1 & 0 & 0 \\ 0 & \cos\theta_{23} & \sin\theta_{23} \\ 0 & -\sin\theta_{23} & \cos\theta_{23} \end{pmatrix} \begin{pmatrix} \cos\theta_{13} & 0 & \sin\theta_{13} e^{-i\delta} \\ 0 & 1 & 0 \\ -\sin\theta_{13} e^{i\delta} & 0 & \cos\theta_{13} \end{pmatrix} \begin{pmatrix} \cos\theta_{12} & \sin\theta_{12} & 0 \\ -\sin\theta_{12} & \cos\theta_{12} & 0 \\ 0 & 0 & 1 \end{pmatrix}$$

Atmospheric/Accelerators:
θ_{23}~45°

Solar/KamLAND:
θ_{12}~23°

θ_{13} only recently well-established at Daya Bay

Reactor Oscillation Experiments

- Reactors: an intense, pure source of $\bar{\nu}_e$
  - Produced in beta decays of neutron-rich fission products
  - Conventional reactor: ~6 x 10^{20} created per second
  - BNB or NuMI: 10-15 x 10^{20} total protons on target!

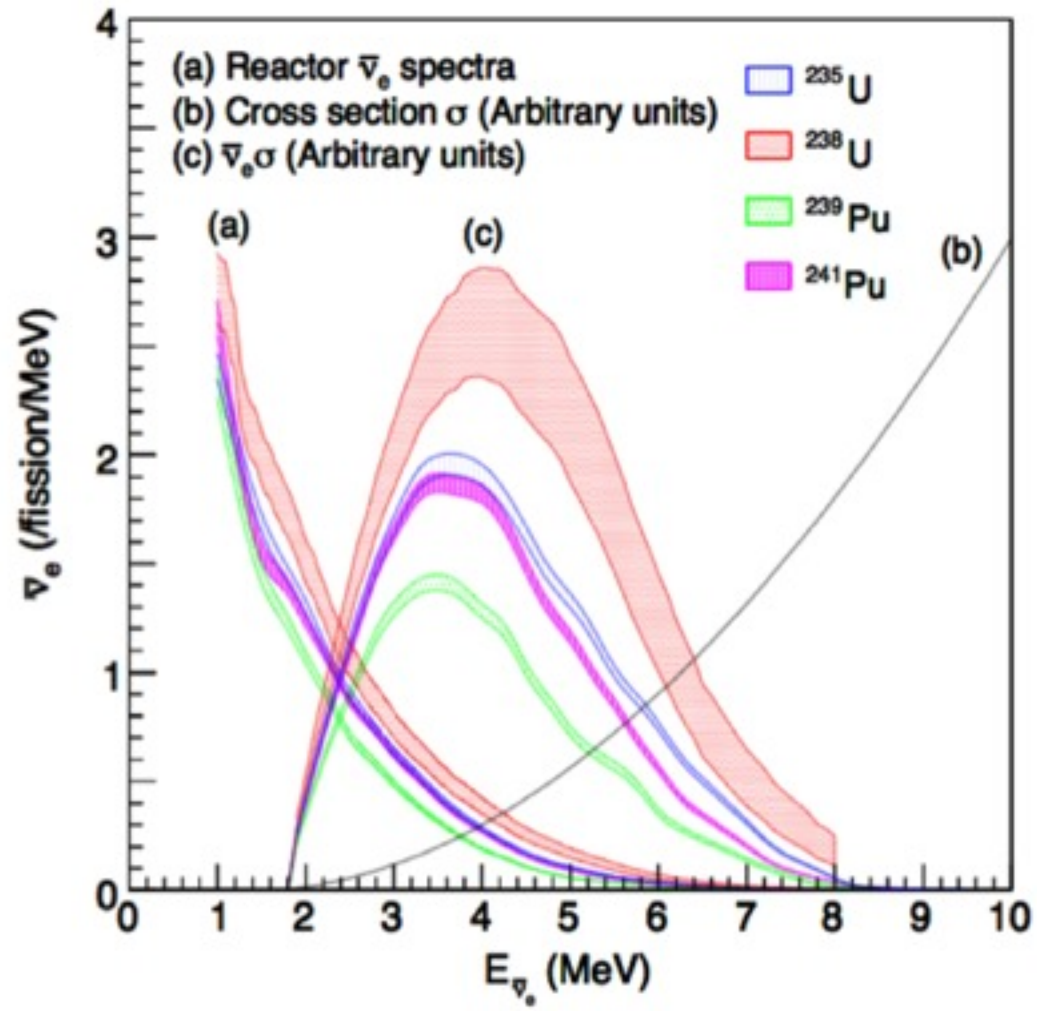

- θ_{13} revealed by deficit of $\bar{\nu}_e$ at ~2 km

$$P_{\bar{\nu}_e \to \bar{\nu}_e} = \boxed{1 - \sin^2(2\boxed{\theta_{13}}) \sin^2\left(\boxed{\Delta m^2_{ee}} \frac{L}{E}\right)}$$
$$\boxed{- \sin^2(2\theta_{12}) \cos^4(\theta_{13}) \sin^2\left(\Delta m^2_{21} \frac{L}{E}\right)}$$

- $\Delta m^2_{ee} \sim \Delta m^2_{32}$ in this case:

$$|\Delta m^2_{ee}| \simeq |\Delta m^2_{32}| \pm 5.21 \times 10^{-5} \mathrm{eV}^2$$

- Second term has small effect at short baselines
- No CP-violation or matter effects

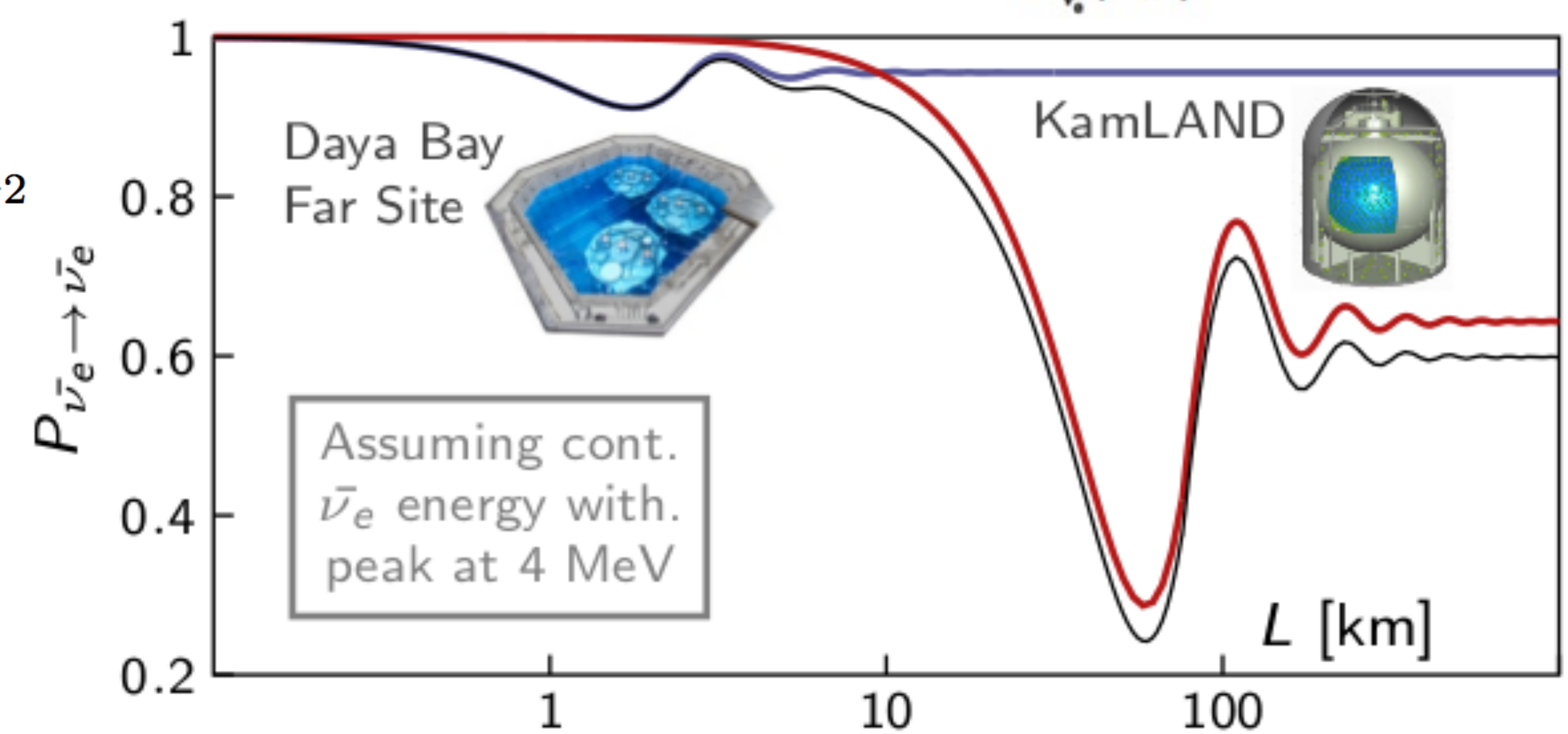

A Powerful Neutrino Source at an Ideal Location

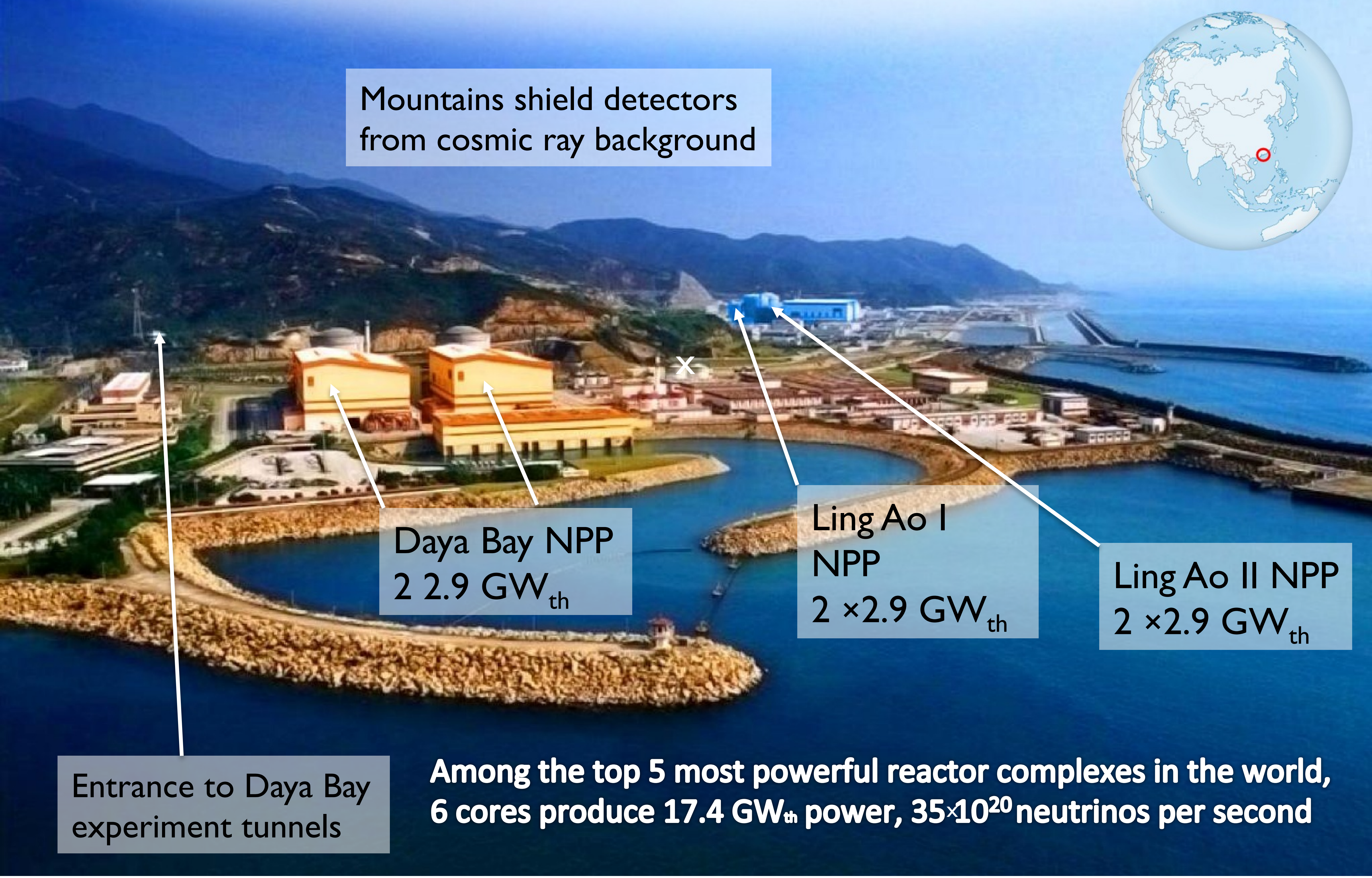

Among the top 5 most powerful reactor complexes in the world, 6 cores produce 17.4 GW_{th} power, $35{\times}10^{20}$ neutrinos per second

Daya Bay Collaboration

- An international effort: 230 collaborators from 40 institutions

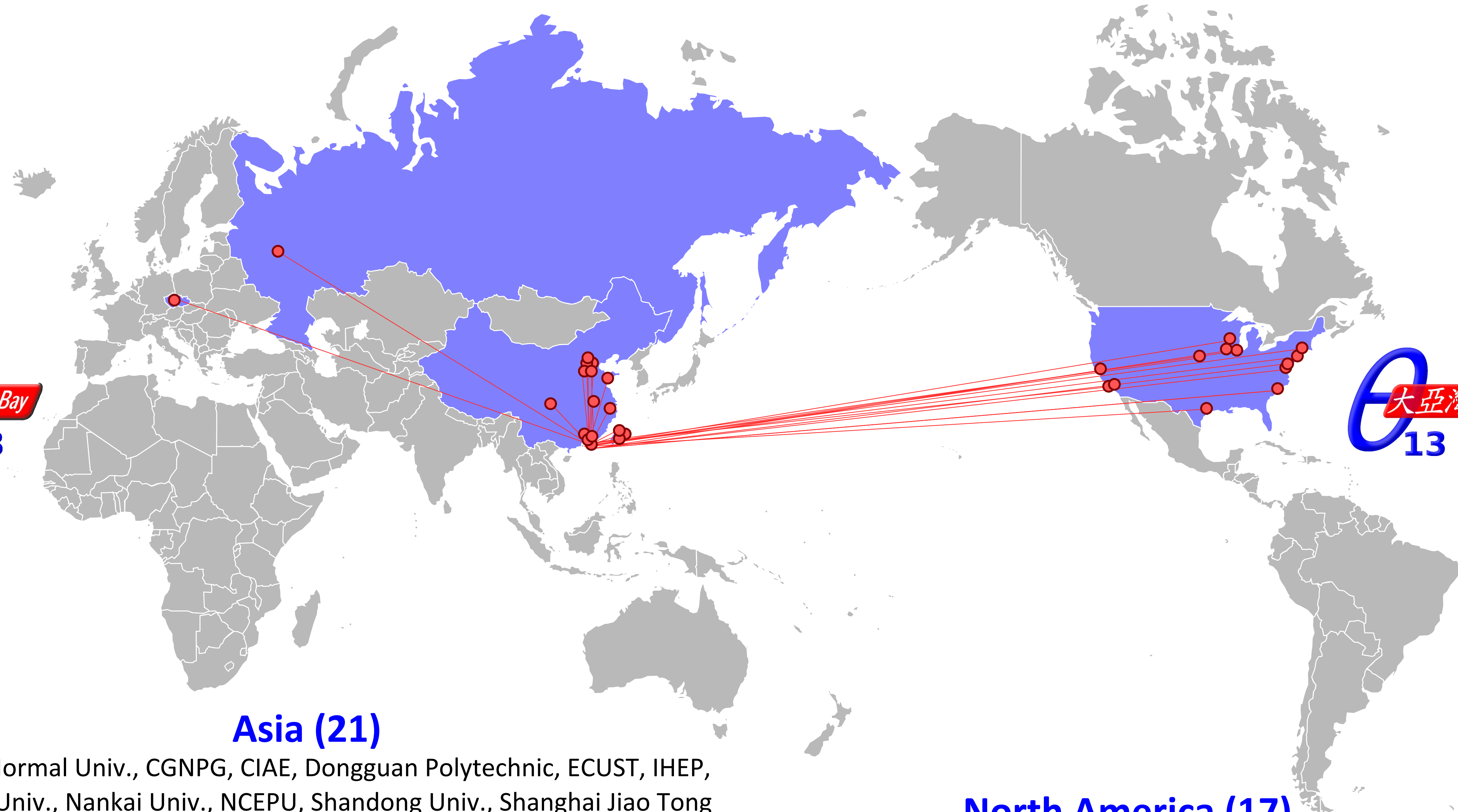

Asia (21)

Beijing Normal Univ., CGNPG, CIAE, Dongguan Polytechnic, ECUST, IHEP, Nanjing Univ., Nankai Univ., NCEPU, Shandong Univ., Shanghai Jiao Tong Univ., Shenzhen Univ., Tsinghua Univ., USTC, Xian Jiaotong Univ., Zhongshan Univ.,
Chinese Univ. of Hong Kong, Univ. of Hong Kong,
National Chiao Tung Univ., National Taiwan Univ., National United Univ.

Europe (2)

Charles University, JINR Dubna

North America (17)

Brookhaven Natl Lab, CalTech, Illinois Institute of Technology, Iowa State, Lawrence Berkeley Natl Lab, Princeton, Rensselaer Polytechnic, Siena College, UC Berkeley, UCLA, Univ. of Cincinnati, Univ. of Houston, UIUC, Univ. of Wisconsin, Virginia Tech, William & Mary, Yale

The Daya Bay Strategy

Relative measurement with 8 functionally identical detectors

- Absolute reactor flux single largest uncertainty in previous measurements

Cancels in near/far ratio: $$\frac{N_f}{N_n} = \left(\frac{N_{p,f}}{N_{p,n}}\right)\left(\frac{L_n}{L_f}\right)^2\left(\frac{\epsilon_f}{\epsilon_n}\right)\left(\frac{P_{sur}(E,L_f)}{P_{sur}(E,L_n)}\right)$$

Baseline Optimization

- Detector locations optimized to known parameter space of $|\Delta m^2_{ee}|$
- Far site maximizes term dependent on $\sin^2 2\theta_{13}$

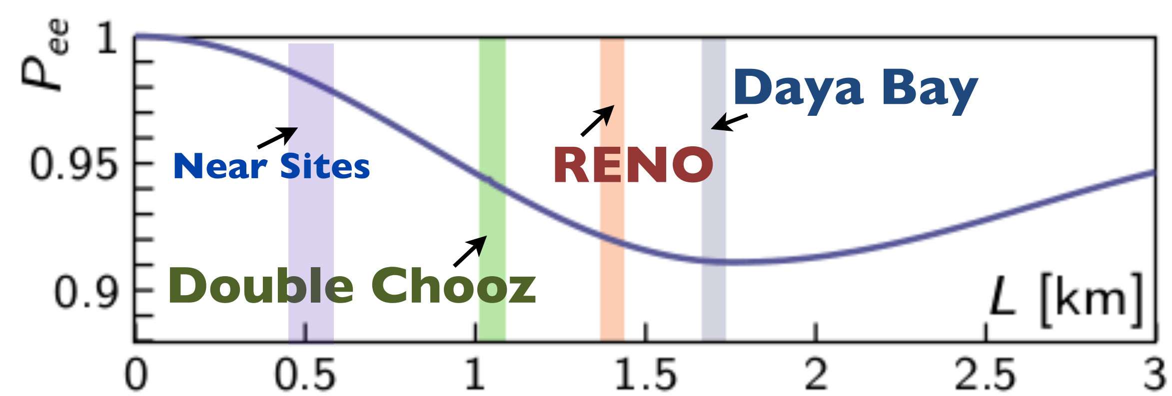

Go strong, big and deep!

	Reactor [GW_{th}]	Target [tons]	Depth [m.w.e]
Double Chooz	8.6	16 (2 × 8)	300, 120 (far, near)
RENO	16.5	32 (2 × 16)	450, 120
Daya Bay	17.4	160 (8 × 20)	860, 250
	Large Signal		Low Background

Daya Bay Site Layout

Far hall measures oscillation

Two near halls constrain reactor flux

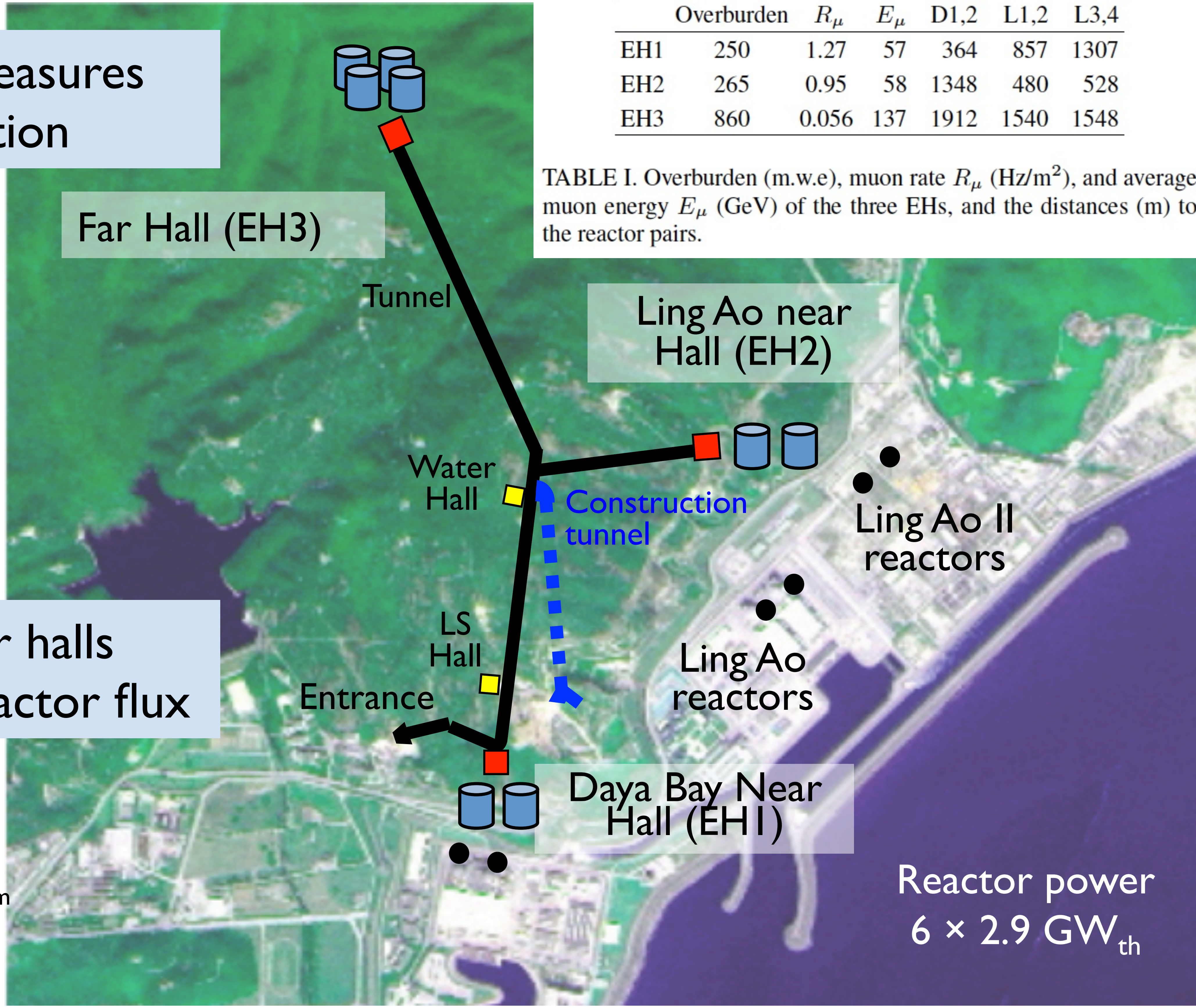

	Overburden	R_μ	E_μ	D1,2	L1,2	L3,4
EH1	250	1.27	57	364	857	1307
EH2	265	0.95	58	1348	480	528
EH3	860	0.056	137	1912	1540	1548

TABLE I. Overburden (m.w.e), muon rate R_μ (Hz/m^2), and average muon energy E_μ (GeV) of the three EHs, and the distances (m) to the reactor pairs.

Daya Bay $\overline{\nu}_e$ Detectors (ADs)

- A Daya Bay AD: three-zone liquid scintillator detector

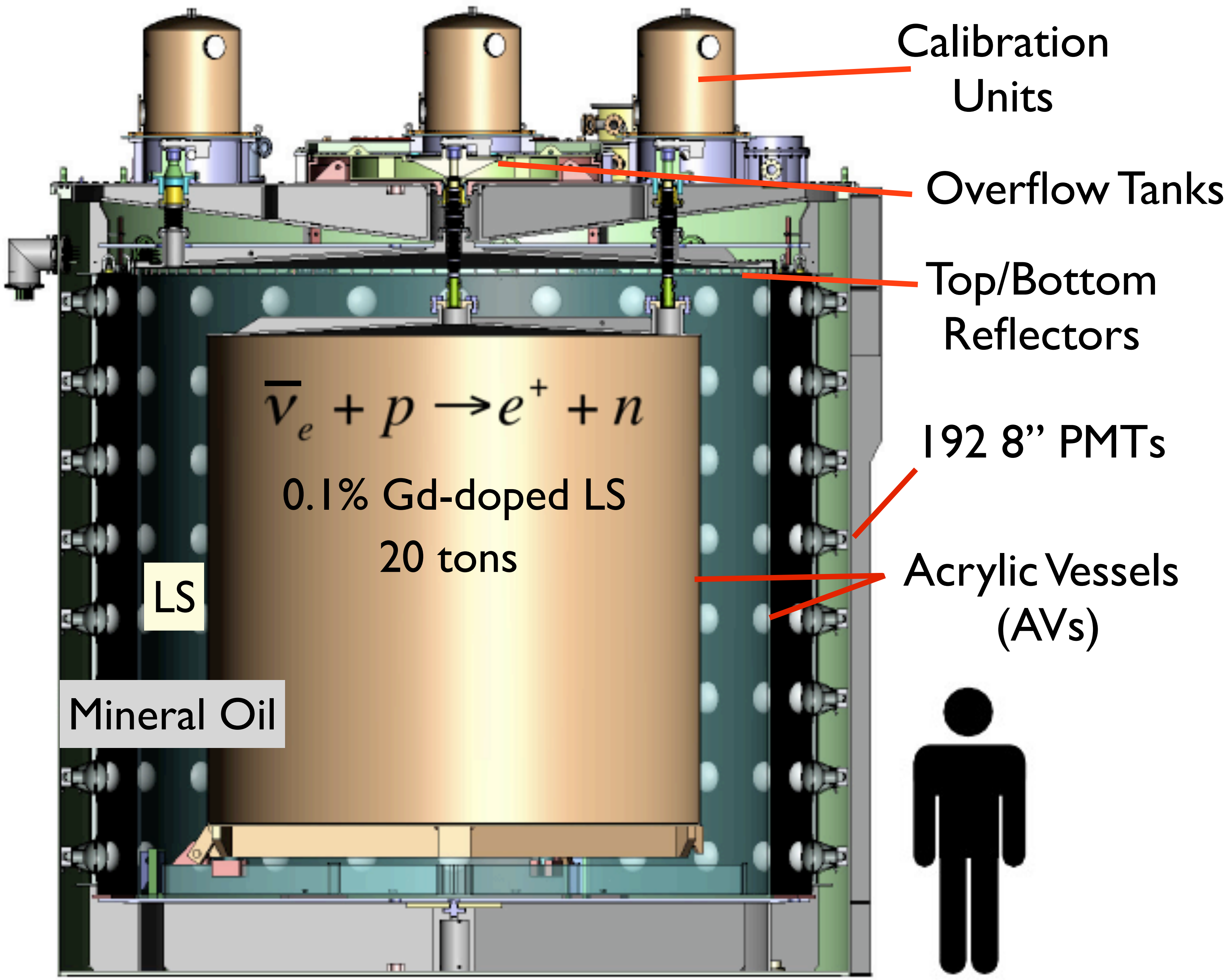

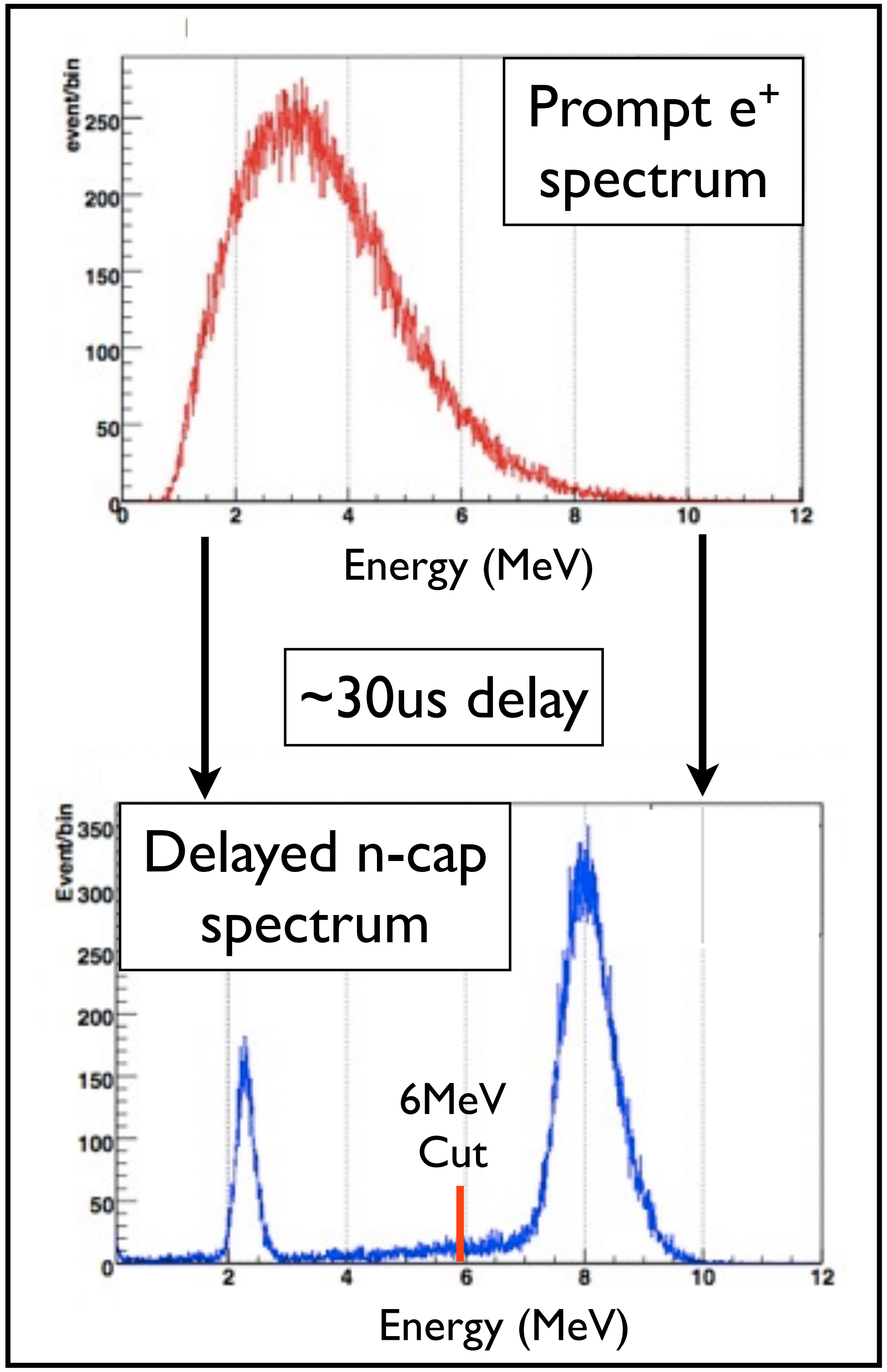

Daya Bay Monte Carlo Data

Detector Calibration

- Weekly calibration unit (ACU) runs:
  - Co-60 Ge-68 gamma sources
  - 0.5 Hz AmC fast neutron source
  - Low-intensity LED light source
- Muon-produced spallation neutrons
  - Same position, energy distribution as IBD delayed signals
  - Will calibrate delayed energy cut with low uncertainty!

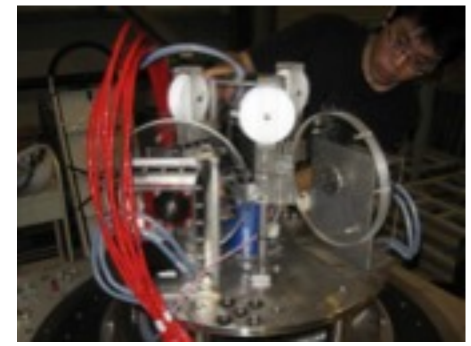

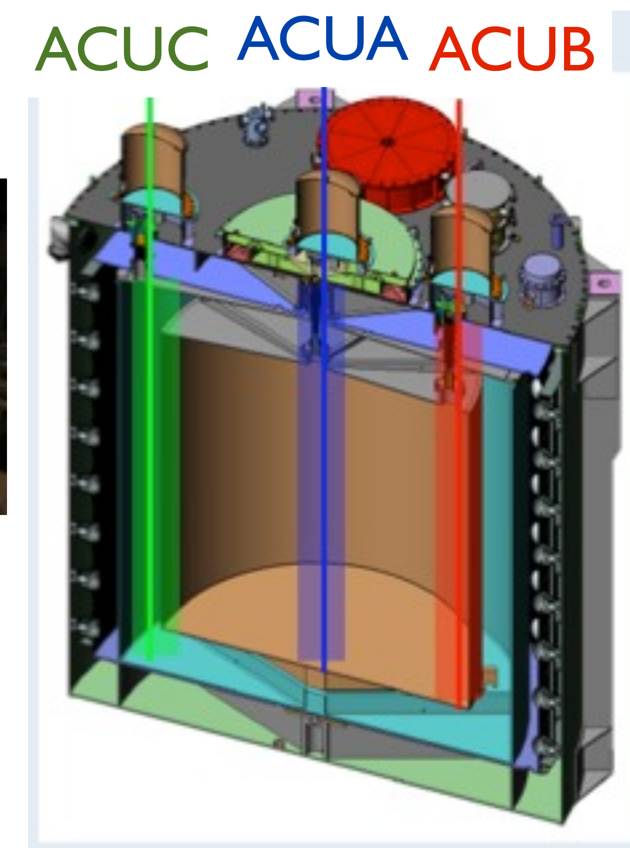

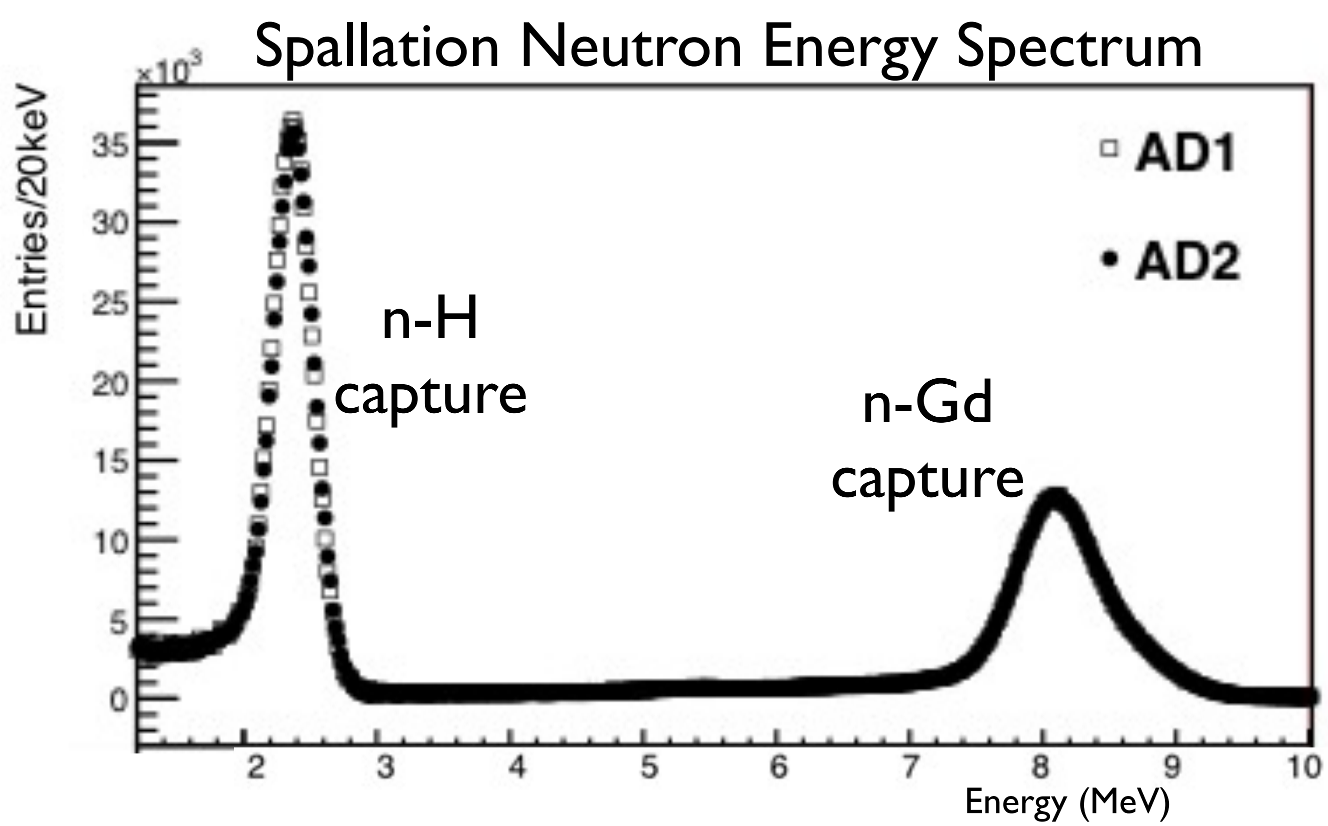

Detector Interior, Before Filling

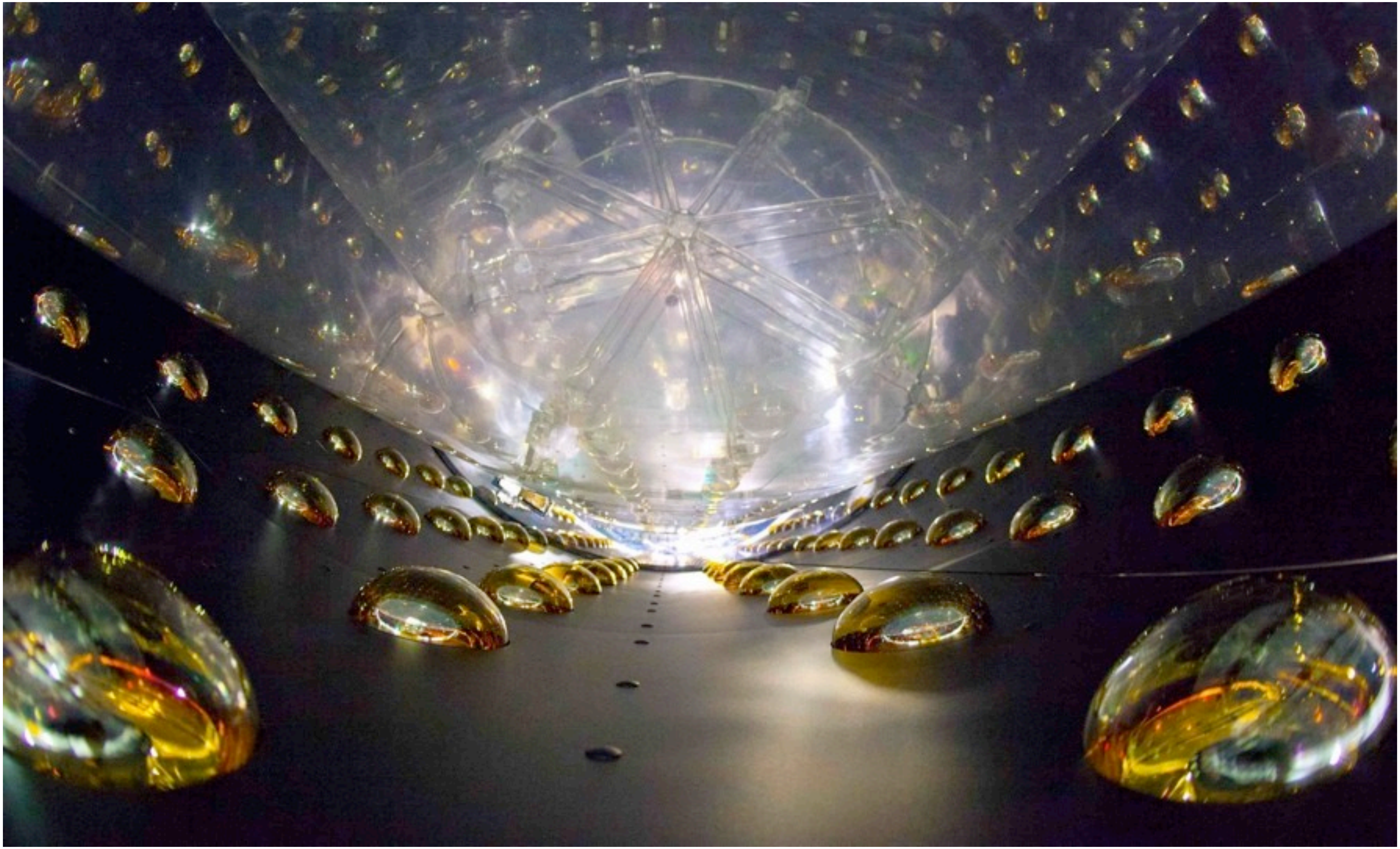

Daya Bay Muon Veto System

- A three-part muon detector:
  - Optically separated inner and outer water pool
    - Passive gamma and neutron shielding
    - Active muon ID for rejecting cosmogenic backgrounds: 288 (near) and 384 (far) PMTs
  - RPC: Resistive plate chambers
    - Independent muon tagging

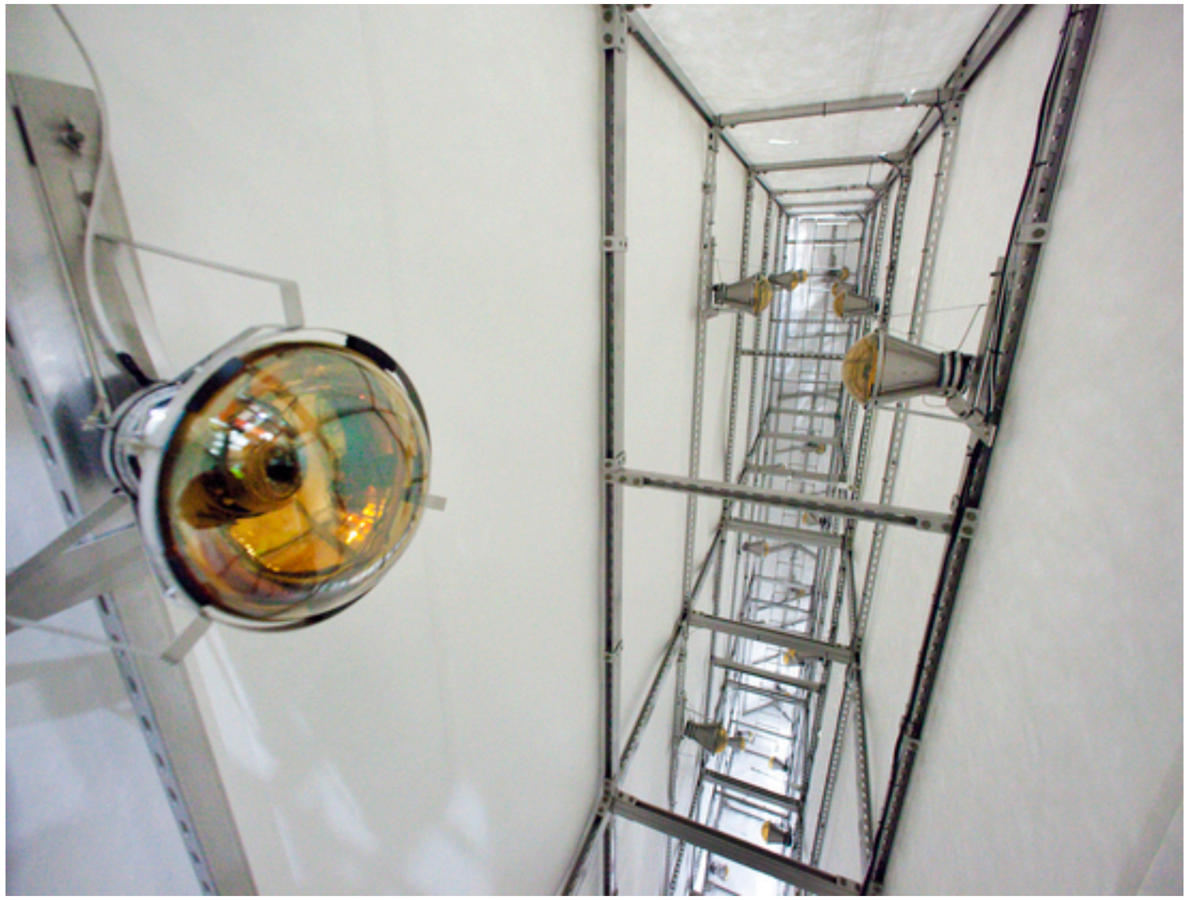

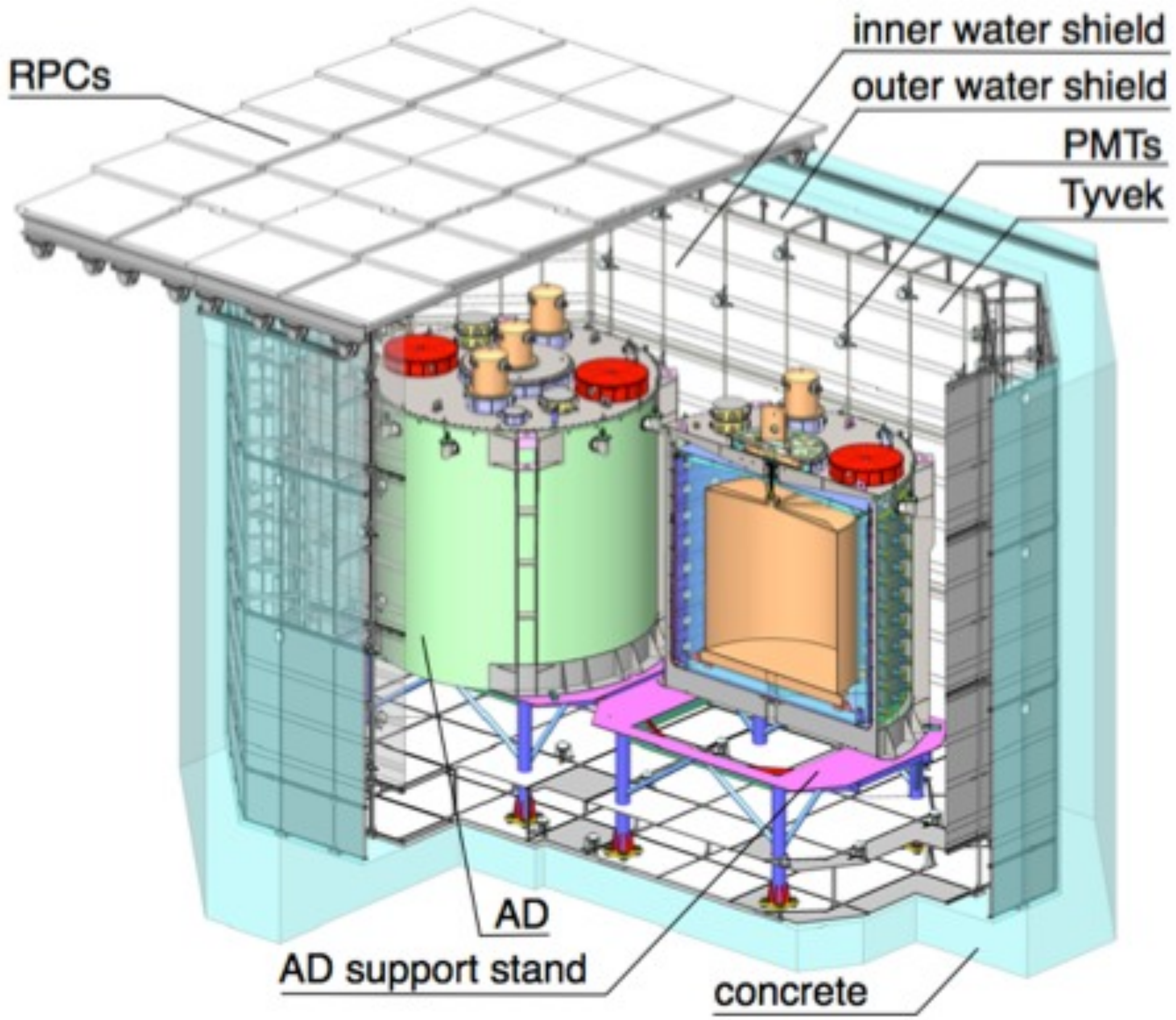

Underground Construction: Before

Underground Construction: After

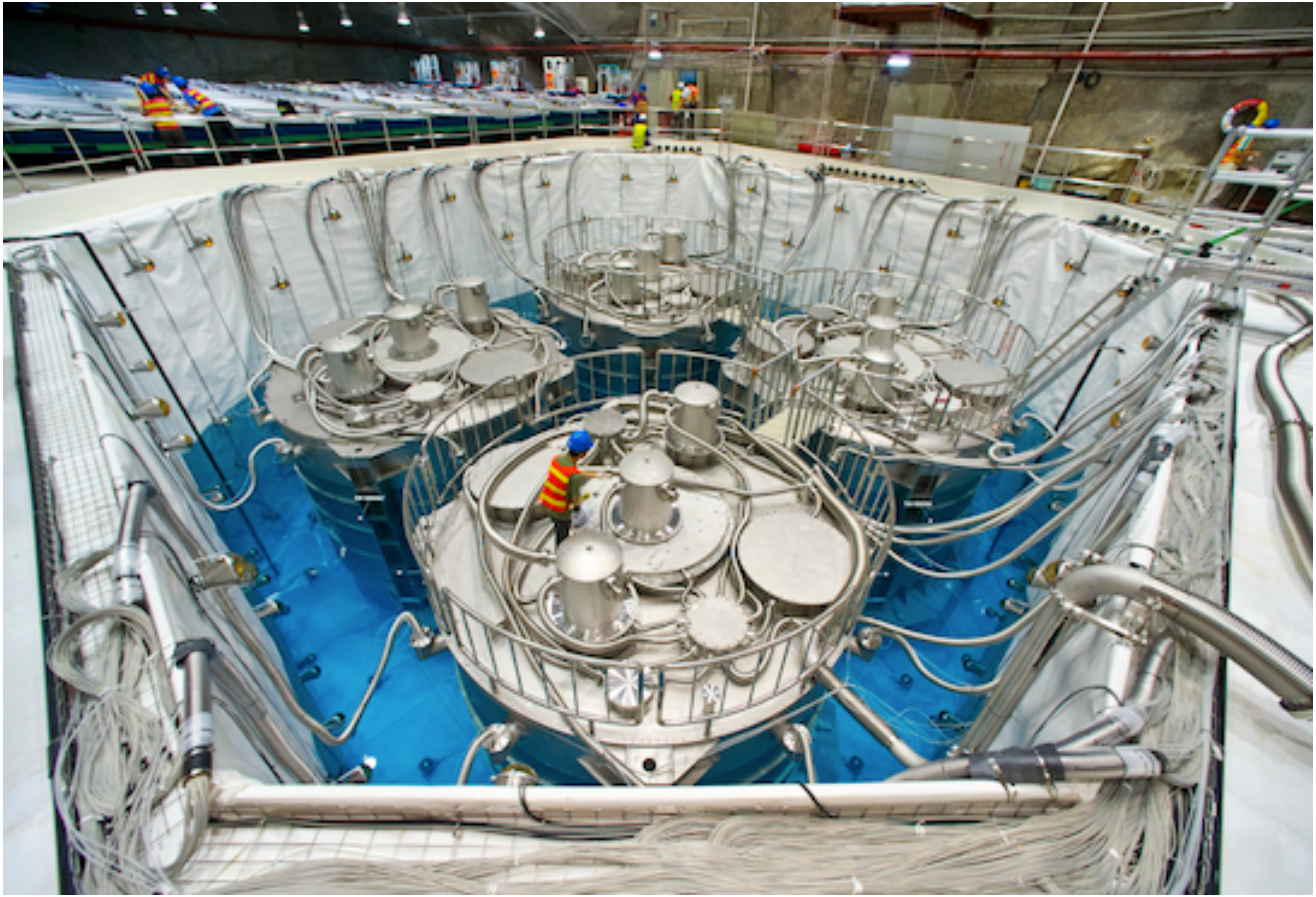

Data Set

Two detector comparison ins-det[1202.6181]

- 90 days of data, Daya Bay near site only
- NIM A 685 (2012), 78-97

First oscillation analysis hep-ex[1203:1669]

- 55 days of data, 6 ADs near+far
- PRL 108 (2012), 171803

Improved oscillation analysis hep-ex[1210.6327]

- 139 days of data, 6 ADs near+far
- CPC 37 (2013), 011001

Spectral Analysis

- 217 days, complete 6 AD period
- 55% more statistics than CPC result

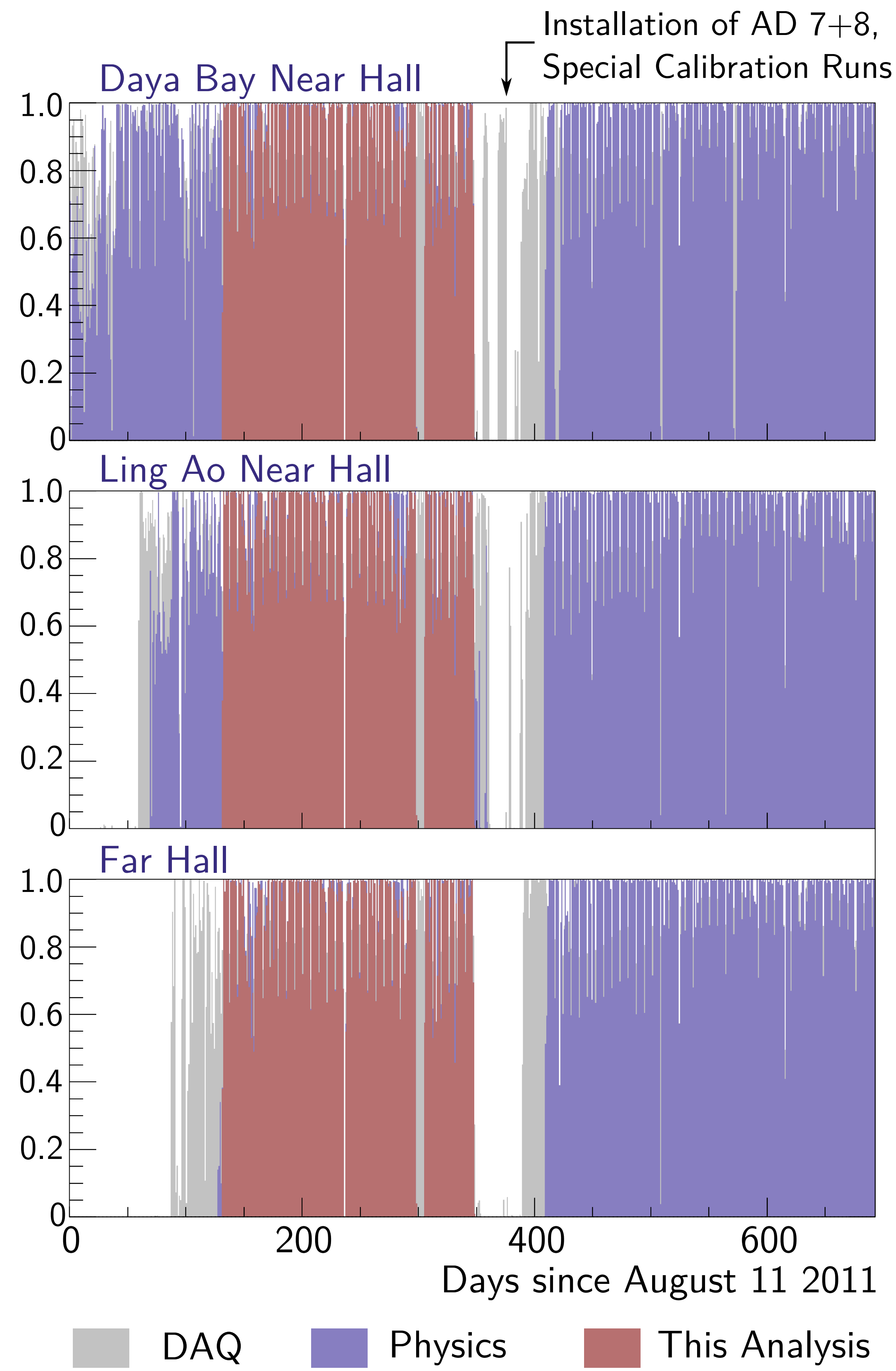

Previous Analysis: Rate-only

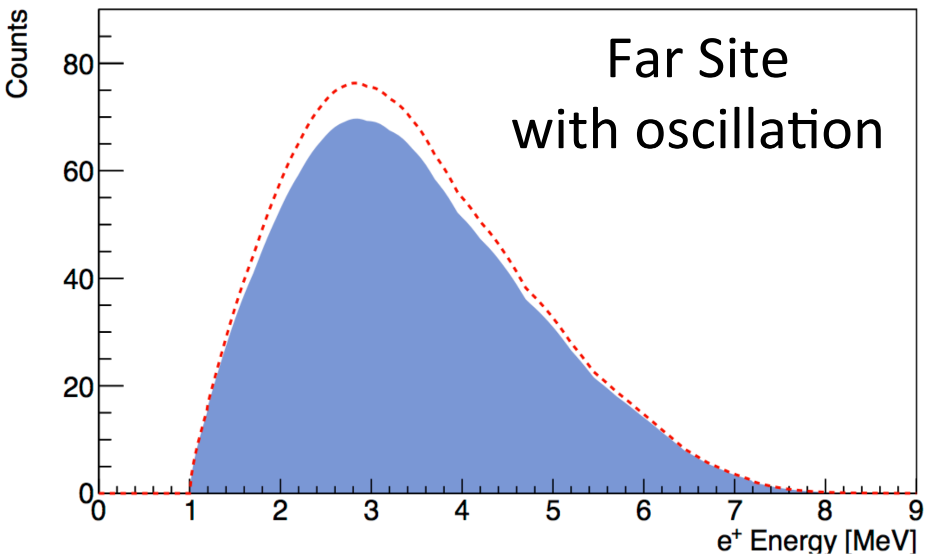

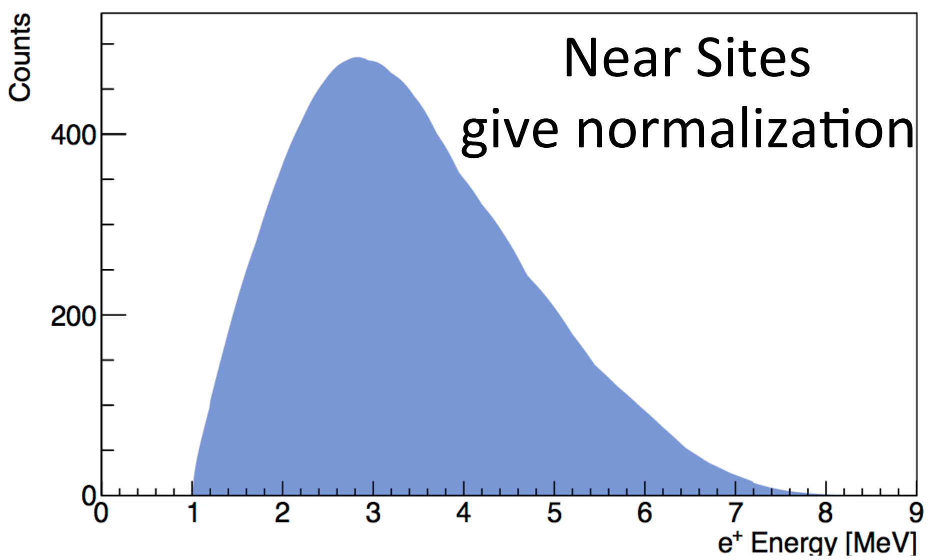

Compare total rate at near and far sites to look for relative rate deficit at far site

Integrate all energies

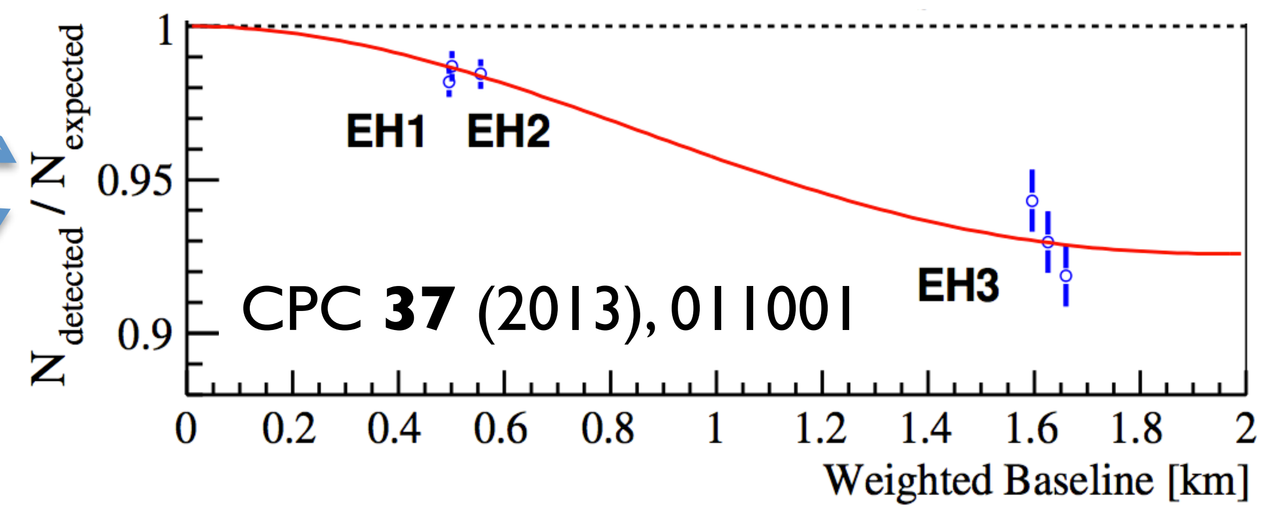

CPC **37** (2013), 011001

Advantage: Fewer systematic uncertainties

Disadvantages: Less sensitive; can't constrain Δm^2_{ee}

This simple analysis has served the collaboration very well

Can start by repeating rate analysis with full 6-AD dataset

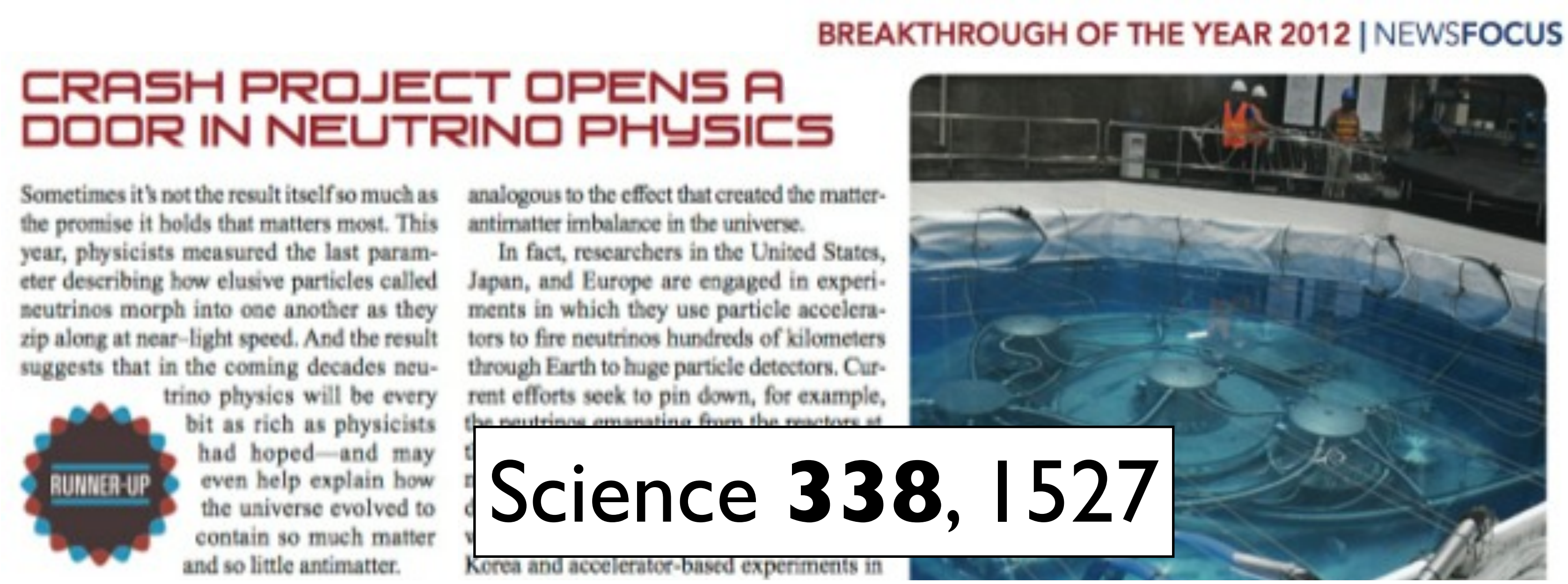
BREAKTHROUGH OF THE YEAR 2012 | NEWSFOCUS

CRASH PROJECT OPENS A DOOR IN NEUTRINO PHYSICS

Sometimes it's not the result itself so much as the promise it holds that matters most. This year, physicists measured the last parameter describing how elusive particles called neutrinos morph into one another as they zip along at near-light speed. And the result suggests that in the coming decades neutrino physics will be every bit as rich as physicists had hoped—and may even help explain how the universe evolved to contain so much matter and so little antimatter.

RUNNER-UP

analogous to the effect that created the matter-antimatter imbalance in the universe.

In fact, researchers in the United States, Japan, and Europe are engaged in experiments in which they use particle accelerators to fire neutrinos hundreds of kilometers through Earth to huge particle detectors. Current efforts seek to pin down, for example,

Korea and accelerator-based experiments in

Science **338**, 1527

Antineutrino Selection

1. Reject spontaneous PMT light emission ("flashers")
2. Prompt positron:
   0.7 MeV < Ep < 12 MeV
3. Delayed neutron:
   6.0 MeV < Ed < 12 MeV
4. Neutron capture time:
   1 μs < t < 200 μs
5. Muon veto:
   - Water pool muon (>12 hit PMTs): Reject [-2μs; 600μs]
   - AD muon (>3000 photoelectrons): Reject [-2 μs; 1400μs]
   - AD shower muon (>3×10^5 p.e.): Reject [-2 μs; 0.4s]
6. Multiplicity:
   - No additional prompt-like signal
     400μs before delayed neutron
   - No additional delayed-like signal
     200μs after delayed neutron

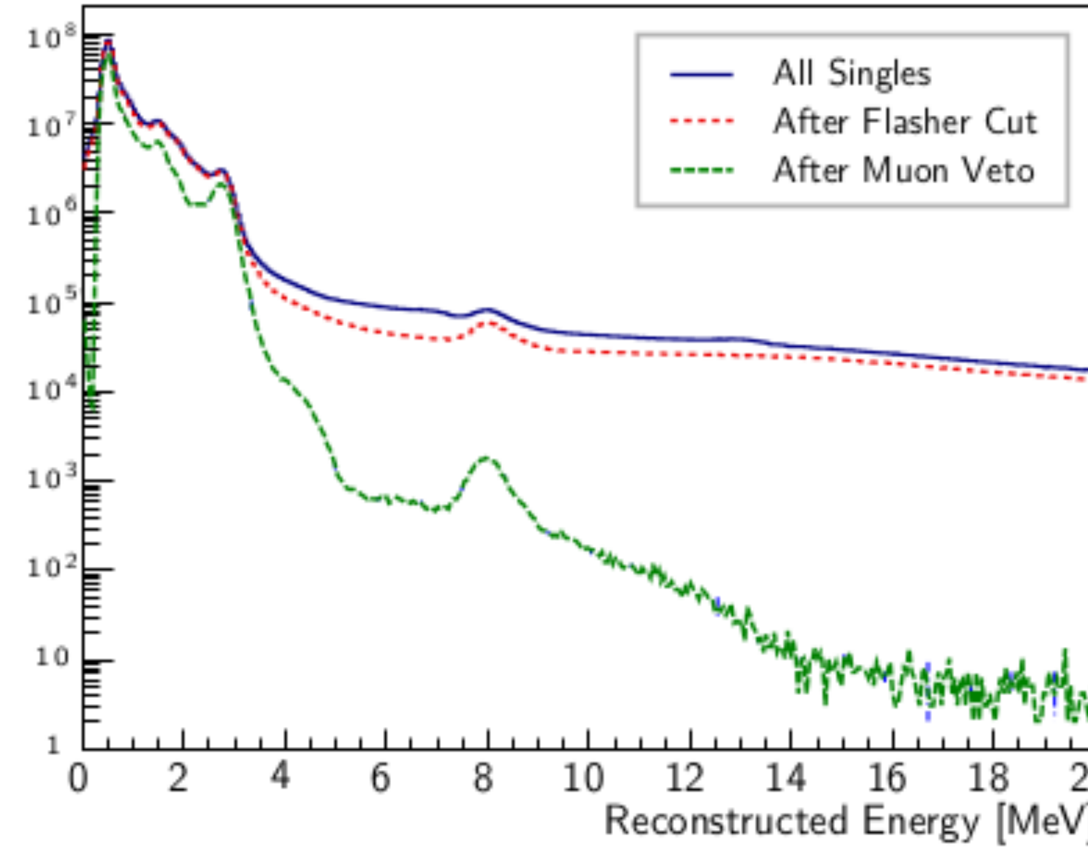

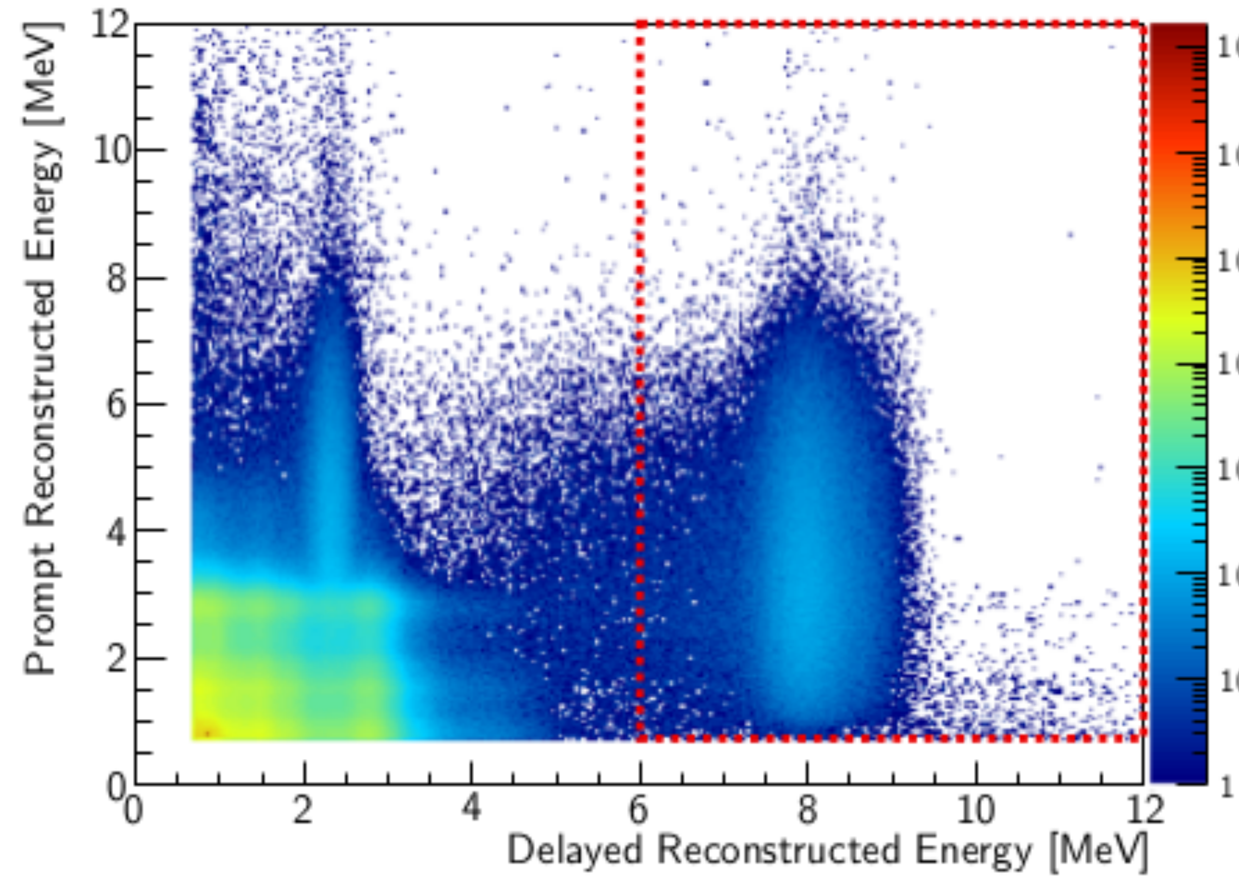

IBD Candidates and Backgrounds

	Near Halls			Far Hall		
	AD 1	AD 2	AD 3	AD 4	AD 5	AD 6
IBD candidates	101290	102519	92912	13964	13894	13731
DAQ live time (days)	191.001		189.645	189.779		
Efficiency $\epsilon_\mu \cdot \epsilon_m$	0.7957	0.7927	0.8282	0.9577	0.9568	0.9566
Accidentals (per day)*	9.54±0.03	9.36±0.03	7.44±0.02	2.96±0.01	2.92±0.01	2.87±0.01
Fast-neutron (per day)*	0.92±0.46		0.62±0.31	0.04±0.02		
^{9}Li/^{8}He (per day)*	2.40±0.86		1.2±0.63	0.22±0.06		
Am-C corr. (per day)*			0.26±0.12			
^{13}C^{16}O backgr. (per day)*	0.08±0.04	0.07±0.04	0.05±0.03	0.04±0.02	0.04±0.02	0.04±0.02
IBD rate (per day)*	653.30±2.31	664.15±2.33	581.97±2.07	73.31±0.66	73.03±0.66	72.20± 0.66

* Background and IBD rates were corrected for the efficiency of the muon veto and multiplicity cuts $\epsilon_\mu \cdot \epsilon_m$

- Over 350k detected electron antineutrinos!
- Far site statistical uncertainty (~0.5%) still dominates background (~0.2%), reactor, and detector (~0.2%) systematics

	Efficiency	Correlated	Uncorrelated
Target protons		0.47%	0.03%
Flasher cut	99.98%	0.01%	0.01%
Delayed energy cut	90.9%	0.6%	0.12%
Prompt energy cut	99.88%	0.10%	0.01%
Multiplicity cut		0.02%	<0.01%
Capture time cut	98.6%	0.12%	0.01%
Gd capture fraction	83.8%	0.8%	<0.1%
Spill-in	105.0%	1.5%	0.02%
Livetime	100.0%	0.002%	<0.01%
Combined	78.8%	1.9%	0.2%

New Rate Analysis

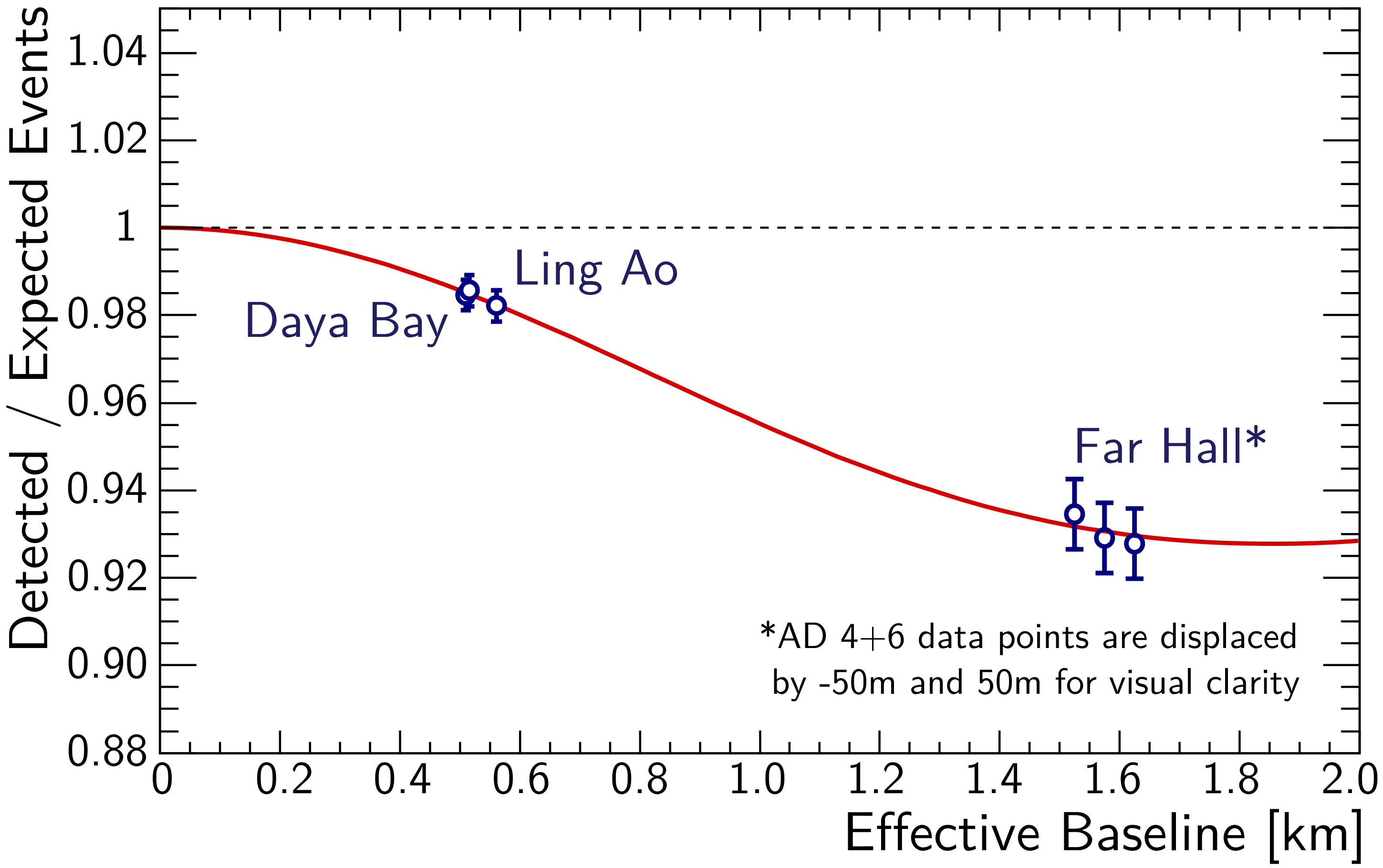

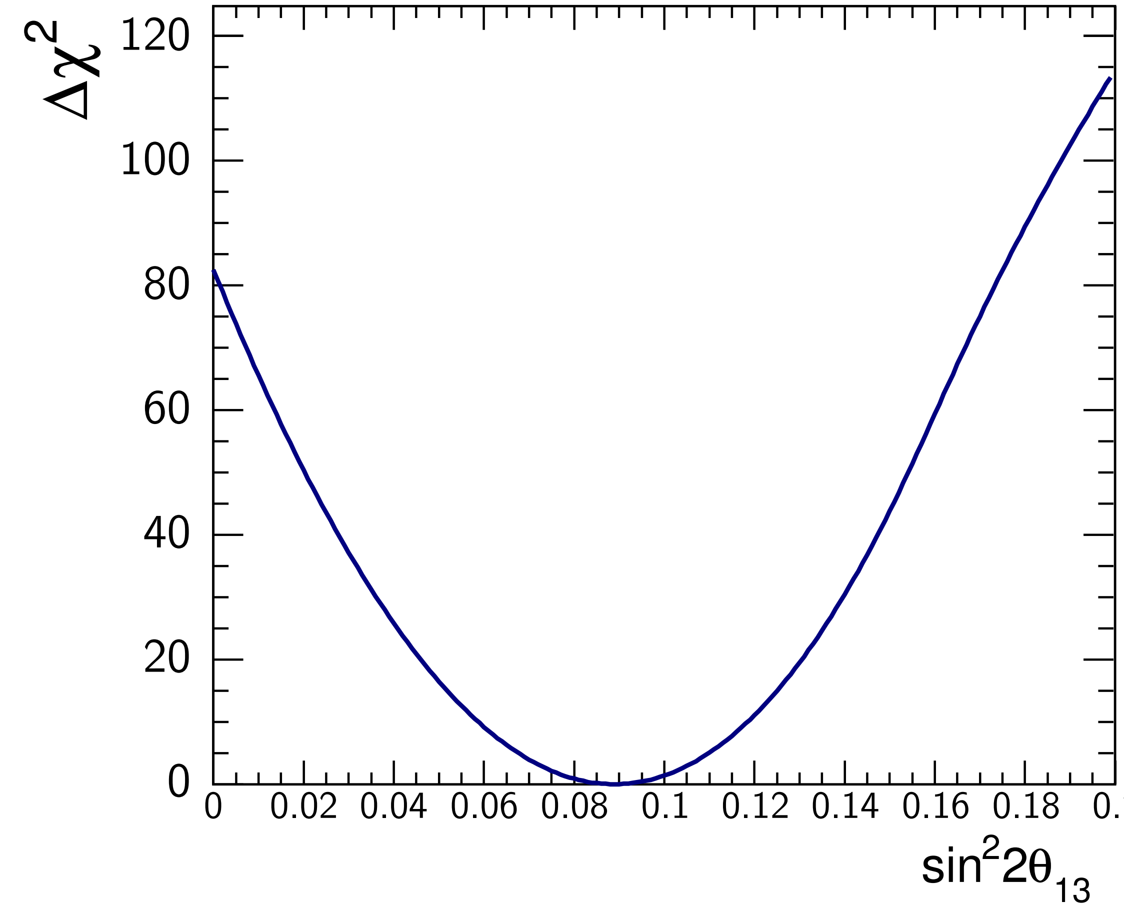

$\sin^2 2\theta_{13} = 0.089 \pm 0.009$

- Uncertainty reduced by statistics of complete 6 AD data period
- Standard approach: $\chi^2/N_{DoF} = 0.48/4$
- $|\Delta m^2_{ee}|$ constrained by MINOS result for $|\Delta m^2_{\mu\mu}|$
- Far vs. near relative measurement: absolute rate not constrained
- Consistent results from independent analyses, different reactor flux models

New Rate+Shape Analysis

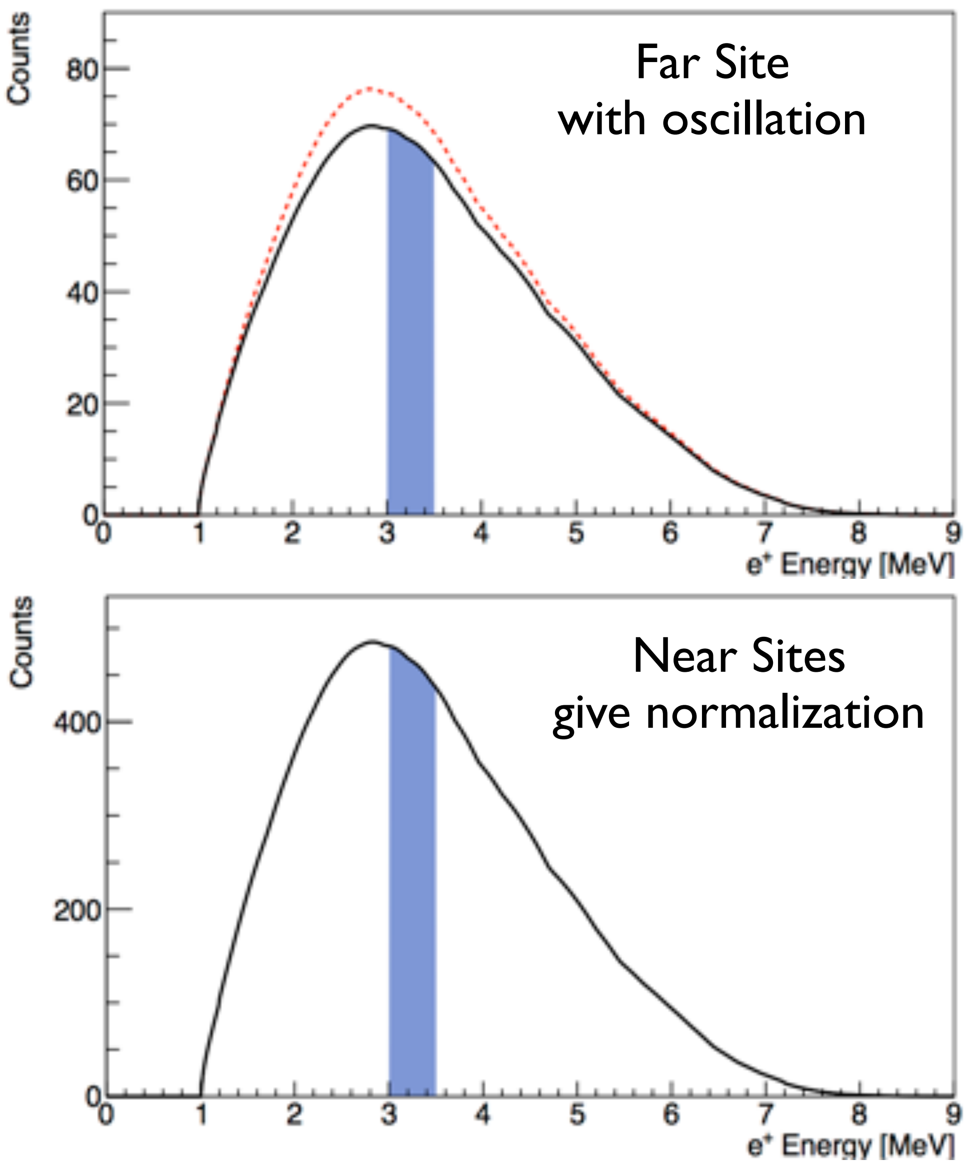

Compare rates in each energy bin between near and far detectors

Compare each energy

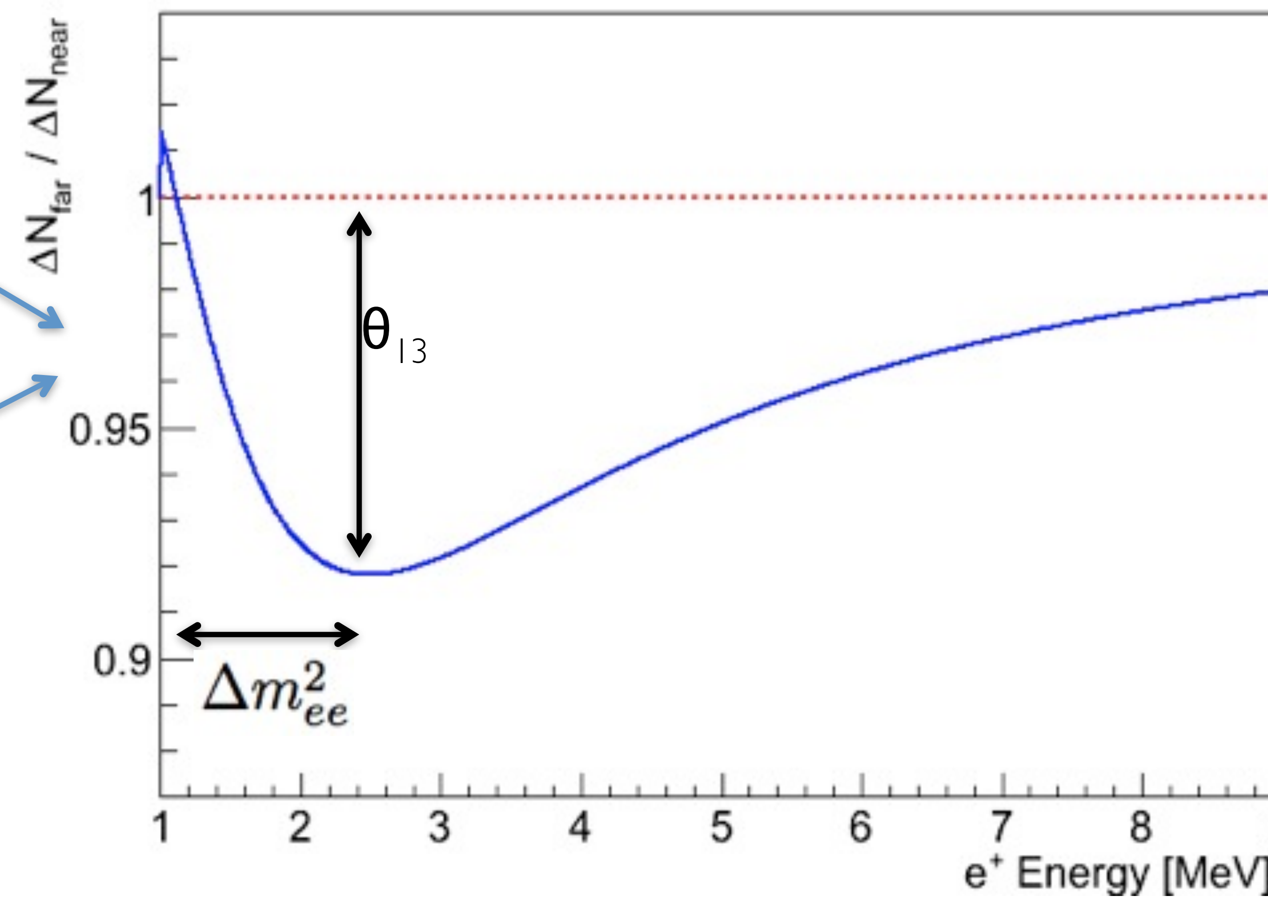

- Advantages: increased sensitivity from shape info; can measure mass splitting
  - First-ever measurement of atmospheric mass splitting at reactors
- Disadvantage: must have detailed understanding of detector response, backgrounds

Energy Response: Relative Calibration

Relative shift in energy between detectors can bias oscillation

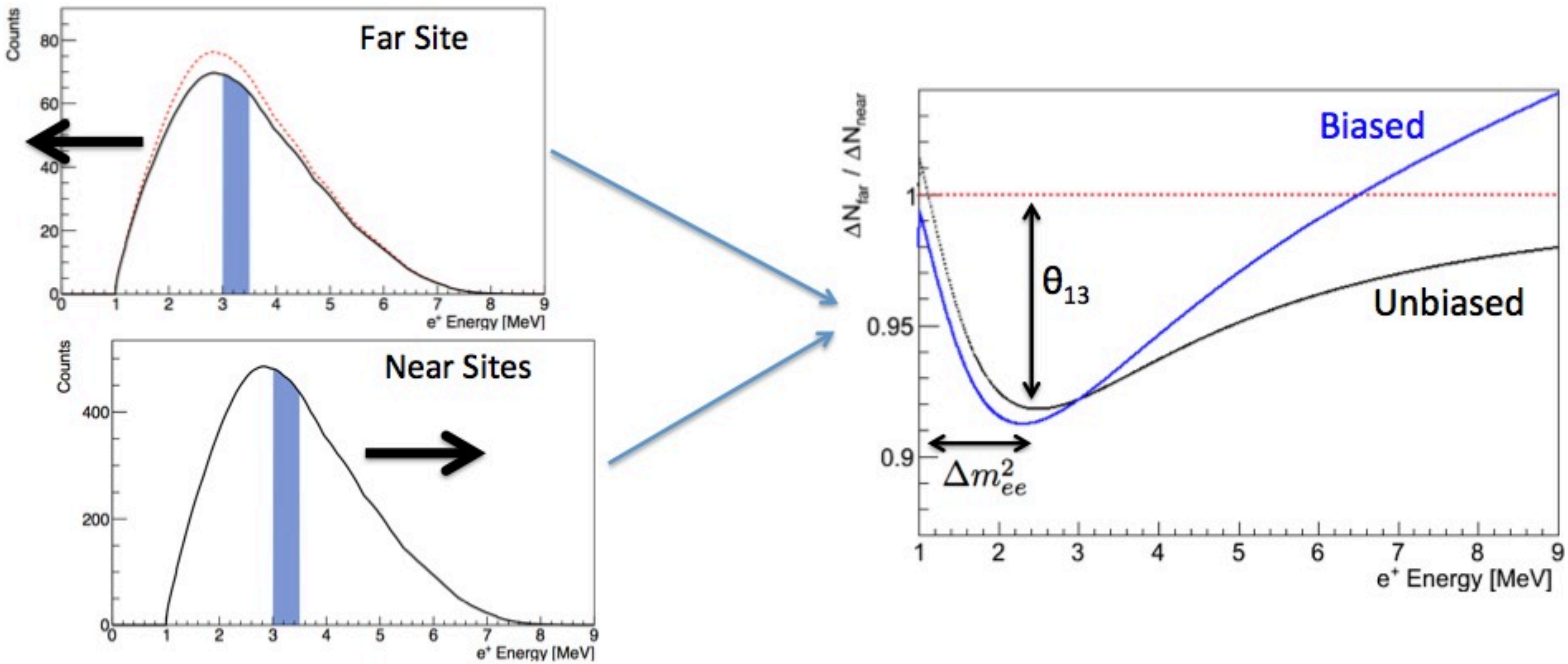

Requires careful detector calibration

Energy Response: Relative Calibration

- Obtain a stable energy response consistent between detectors
  - Use spallation neutron nGd peak to benchmark energy scale
  - Stability of < 0.1% in all detectors with time
  - Energy scales consistent for all measured energies and particles to 0.35%

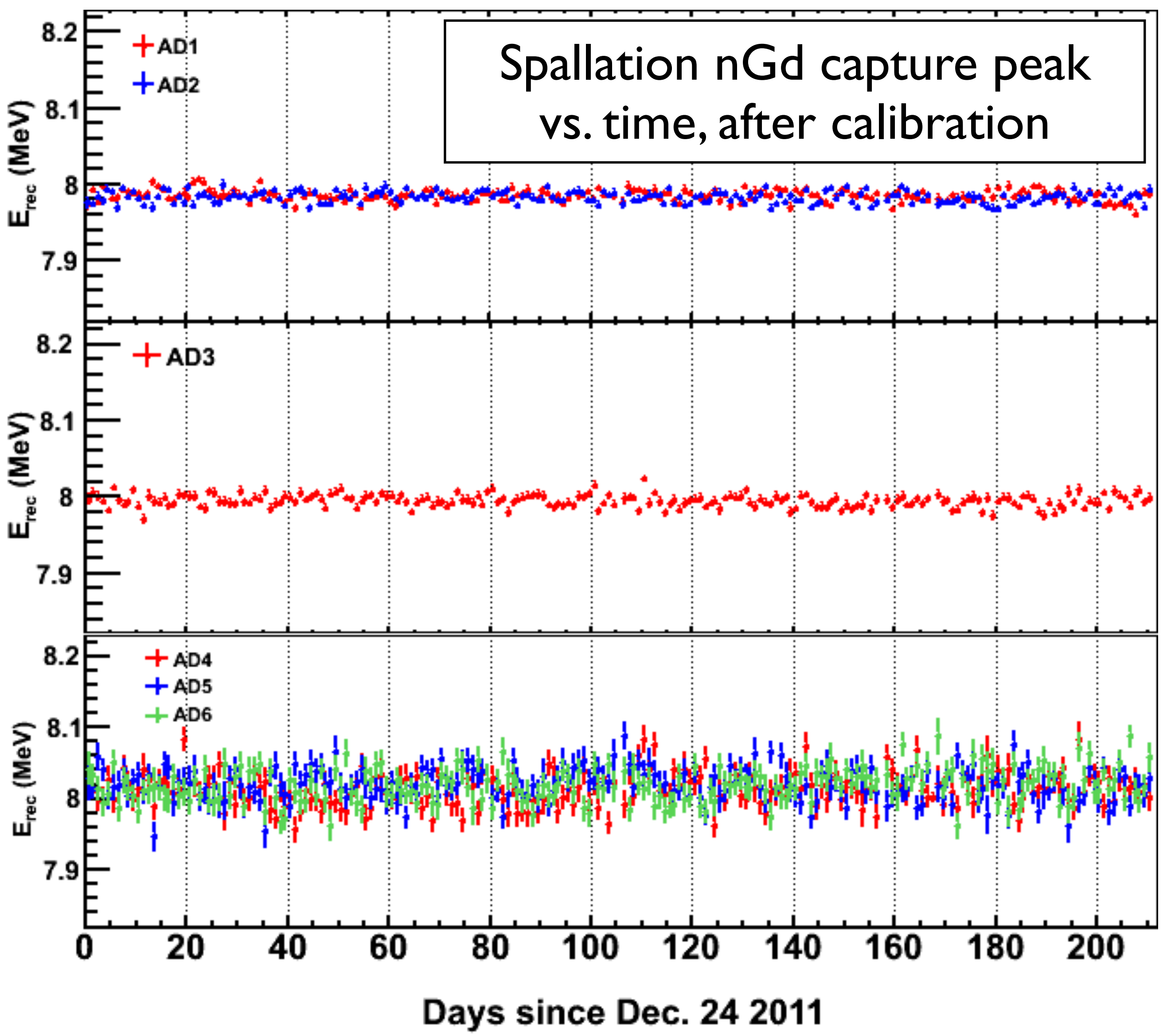

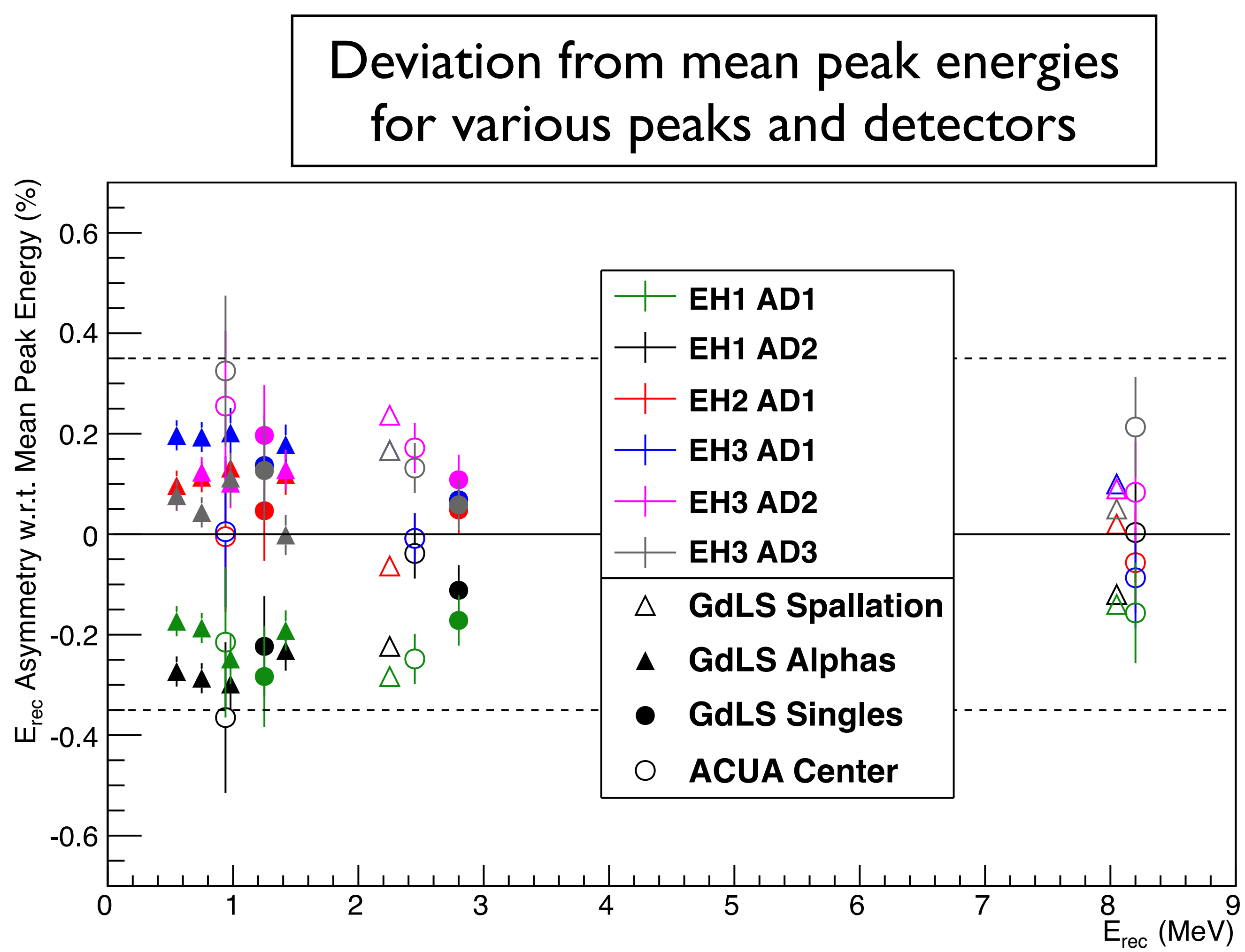

Energy Response: Absolute Calibration

Absolute energy shift common between detectors can also bias measured oscillation

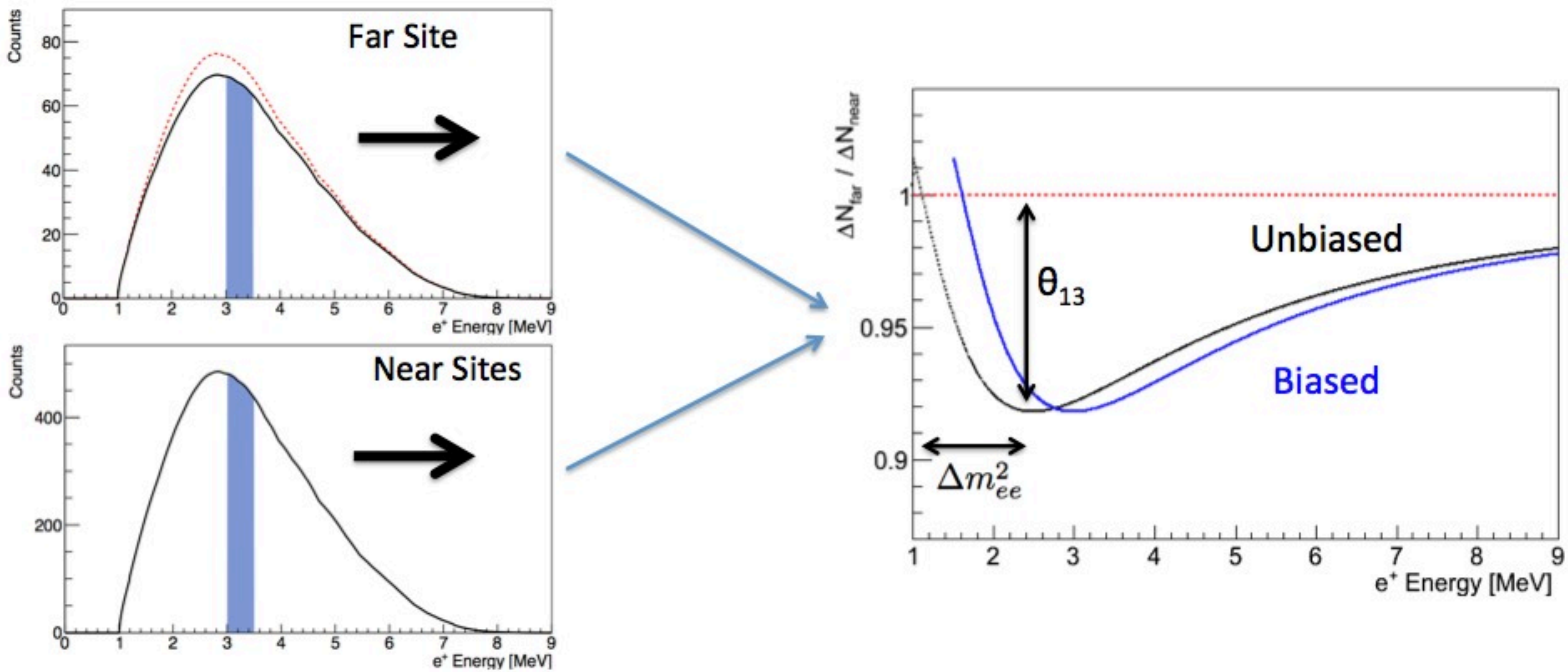

Requires detailed translation between true and detected energies

Energy Response Model Overview

Must understand absolute energy response of detector

Particle Energy E_{true}

↓

Energy Deposited in Scintillator E_{dep}

↓

Energy Converted to Visible Light E_{vis}

↓

Reconstructed Energy E_{rec}

Energy Losses in Acrylic

Acrylic vessels non-scintillating

- Induce shape distortion
- Correction from MC

Energy Resolution

- Light production
- Light collection
- PMT/electronics response

Two major sources of non-linearity. Difficult to decouple !

1: Scintillator Response

- Quenching effects
- Cherenkov radiation

2: Readout Electronics

- Charge collection efficiency decreases with visible light

Use energy response model to provide spectral prediction for signal, background

Starting Point: True Prompt Spectrum

Start with a per-AD true spectrum prediction

- Predict spectrum at each AD given powers and fission fractions of each reactor
- Translate to positron energy (Shift low-energy down to 1 MeV)

	^{235}U	^{238}U	^{239}Pu	^{241}Pu
AD 1	63.3	12.2	19.5	4.8
AD 2	63.3	12.2	19.5	4.8
AD 3	61.0	12.5	21.5	4.9
AD 4	61.5	12.4	21.1	4.9
AD 5	61.5	12.4	21.1	4.9
AD 6	61.5	12.4	21.1	4.9

Approximate percentage of IBDs from each fission isotope at each detector

New model:

P. Huber, Phys. Rev. C84, 024617 (2011),
T. Mueller et al., Phys. Rev. C83, 054615 (2011)

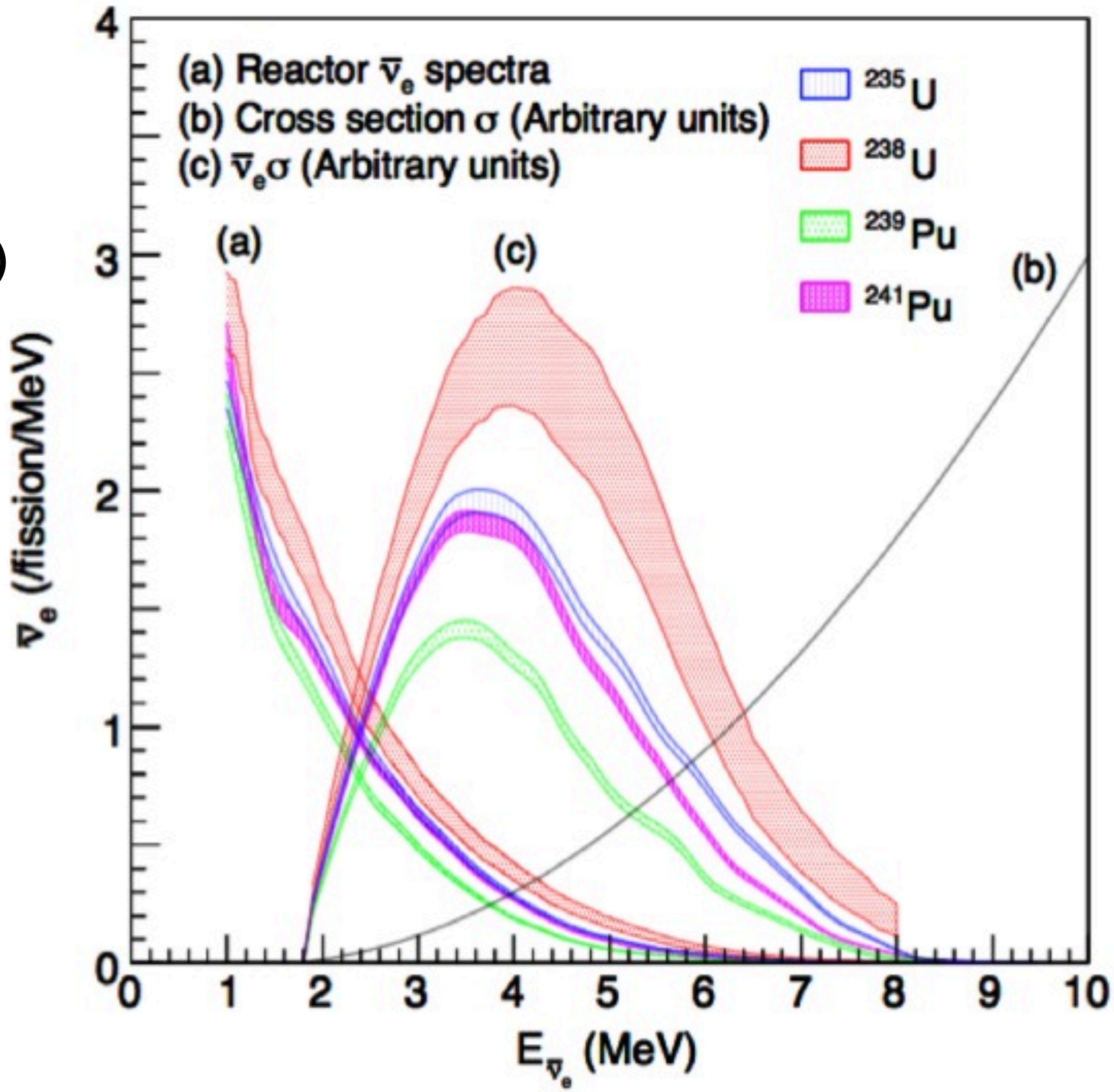

Energy Response: Non-scintillating Volumes

Energy loss in acrylic causes small distortion of energy spectrum

If antineutrino interacts in or near acrylic vessel, a portion of the kinetic energy of inverse beta positrons will not be detected

Annihilation gammas with longer range can also deposit energy in the vessels

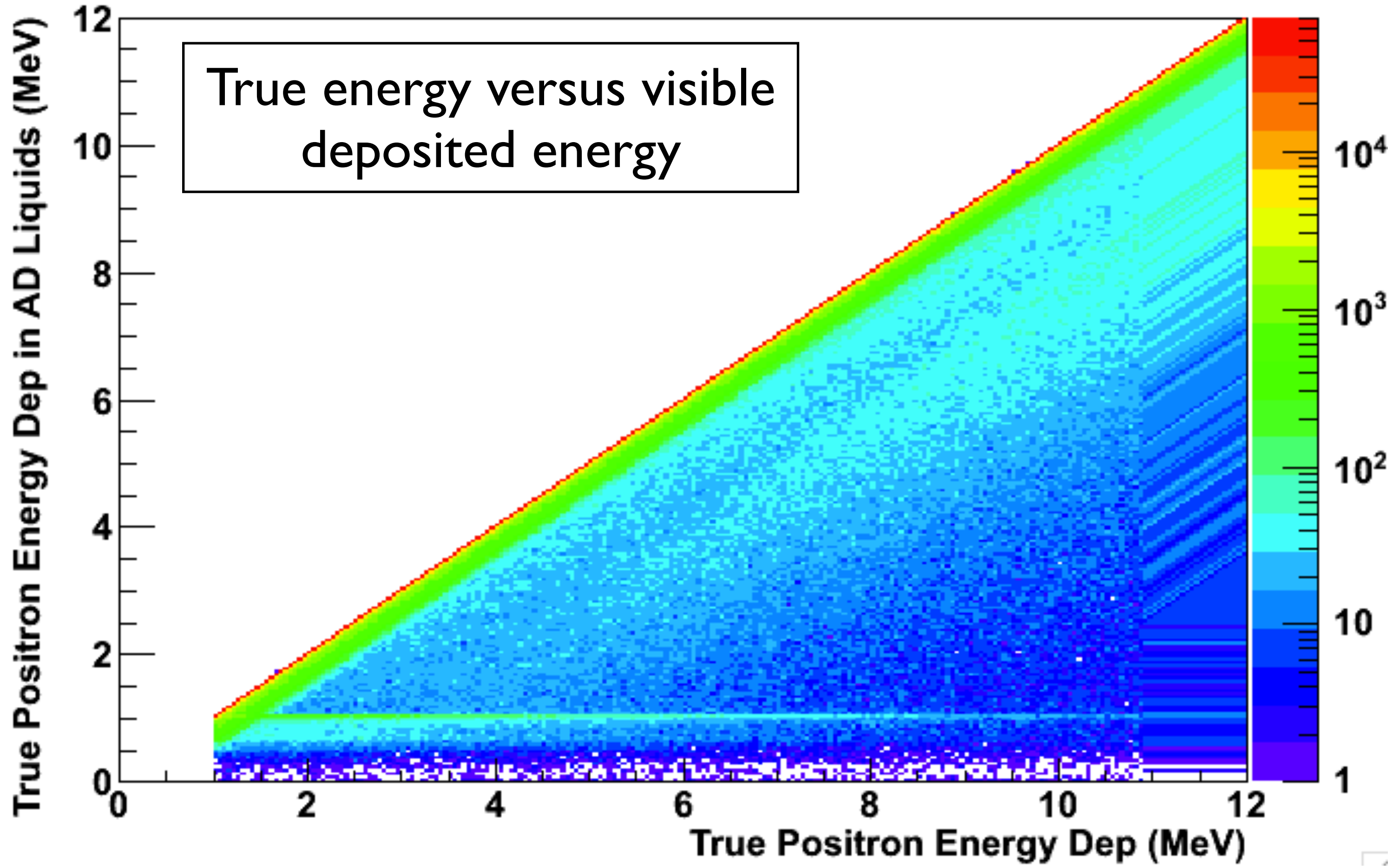

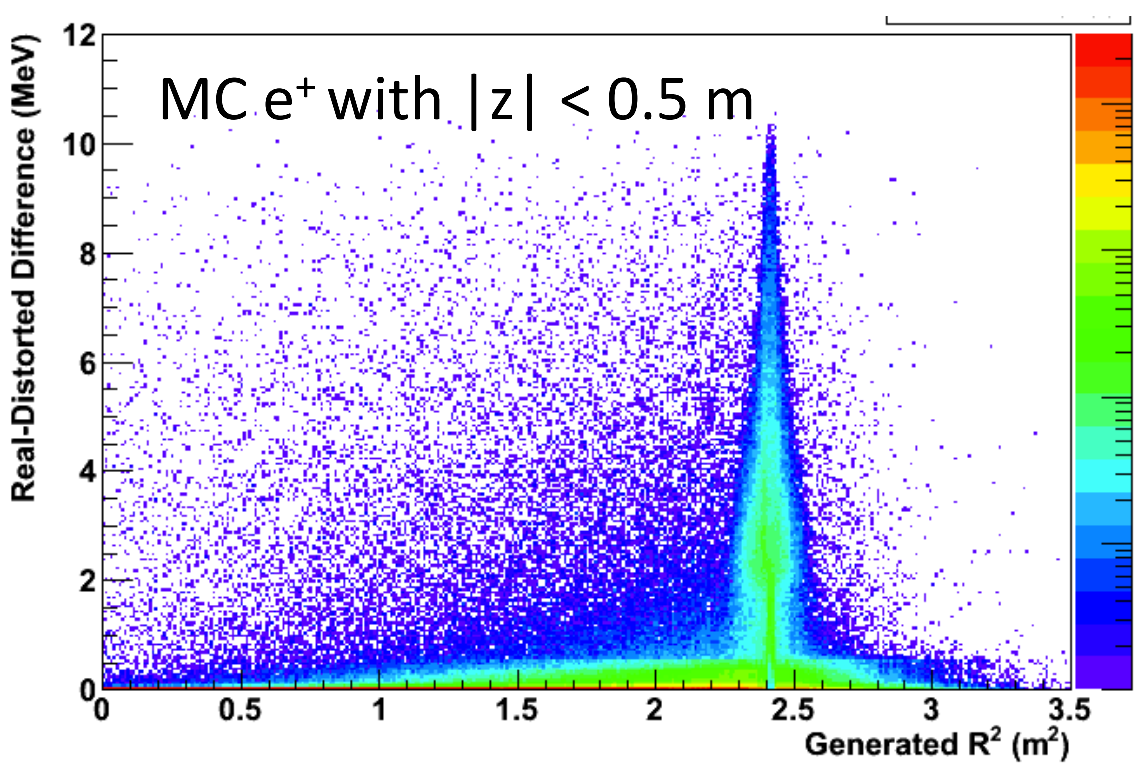

Generated 2D distortion matrix from MC to correct predicted positron energy spectrum

Uncertainties from varying acrylic vessel thicknesses and MC statistics incorporated into analysis.

Energy Response: Scintillator

Electron response

2 parameterizations to model quenching effects and Cherenkov radiation:

1) 3-parameter purely empirical model:

$$\frac{E_{\text{vis}}}{E_{\text{true}}} = \frac{1 + p_3 \cdot E_{true}}{1 + p_1 \cdot e^{-p_2 \cdot E_{\text{true}}}}$$

2) Semi-emp. model based on Birks' law:

$$\frac{E_{\text{vis}}}{E_{\text{true}}} = f_q(E_{\text{true}}; k_B) + k_C \cdot f_c(E_{\text{true}})$$

k_B: Birks' constant
k_C: Cherenkov contribution

Gammas + positrons

- Gammas connected to electron model through MC:

$$E^{\gamma}_{\text{vis}} = \int E^{e^-}_{\text{vis}}\left(E^{e^-}_{\text{true}}\right) \cdot \frac{dN}{dE}\left(E^{e^-}_{\text{true}}\right) dE^{e^-}_{\text{true}}$$

- Positrons connected to electron model through MC:

$$E^{e^+}_{\text{vis}} = E^{e^-}_{\text{vis}} + 2 \cdot E^{\gamma}_{\text{vis}}(0.511\,\text{MeV})$$

Simulation of individual e⁻, e⁺ energies due to gamma interaction in scintillator.

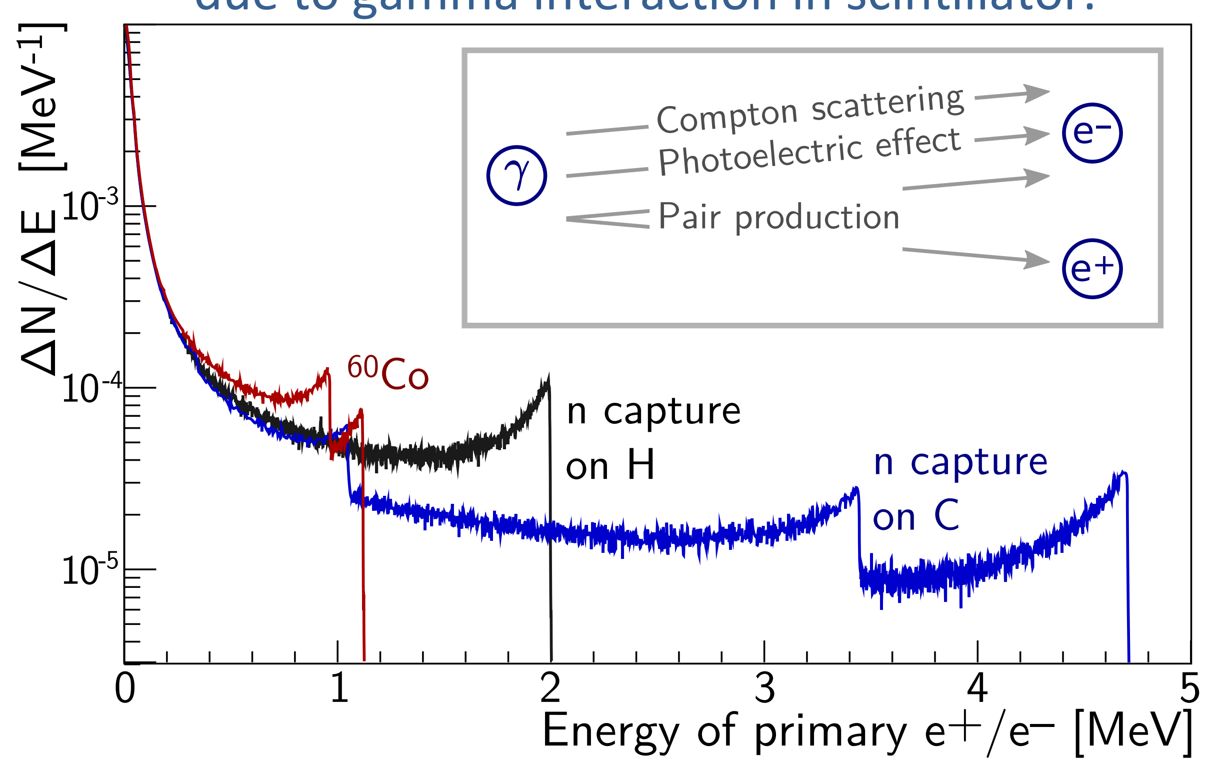

Energy Response: Electronics

PMT readout electronics introduces additional biases

Electronics does not fully capture late secondary hits

- Slow scintillation component missed at high energies
- Charge collection efficiency decreases with visible light

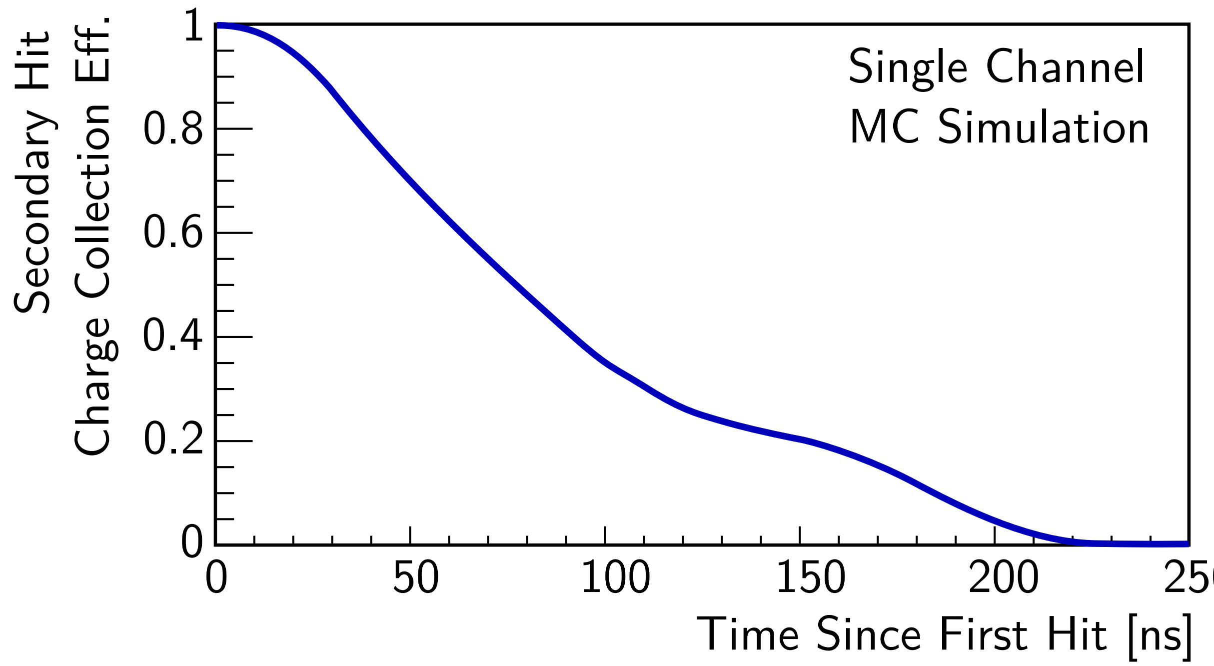

Final Combined Non-linearity Model

- Effective model as a function of total visible energy
- 2 empirical parameterizations: exponential and quadratic
- Total effective non-linearity f from both scintillation and electronics effects:

$$f = \frac{E_{rec}}{E_{true}} = \underbrace{\frac{E_{rec}}{E_{vis}}}_{\boxed{1}} \cdot \underbrace{\frac{E_{vis}}{E_{true}}}_{\boxed{2}}$$

$\boxed{1}$ Electronics non-linearity

$\boxed{2}$ Scintillator non-linearity

Energy Response: Constraining With Data

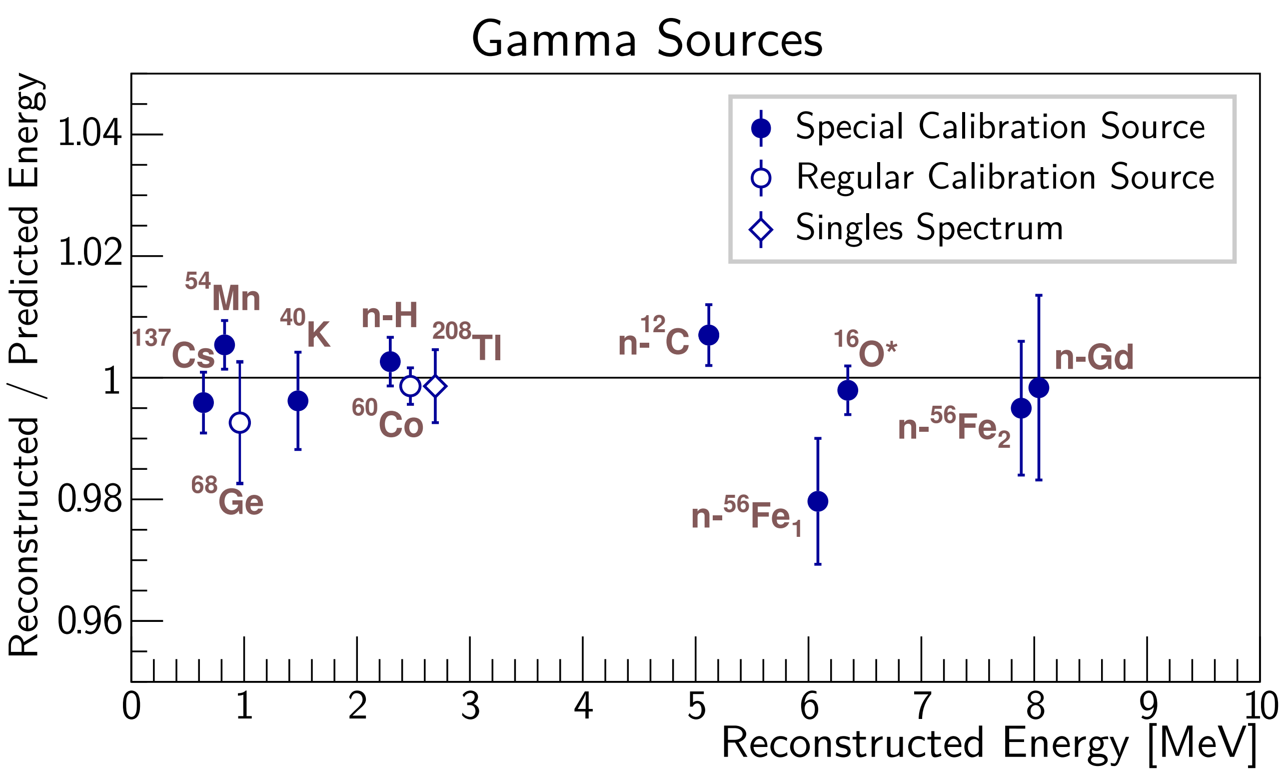

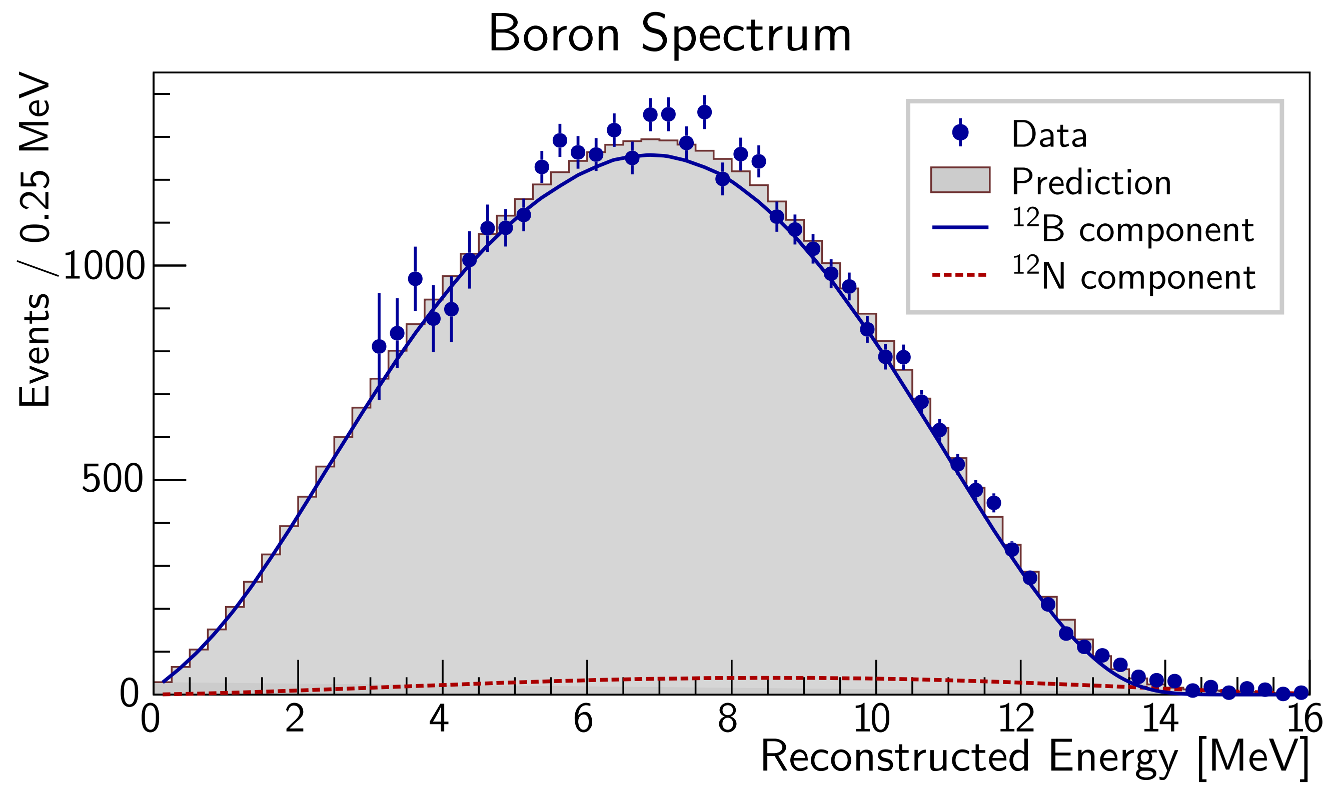

Full detector calibration data

1. Monoenergetic gamma lines from various sources
   - Radioactive calibration sources, employed regularly: ^{68}Ge, ^{60}Co, ^{241}Am-^{13}C and during special calibration periods: ^{137}Cs, ^{54}Mn, ^{40}K, ^{241}Am-^{9}Be, Pu-^{13}C
   - Singles and correlated spectra in regular physics runs (^{40}K, ^{208}Tl, n capture on H)
2. Continuous spectrum from ^{12}B produced by muon spallation inside the scintillator

Standalone measurements

- Scintillator quenching measurements using neutron beams and gamma sources
- Calibration of readout electronics with flash ADC

Energy Response: Cross-Checks

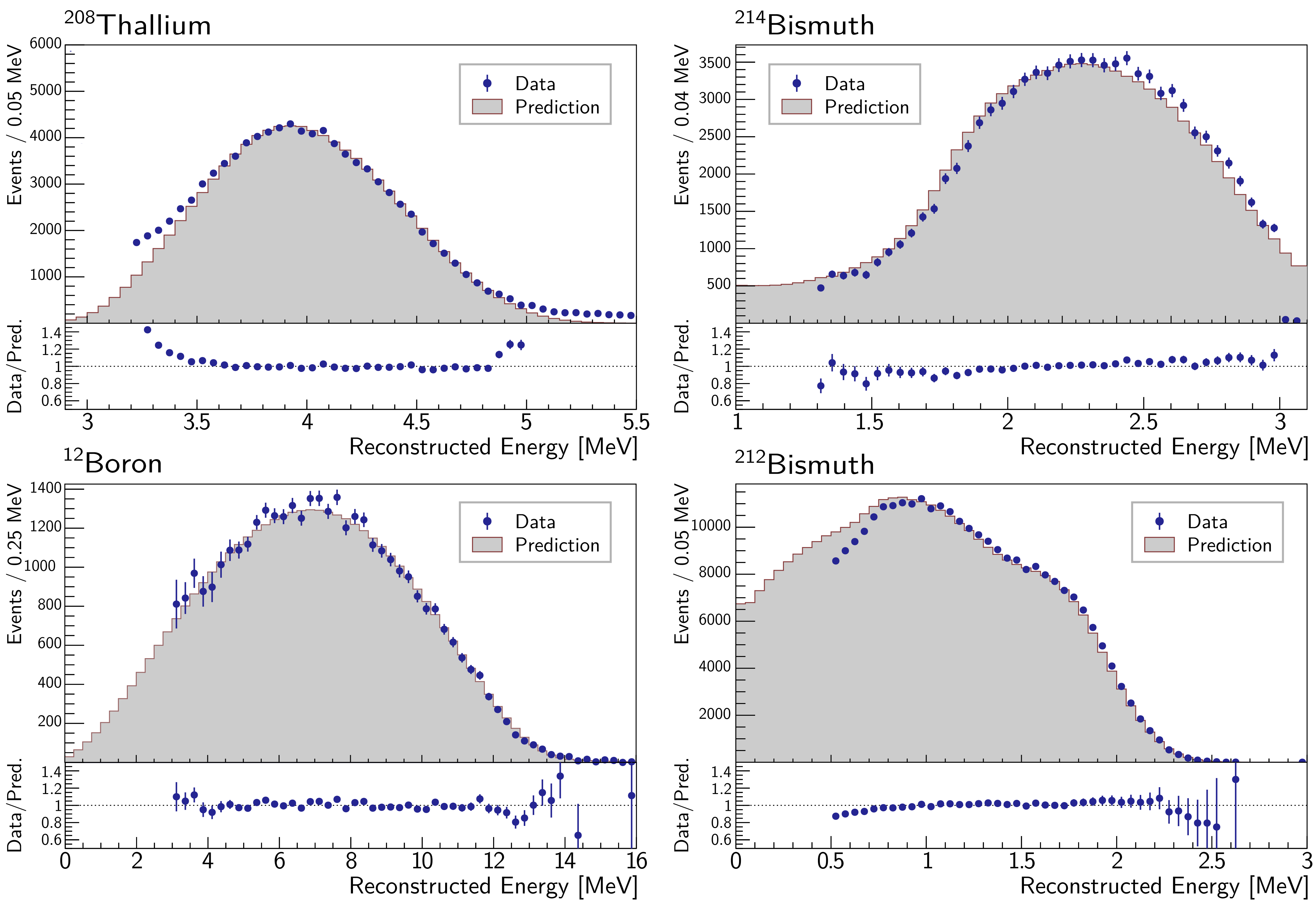

Additional spectra from ^{212}Bi, ^{214}Bi and ^{208}Tl decays

- Sizable theoretical uncertainties from 1st forbidden non-unique beta decays
- ^{212}Bi, ^{214}Bi and ^{208}Tl spectra only utilized to cross-check results

Energy Response: Final Positron Model

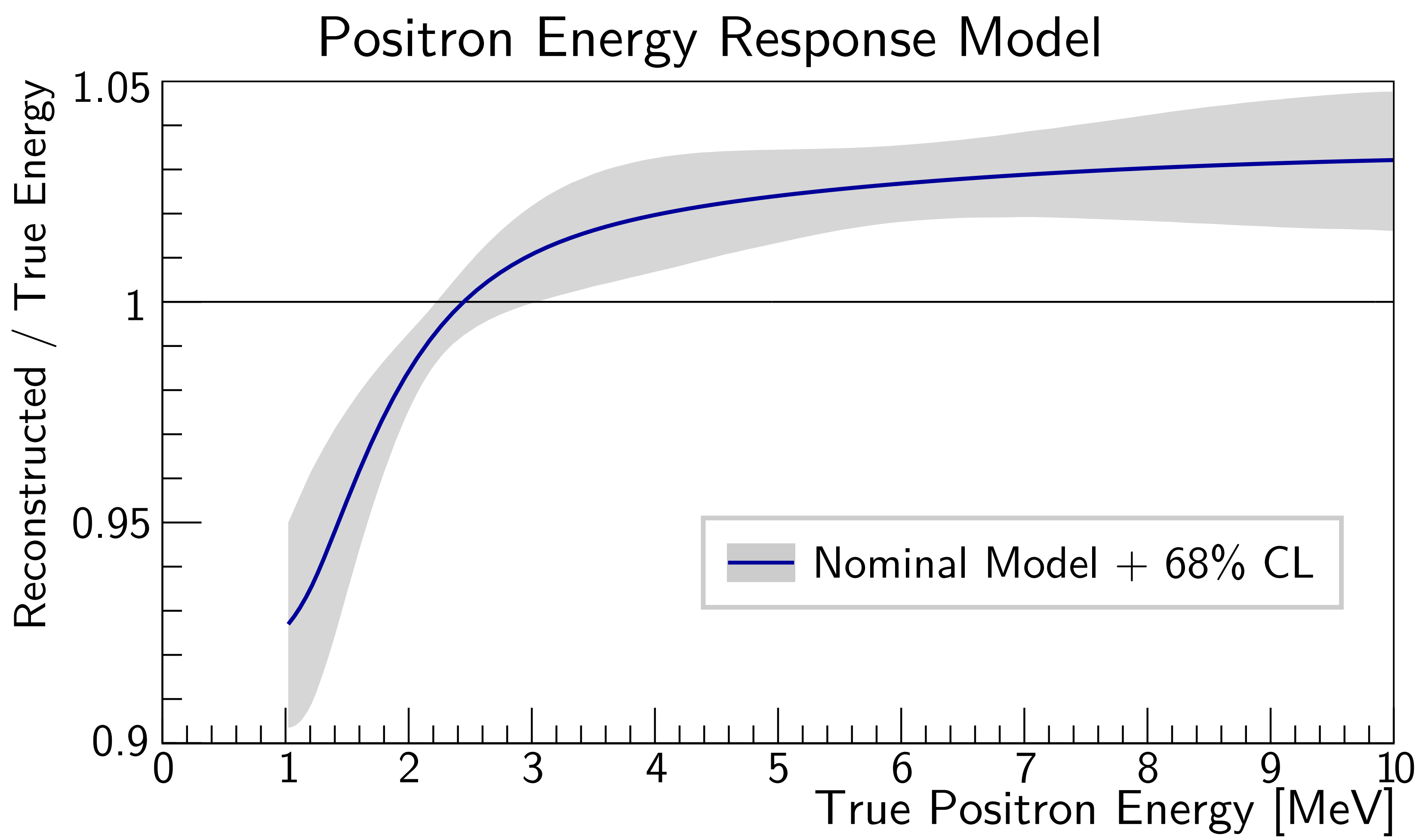

Combination of 5 models to conservatively estimate uncertainty

- Models selected so that
  1. Correlations are minimized
  2. All remaining validated curves with their uncertainties are included in resulting 68% confidence interval
- Nominal: method 1 with empirical scintillator model + exponential electronics
- **Choice of nominal model has negligible impact on oscillation result**

Detector Resolution

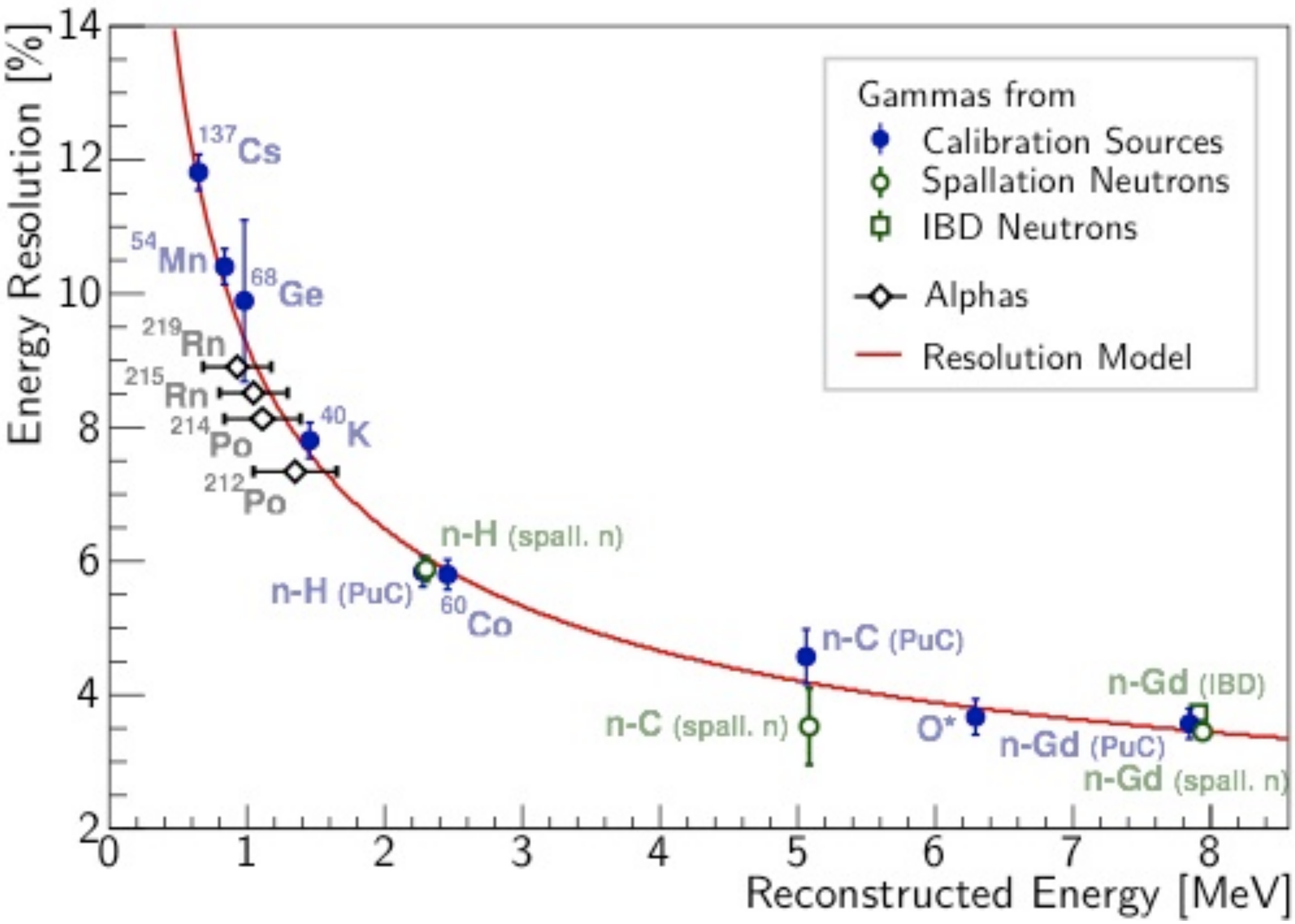

Functional form:

$$\frac{\sigma_E}{E} = \sqrt{a^2 + \frac{b^2}{E} + \frac{c^2}{E^2}}$$

Contributions from:

- a : Spacial/temp. resolution ($\propto$E)
- b : Photon statistics ($\propto\sqrt{E}$)
- c : Dark noise (const:)

Calibrated primarily using monoenergetic gamma sources

- Radioactive calibration sources placed at the detector center
- Additional data from IBD and spallation neutrons, uniformly distributed in LS
- Alpha source data used to cross-check result
  - ➢ Larger uncertainties due to different response from electronics

Backgrounds: Accidentals

- Largest contributor to background rates: two uncorrelated detector triggers passing all selection cuts: 4% (1%) B/S at near (far) sites

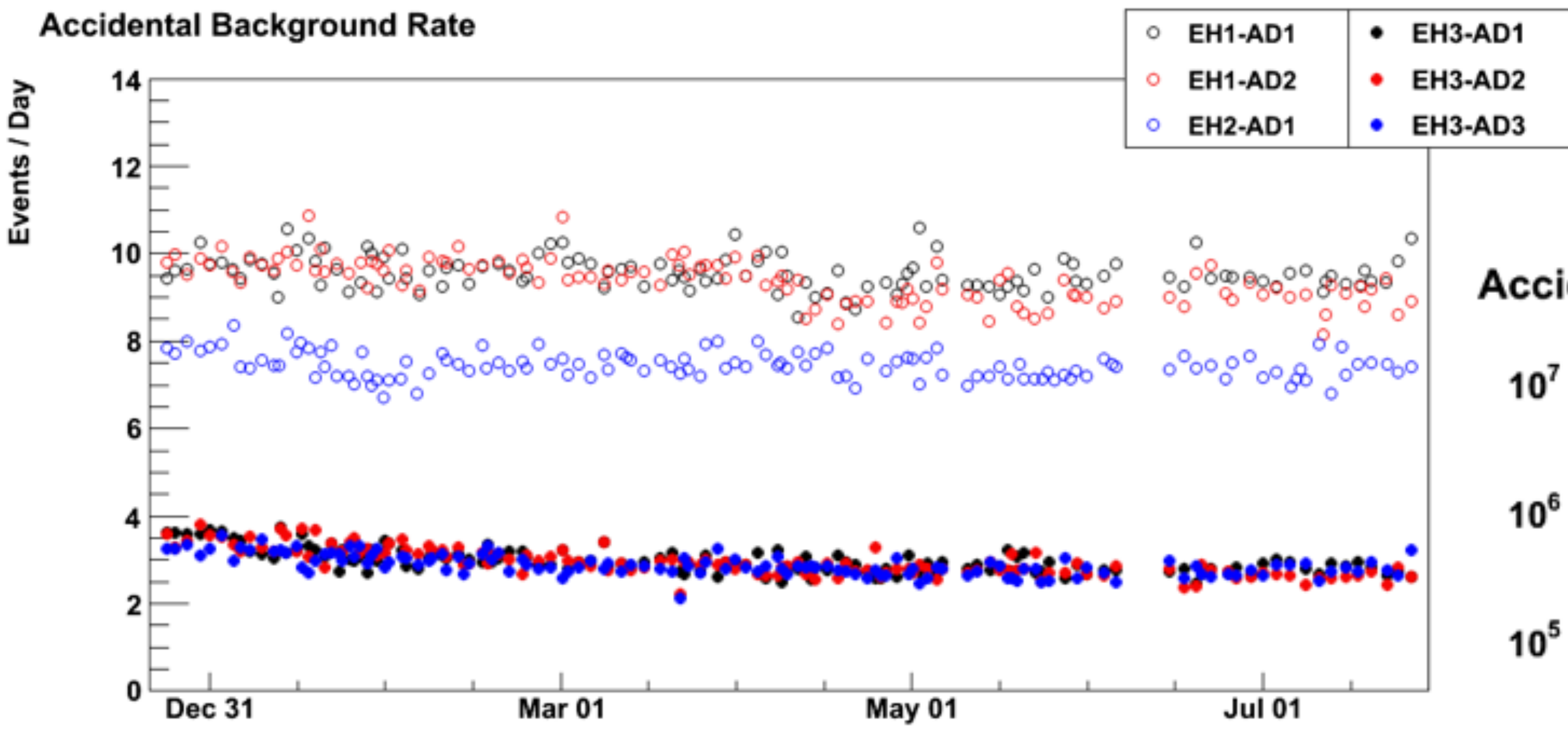

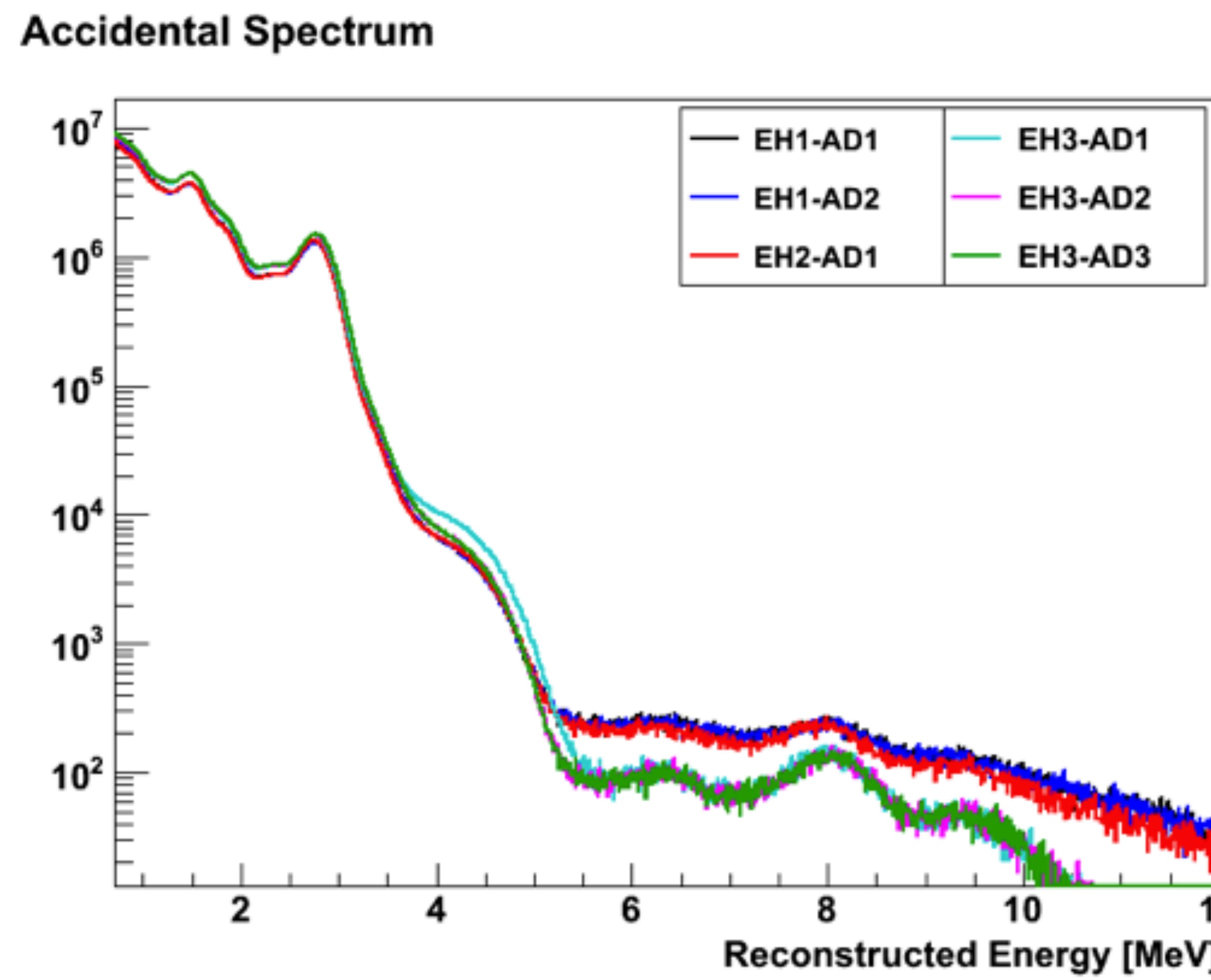

- Accidentals rate, spectrum statistically calculated with excellent precision using rate and spectrum of single triggers

Backgrounds: AmC Source

- Minor low-energy background from AmC neutron calibration sources: ~0.3% B/S
- Contribution to total rate, spectrum calculated using detector Monte Carlo
- MC benchmark: measured rate and spectrum of 80x stronger AmC source on top of AD

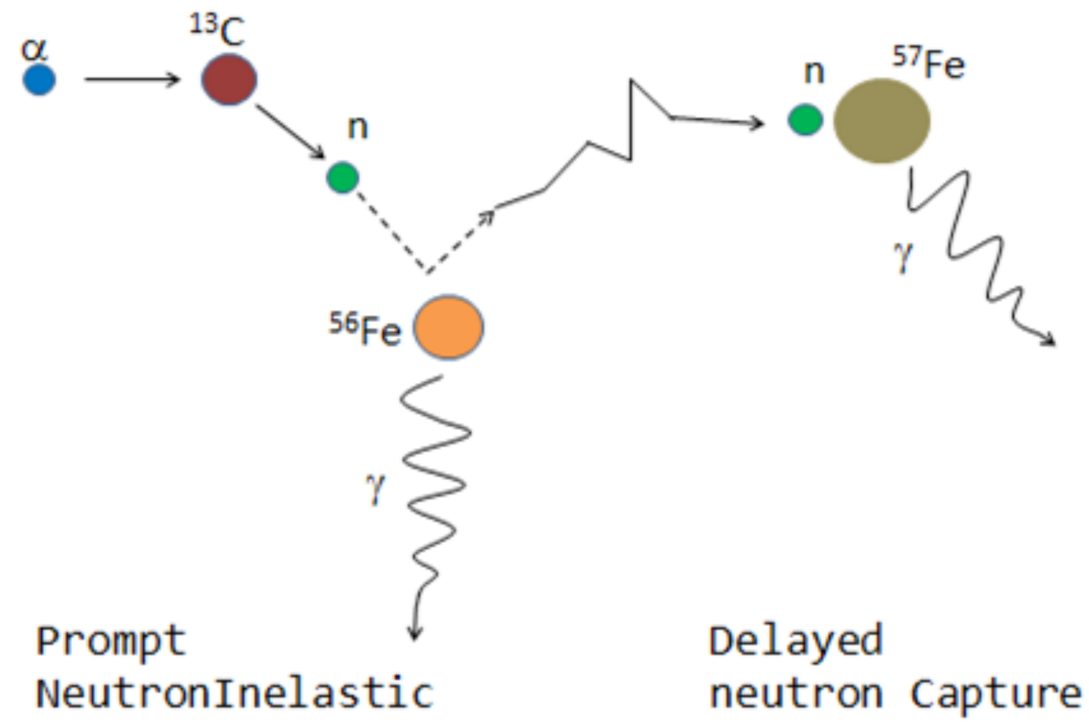

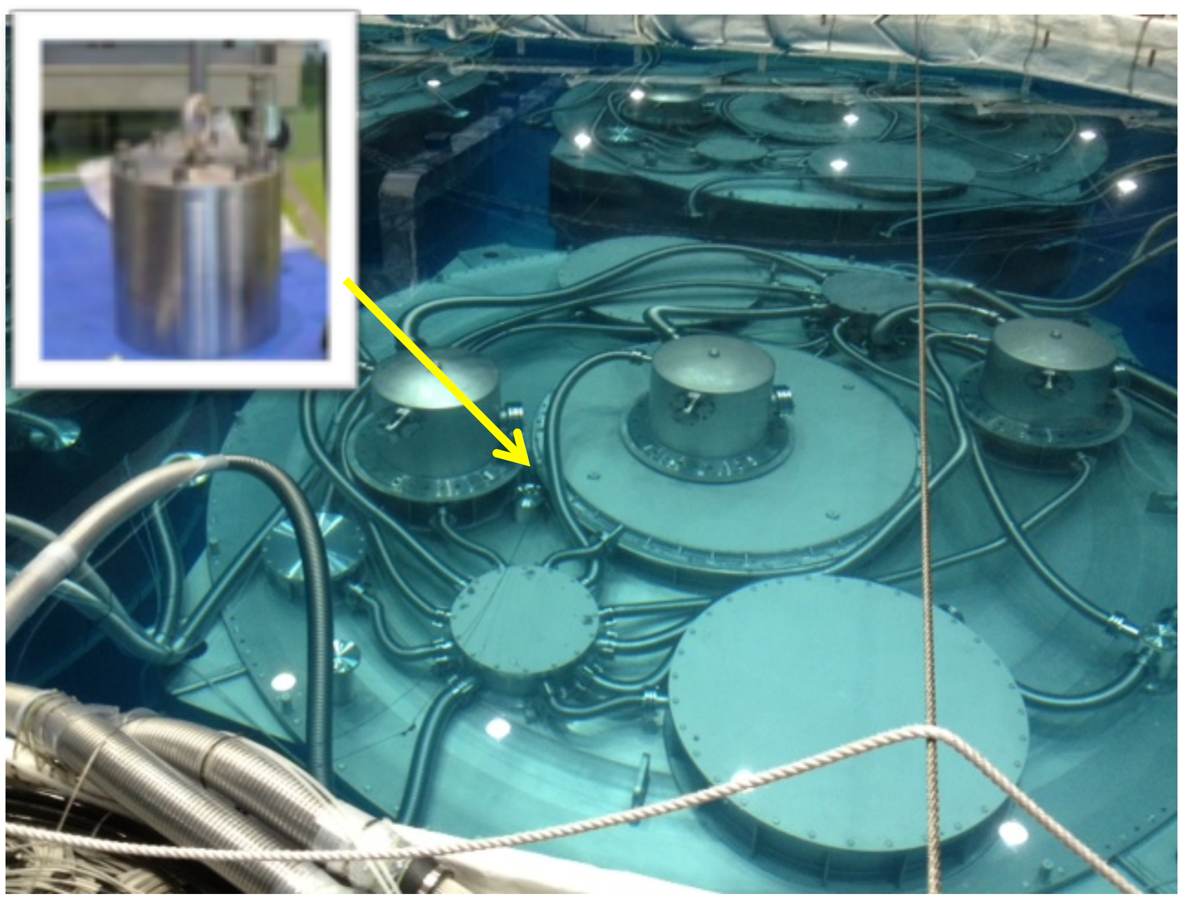

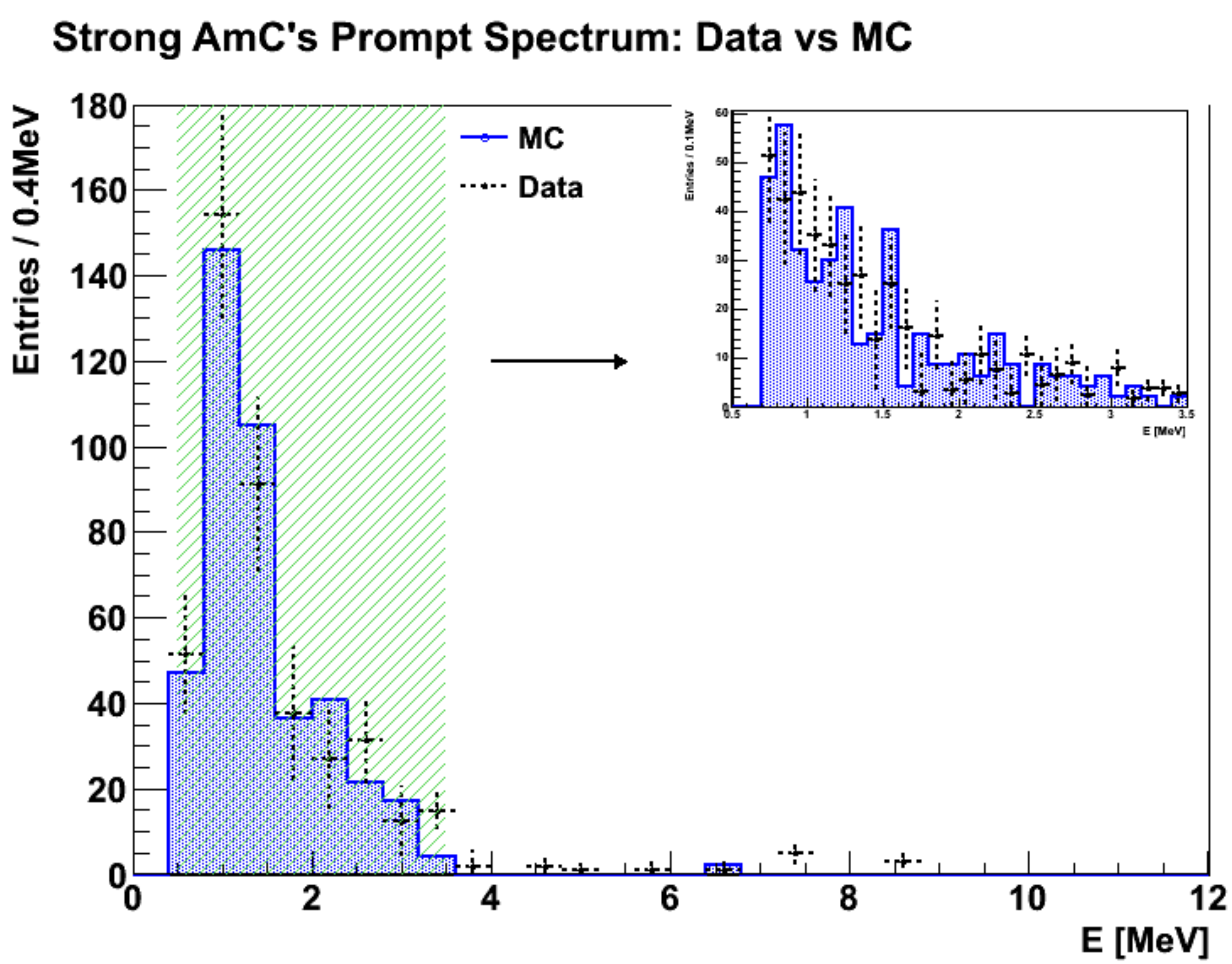

Backgrounds: High Energies

- High-energy backgrounds contributed by spallation: neutrons and beta isotopes
  - Untagged fast neutrons provide estimated 0.1% B/S, with flat spectral shape
  - Unvetoed He-8, Li-9 decays provide 0.3% B/S with spectral shape determined by combining theoretical decay product spectra with detector non-linearity model

β-n decay:

- Prompt: β-decay
- Delayed: neutron capture

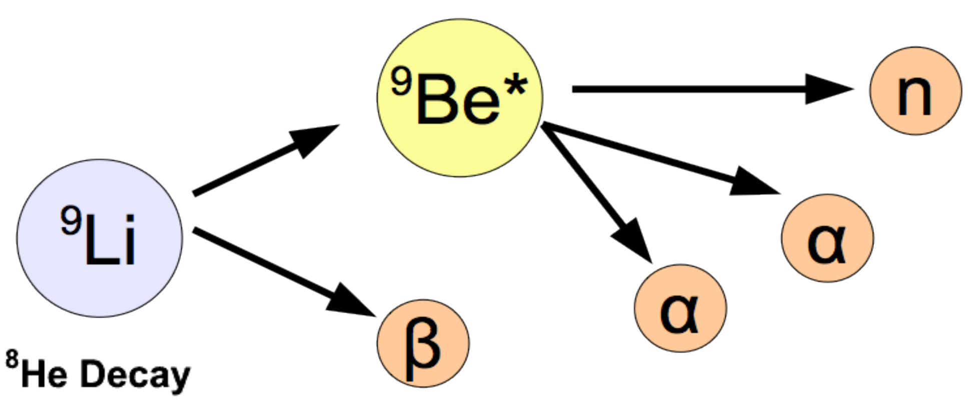

^{9}Li / ^{8}He Decay

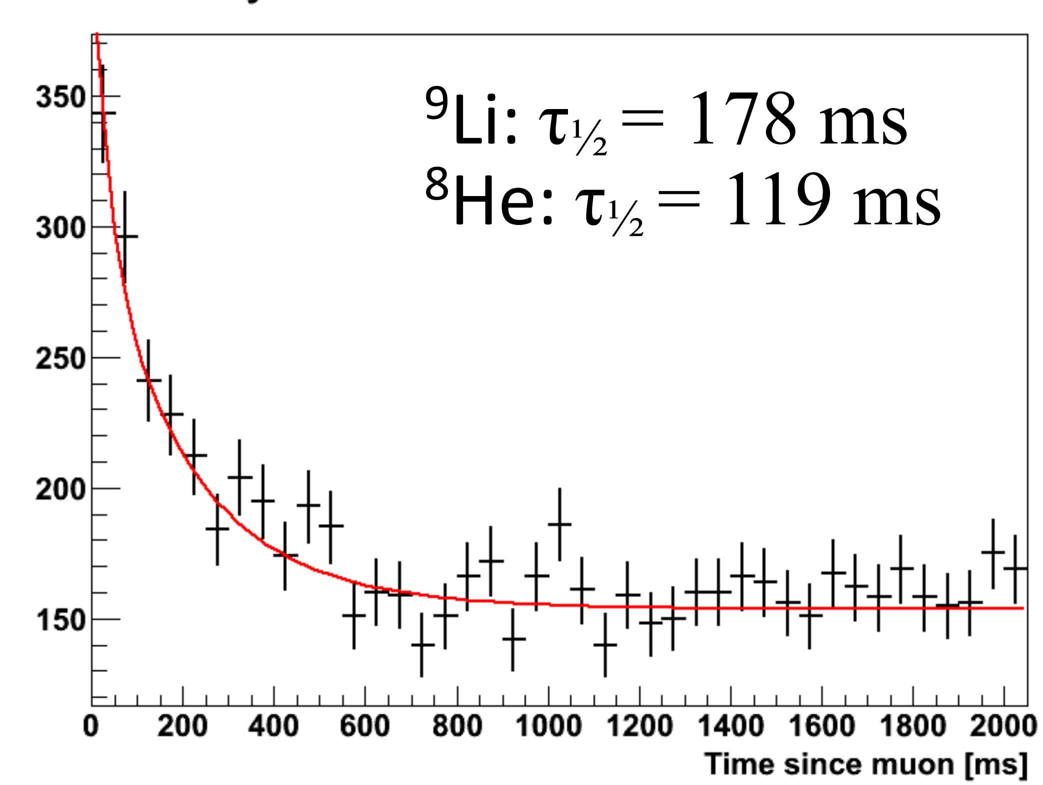

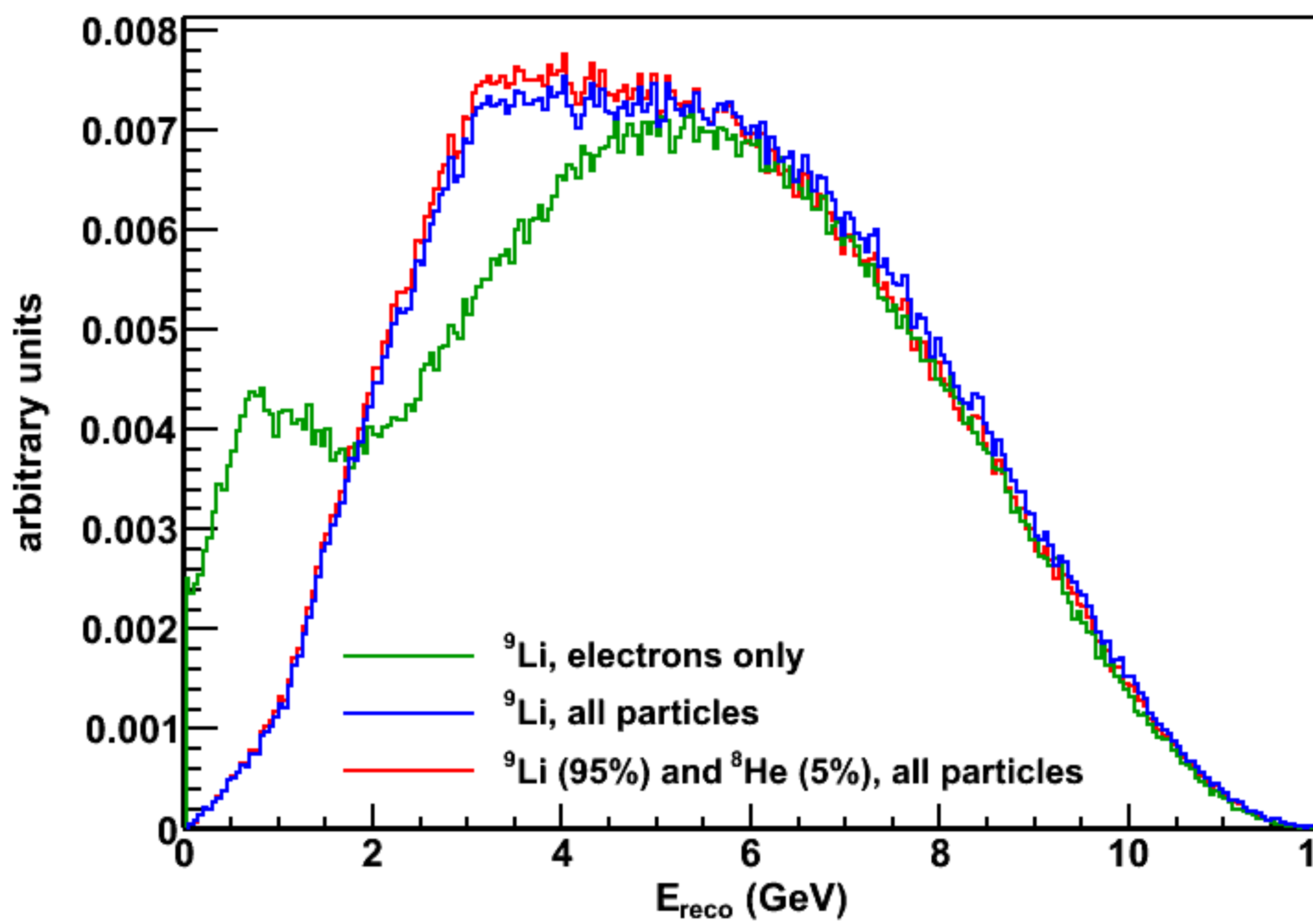

Will eventually provide spectrum of vetoed He-8/Li-9

Rate+Shape Result: Fit Method

$$\chi^2 = \sum_i^{det\times E_p} [N_i^{pred}(\theta_{13},\Delta m^2_{ee},\vec{f},\vec{\eta},\vec{\epsilon},\vec{b}), - N_i^{data} + N_i^{data} \log \frac{N_i^{data}}{N_i^{pred}(\theta_{13},\Delta m^2_{ee},\vec{f},\vec{\eta},\vec{\epsilon},\vec{b})}]$$

$$+ \sum_j^{site\times E_p} \sum_k^{site\times E_p} f_j V_{jk}^{-1} f_k$$ Reactor Flux Model Constraint

$$+ \sum_l^{abs.E} \frac{\eta_l^2}{\sigma_l^2}$$ Energy Model Constraint

$$+ \sum_m^{det\times eff} \frac{\epsilon_m^2}{\sigma_m^2}$$ Detector Efficiency Constraint

$$+ \sum_n^{det\times bg} \frac{b_n^2}{\sigma_n^2}$$ Background Constraint

- Binned maximum likelihood method
- Constrained reactor flux model using covariance matrix approach
- Constrained background and detector uncertainties with pulls, nuisance terms
- No constraint on absolute rate

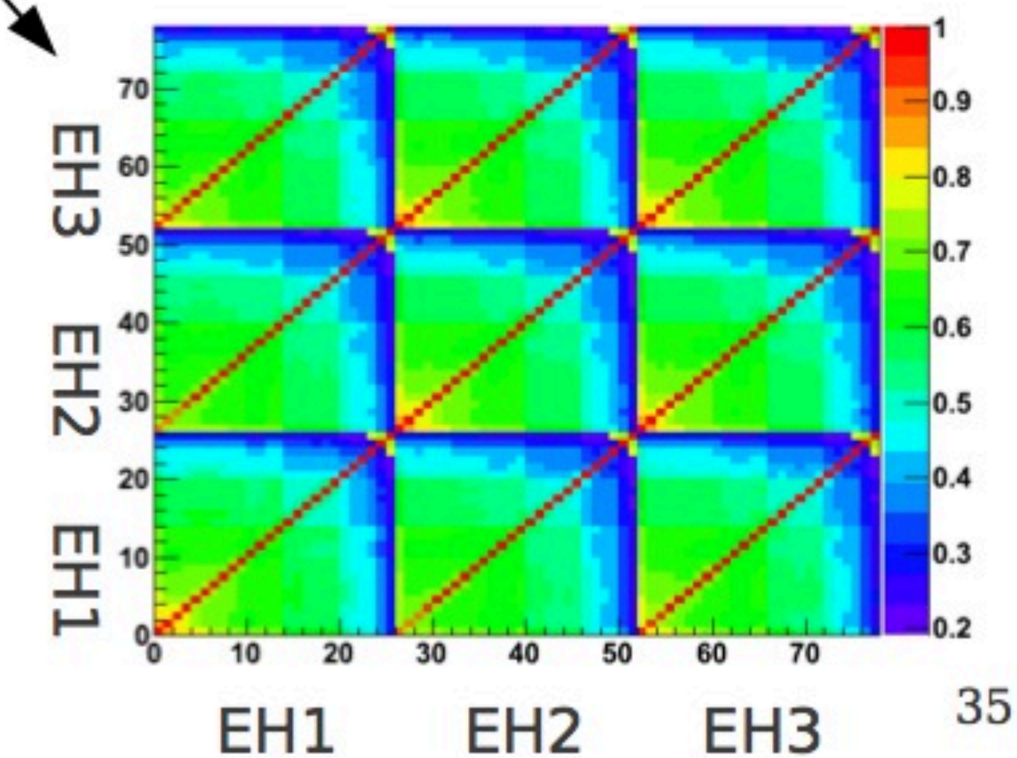

Rate+Shape Result: Prompt Spectra

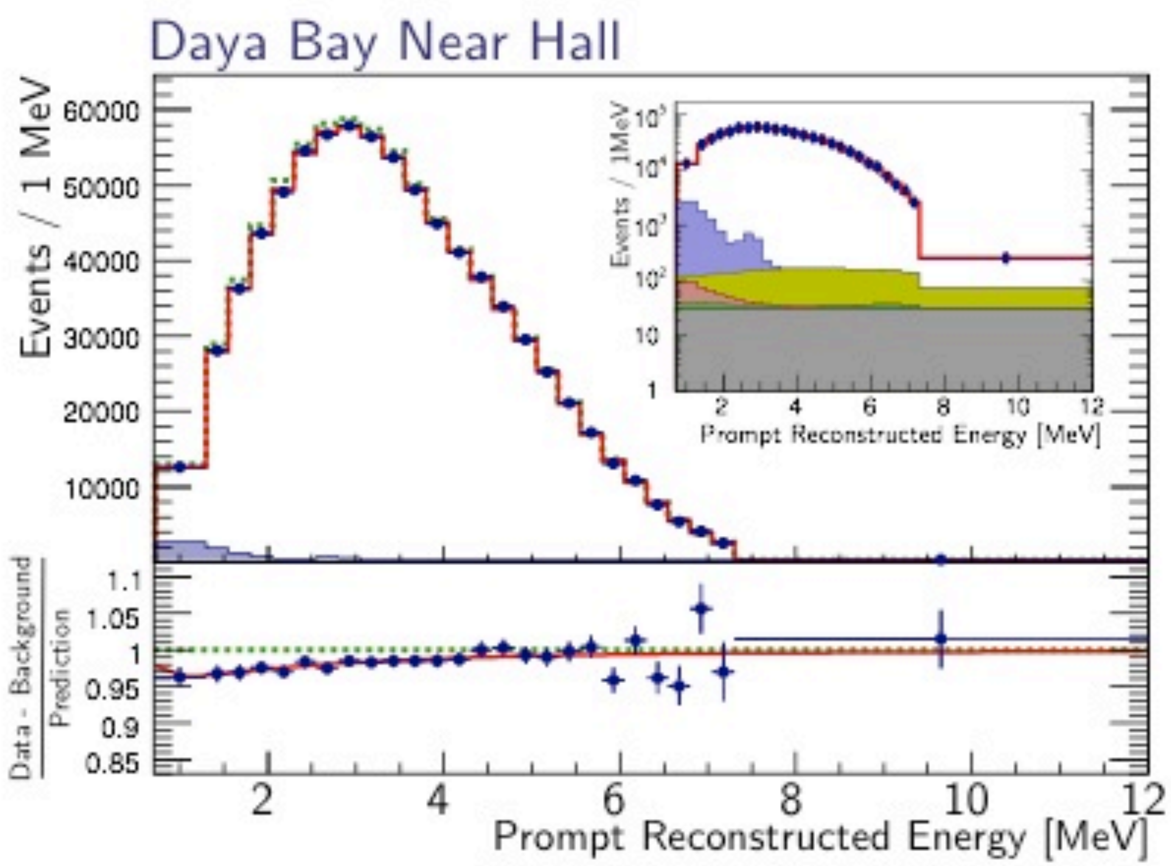

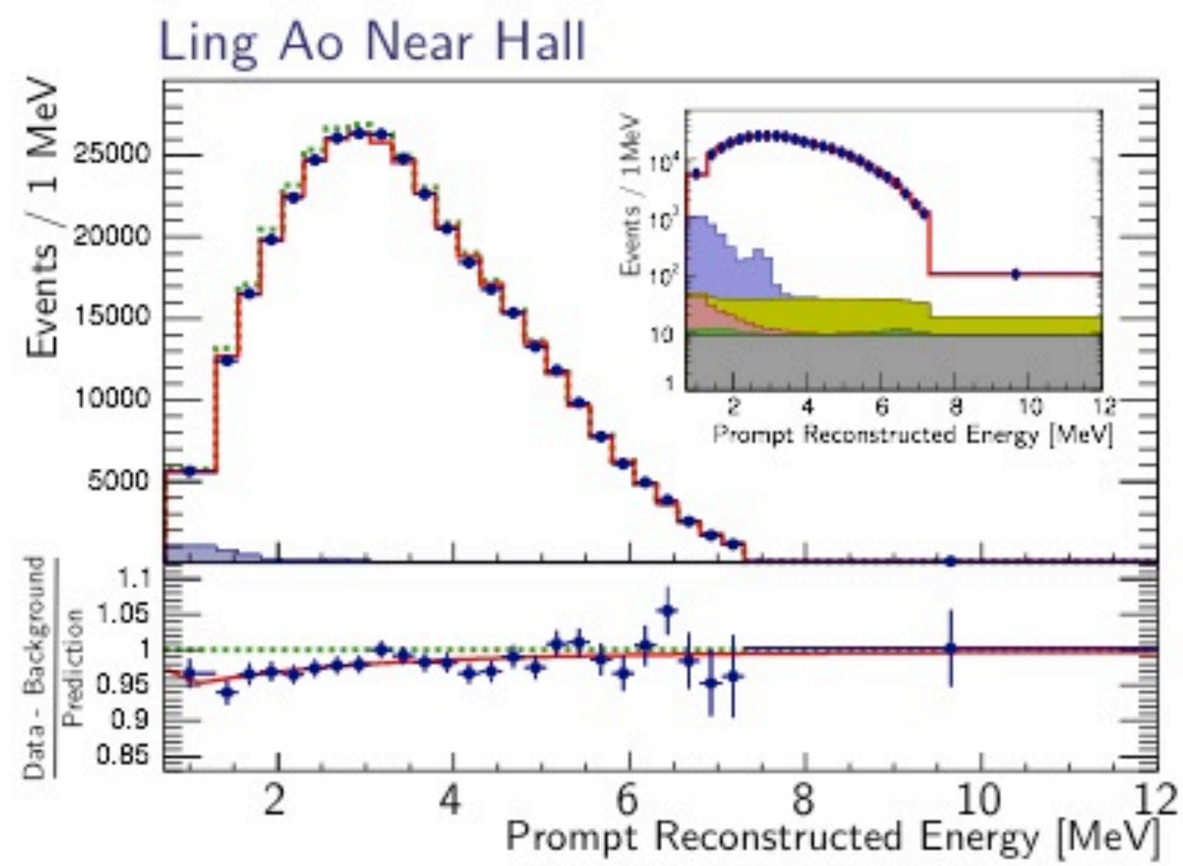

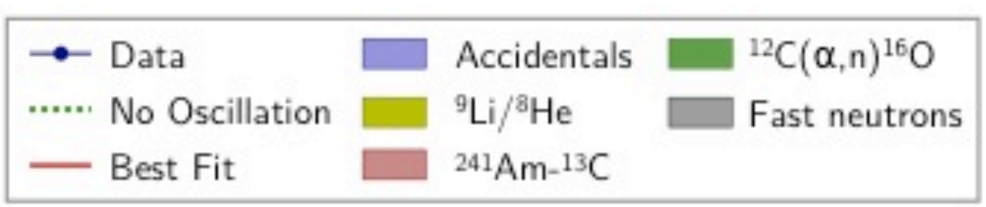

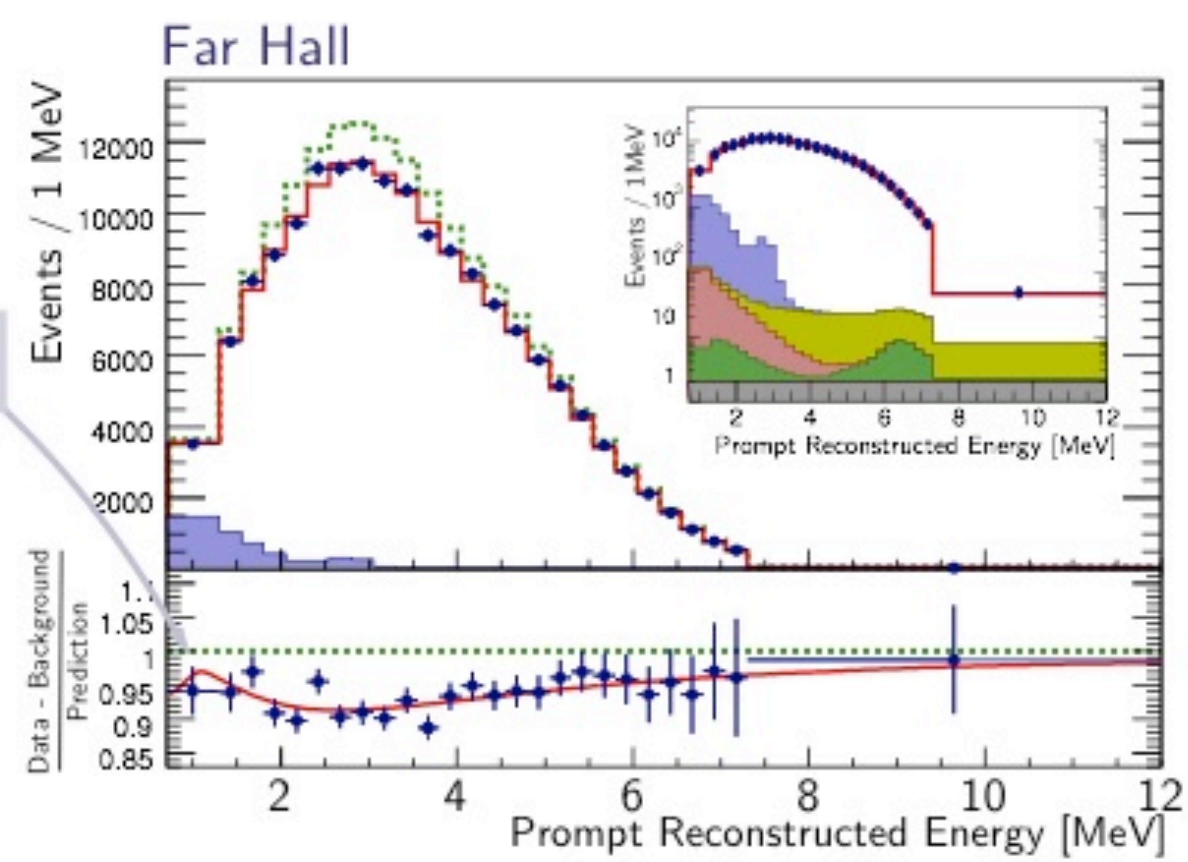

Shape distortion from energy losses in acrylic

Spectral distortion consistent with oscillation

- Both background and predicted no oscillation spectrum determined by best fit
- Errors statistical only

Rate+Shape Result: Oscillation Parameters

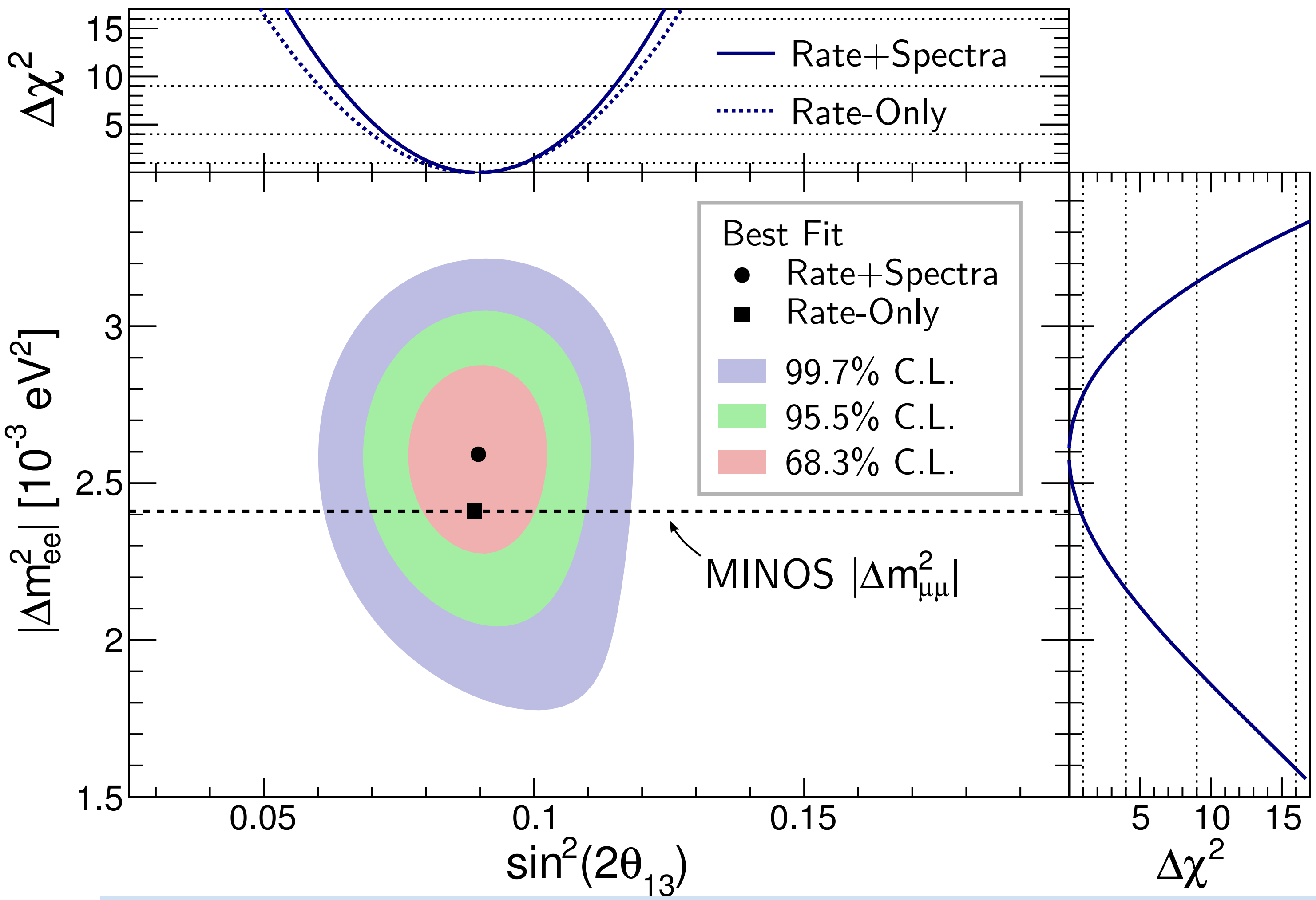

$$\sin^2 2\theta_{13} = 0.090^{+0.008}_{-0.009}$$

$$|\Delta m^2_{ee}| = 2.59^{+0.19}_{-0.20} \cdot 10^{-3}\mathrm{eV}^2$$

$$\chi^2/N_{\mathrm{DoF}} = 162.7/153$$

Strong confirmation of oscillation-interpretation of observed ν_e deficit

	Normal MH Δm^2_{32} [10^{-3}eV^2]	Inverted MH Δm^2_{32} [10^{-3}eV^2]
From Daya Bay Δm^2_{ee}	$2.54^{+0.19}_{-0.20}$	$-2.64^{+0.19}_{-0.20}$
From MINOS $\Delta m^2_{\mu\mu}$	$2.37^{+0.09}_{-0.09}$	$-2.41^{+0.11}_{-0.09}$

A. Radovic, DPF2013

Rate+Shape Result: Cross-Checks

- Performed independent fits using differing fit methods:
  - Pure X^2 covariance matrix approach: use near site spectrum to predict far site
  - Pure pulls-approach X^2 approach
  - All agree well within uncertainties

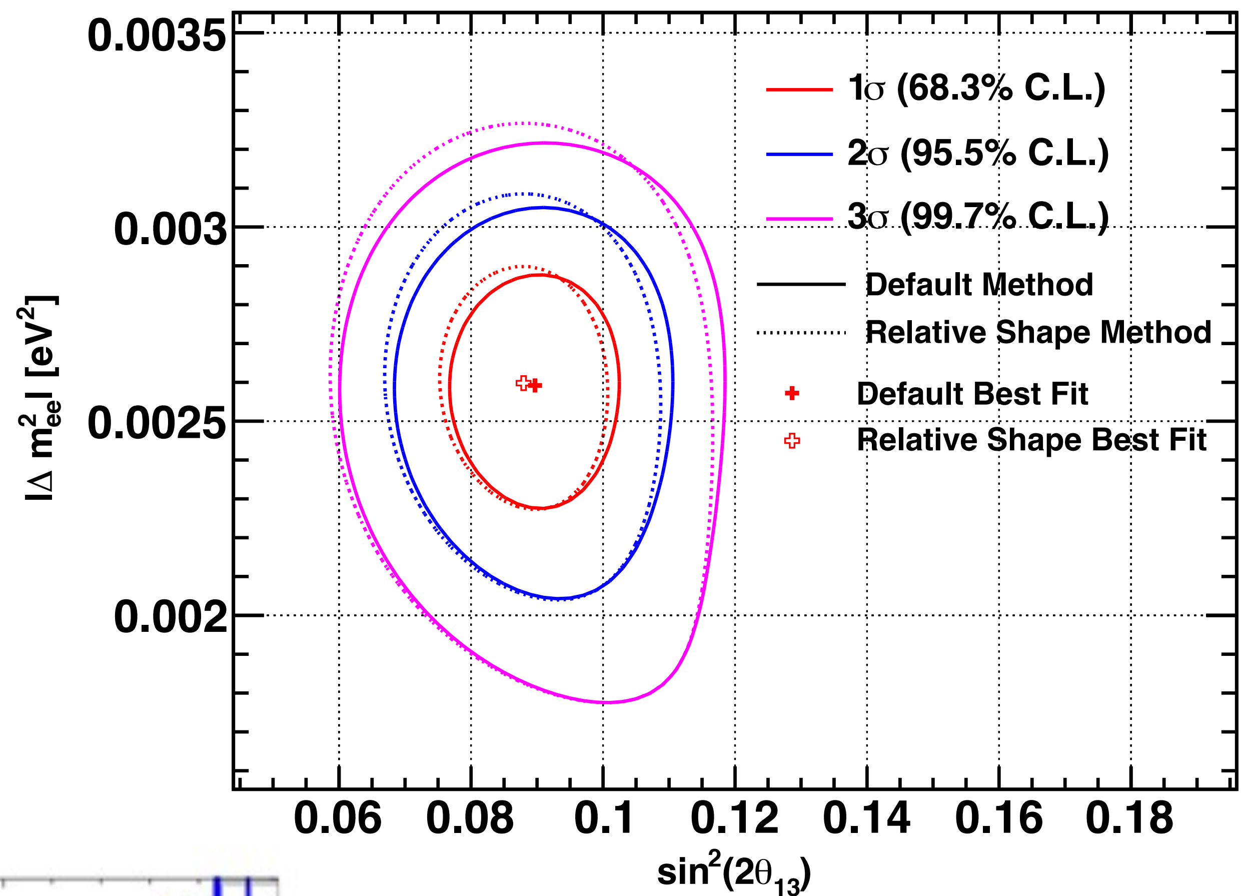

- Fits utilizing differing reactor models yield identical results
  - Vogel (U-238) + ILL (others)
    PRD 39, 1989 Phys Lett: **B218** (1989) Phys Lett **B160** (1985) Phys Lett: **B118** (1982)
  - French(U-238) + Huber (others)
    PRC 83, 2011 PRC 84, 2011

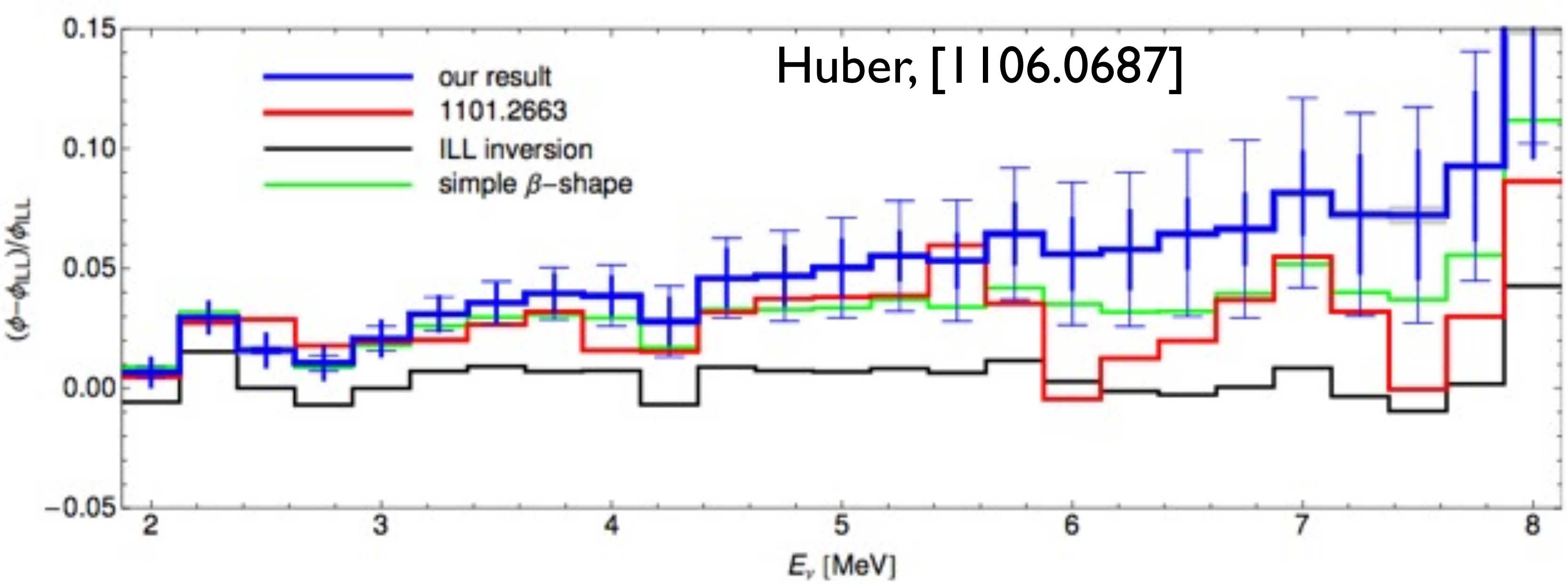

θ_{13} Landscape

Daya Bay remains the most precise of numerous largely consistent θ_{13} measurements

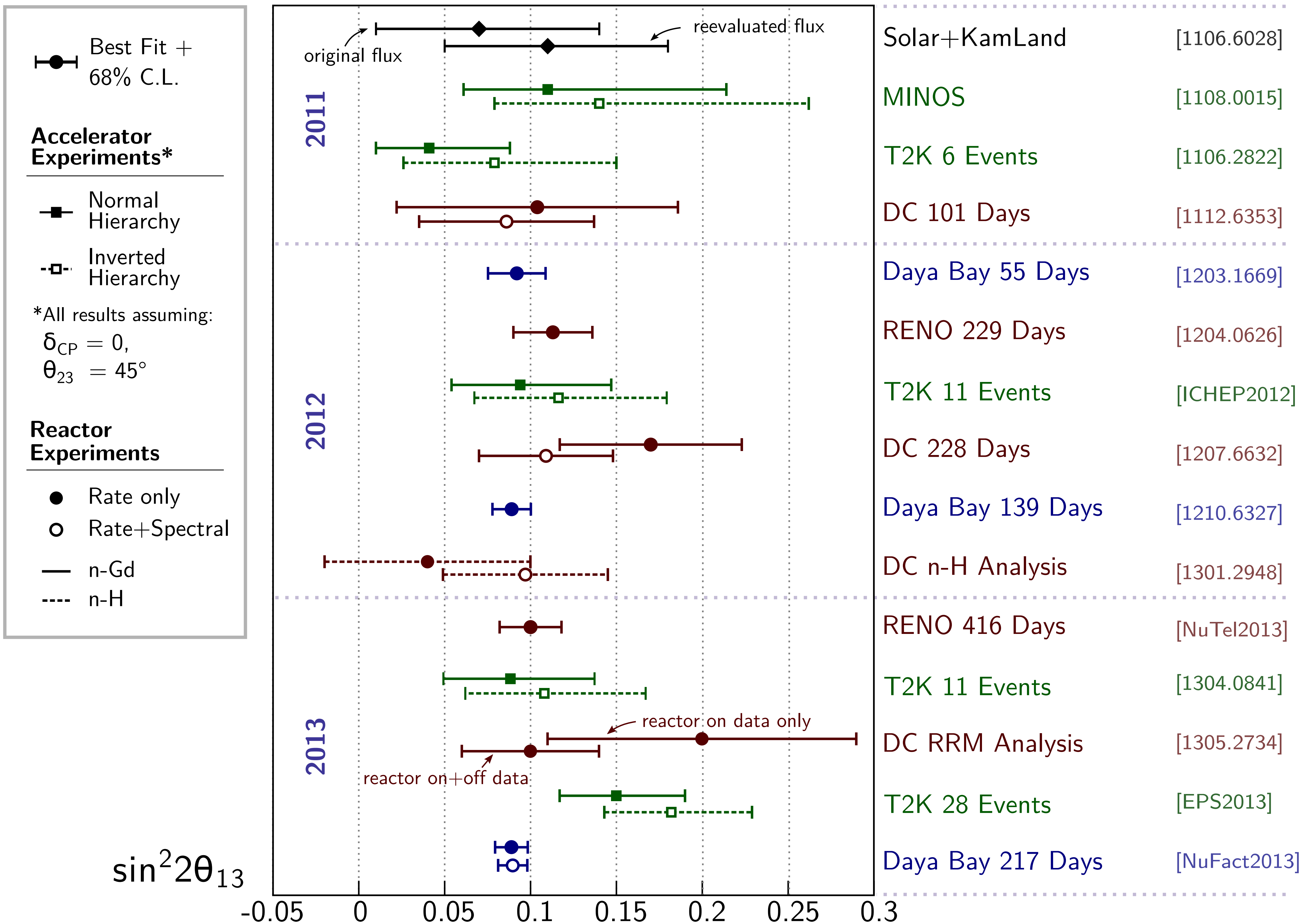

Looking Forward: Impacts of Large θ_{13}

- Many flavor symmetry models and GUTs predicting neutrino oscillation parameters are ruled out by large θ_{13}

Flavor Symmetries

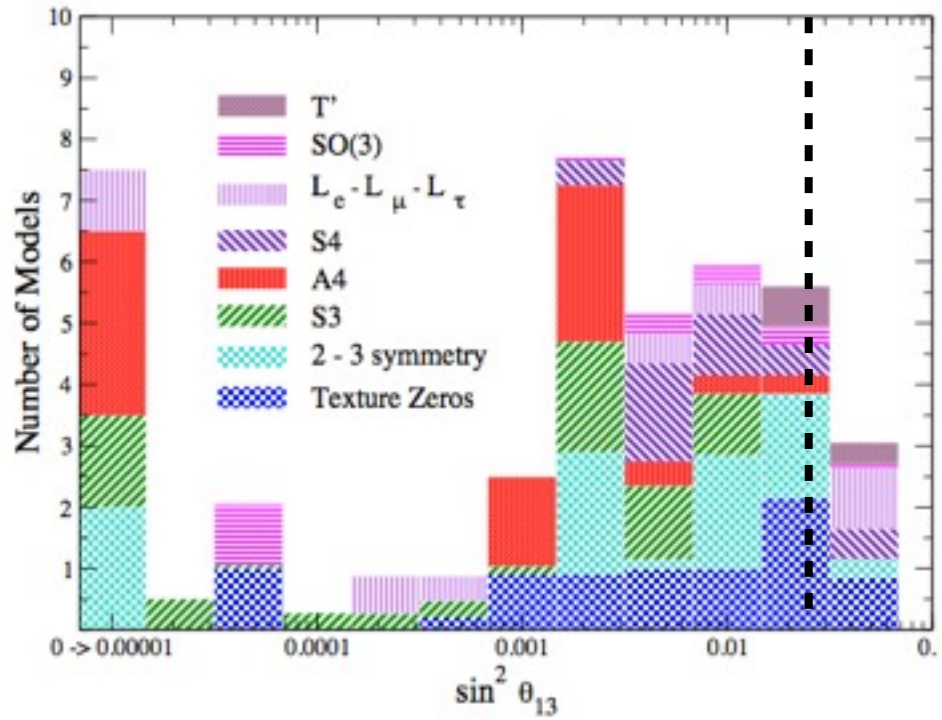

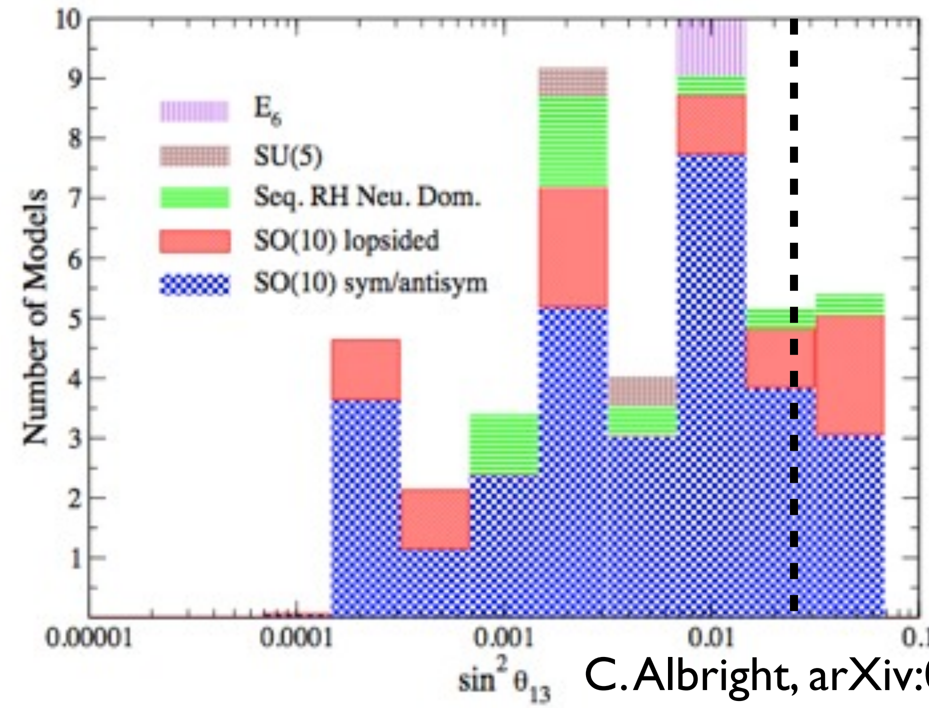

GUTs

C. Albright, arXiv:0911.2437v1 (2009)

- Prospects for mass hierarchy and δ_{cp} are greatly improved

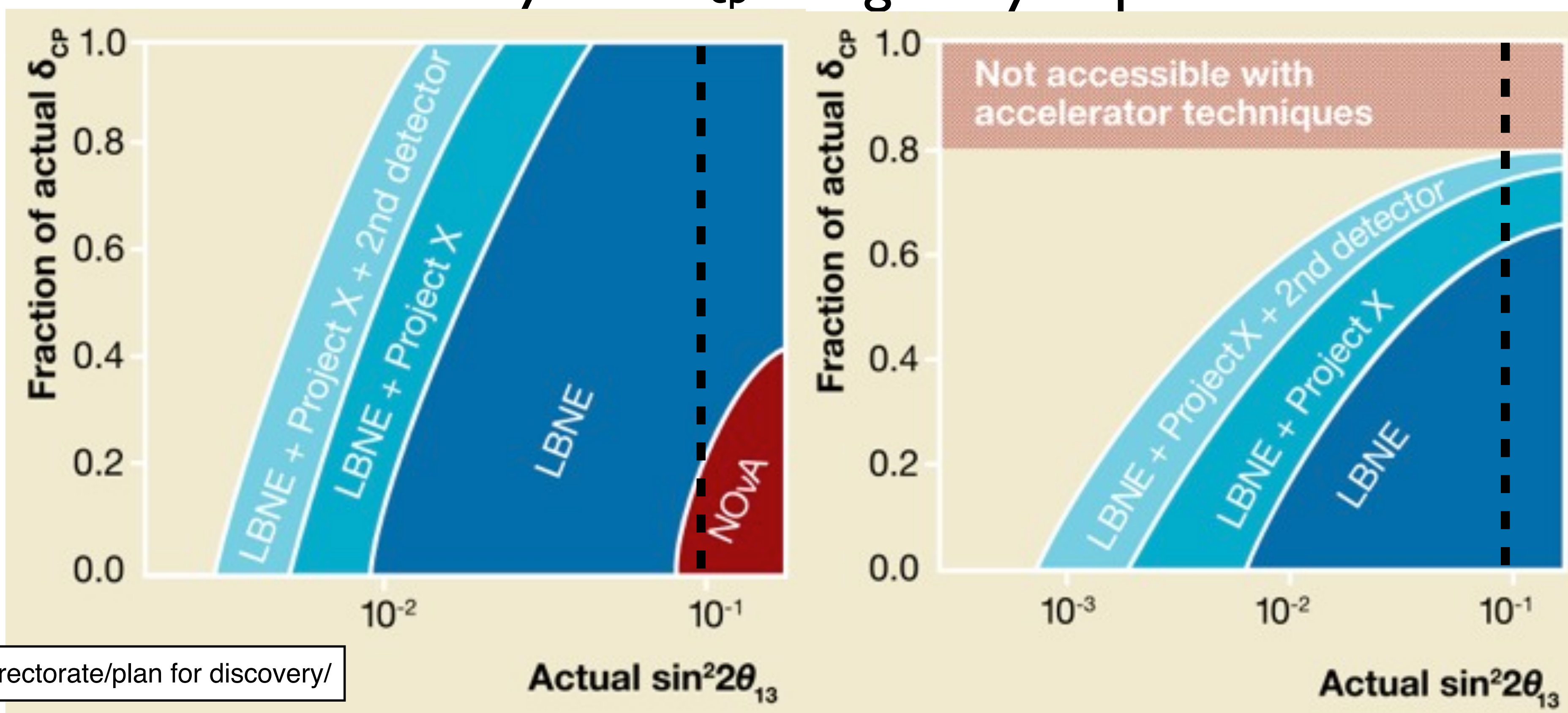

http://www.fnal.gov/directorate/plan for discovery/

42

Looking Forward: On-Site

Final two detectors installed, operating since Oct. 2012.

EH2

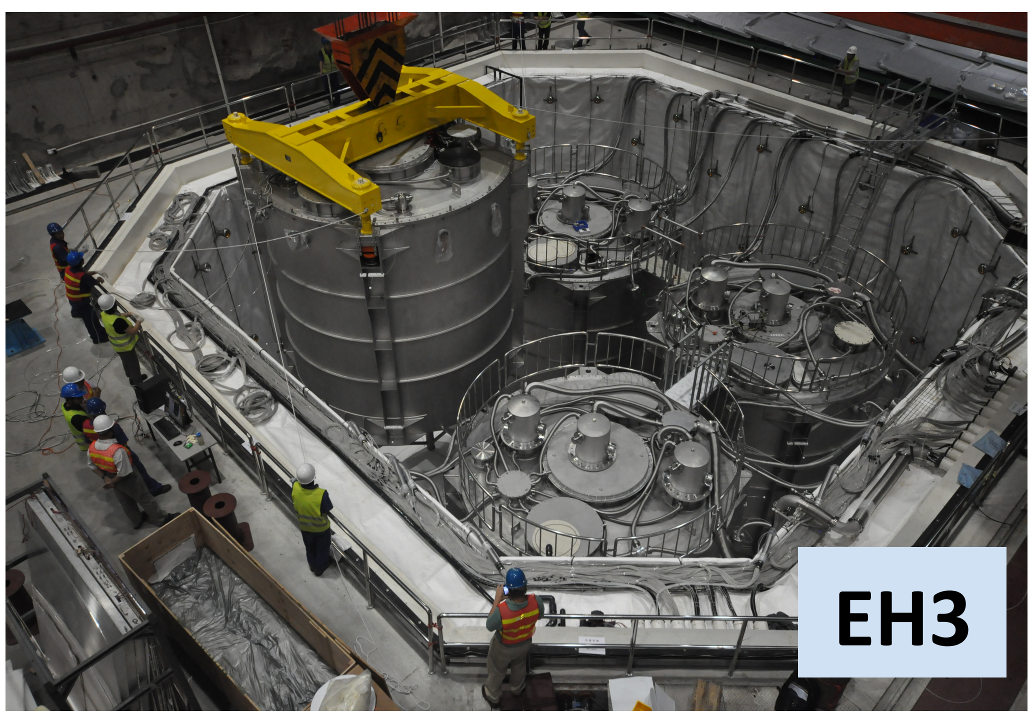

EH3

Full 4π detector calibration in Sep. 2012.

Have many months of 8-AD data in the can; data-taking continues

Looking Forward: Oscillation Sensitivity

- Sensitivity to oscillation parameters continues to improve

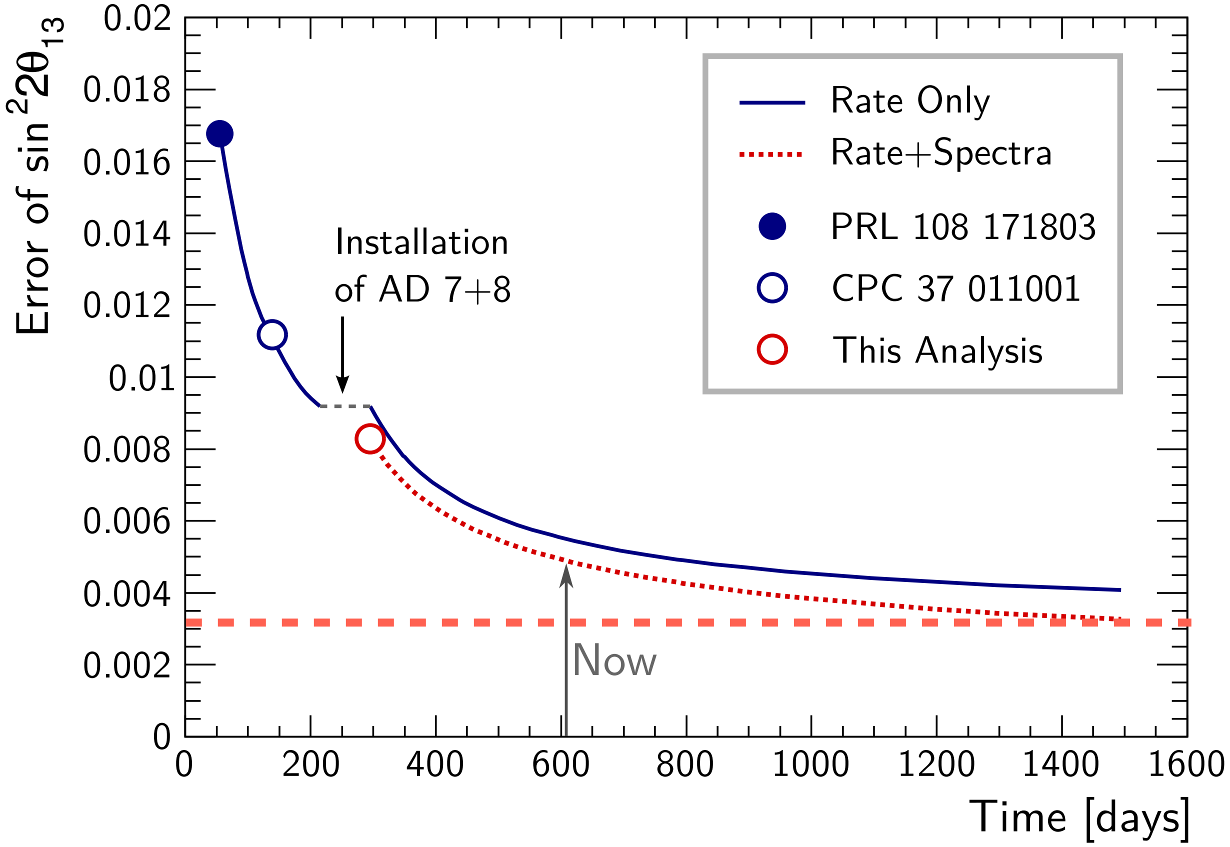

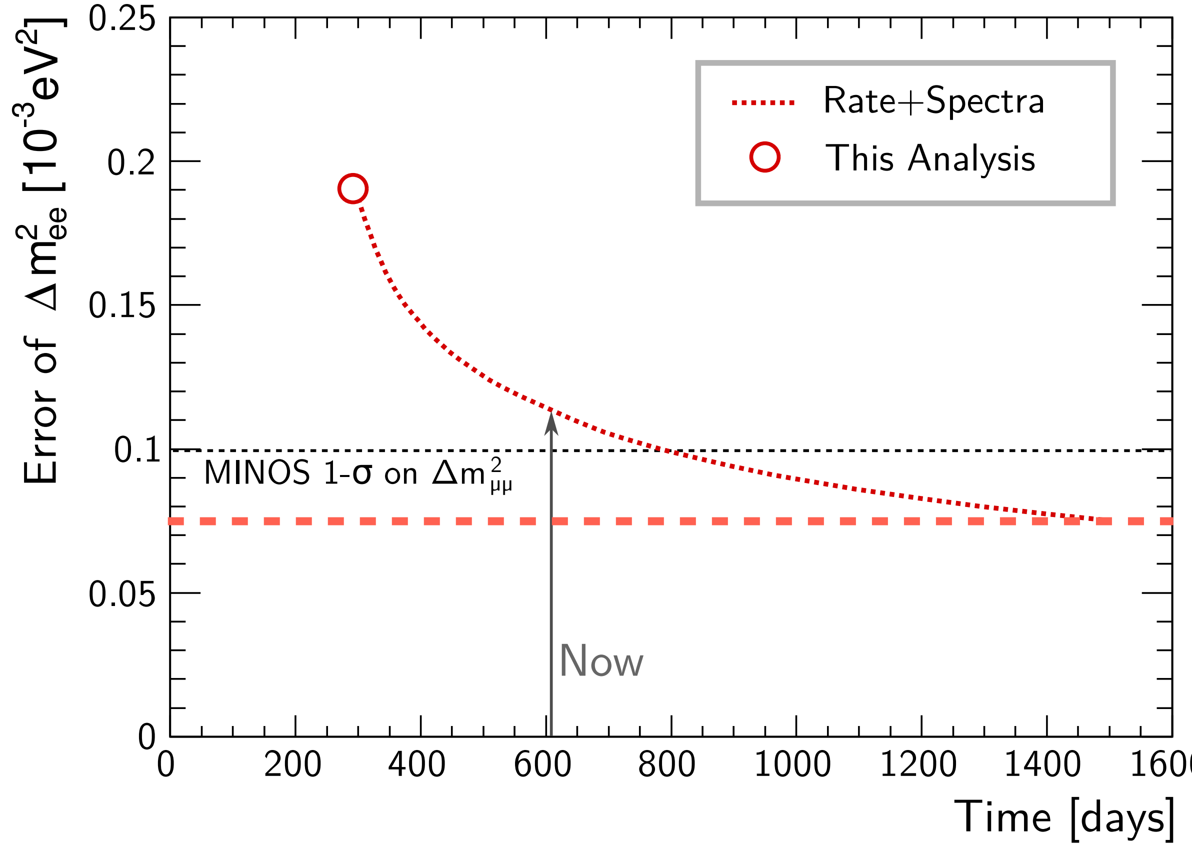

- From statistics alone, precision will improve by over a factor of two by the end of data-taking
- Further reduction of relative energy scale uncertainty seems likely
- Absolute energy response model will likely also see improvements in precision

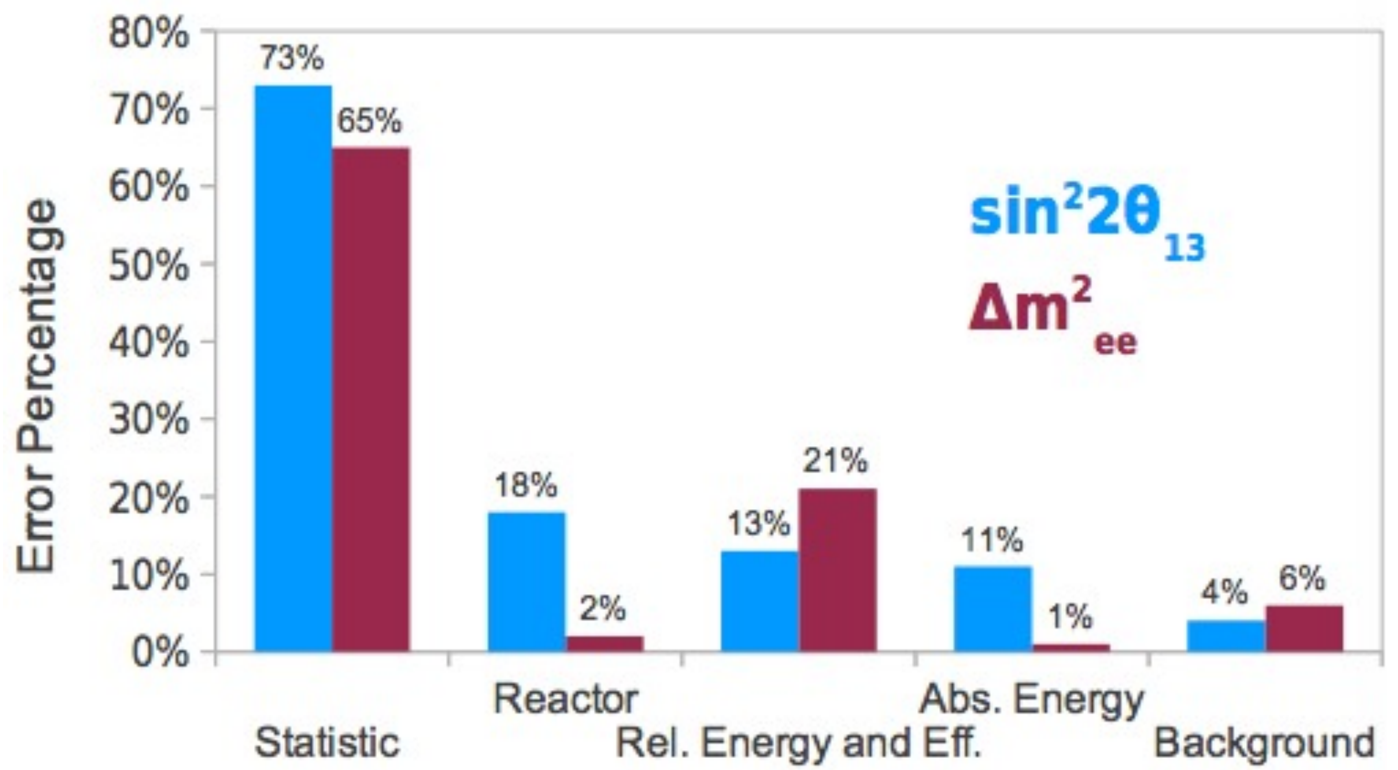

Looking Forward: Global Impacts

- Precision of θ_{13} improves ability to measure CP violation, mass hierarchy in future experiments

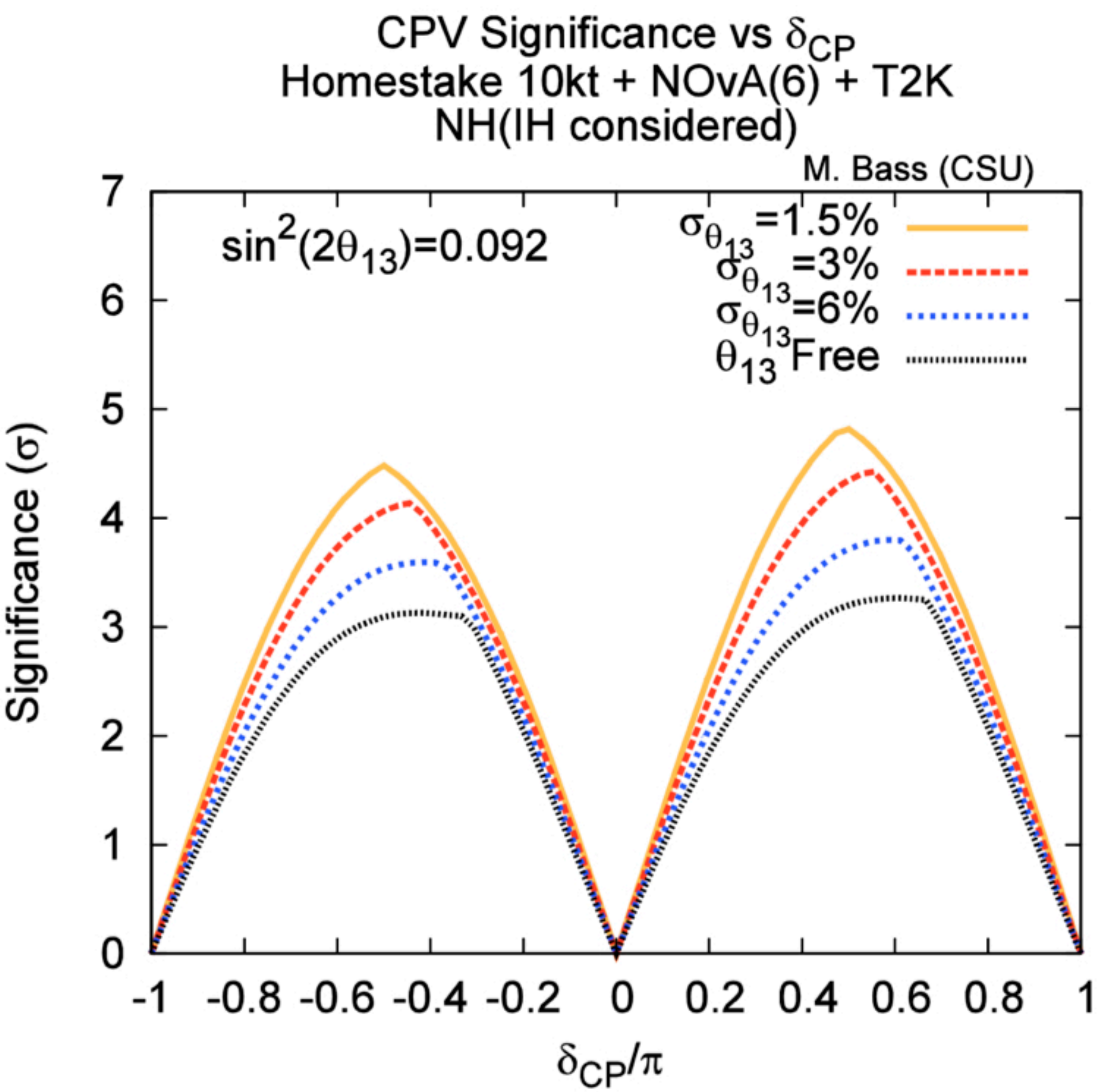

Demonstration of predicted CPV ranges given input uncertainties on mixing angles

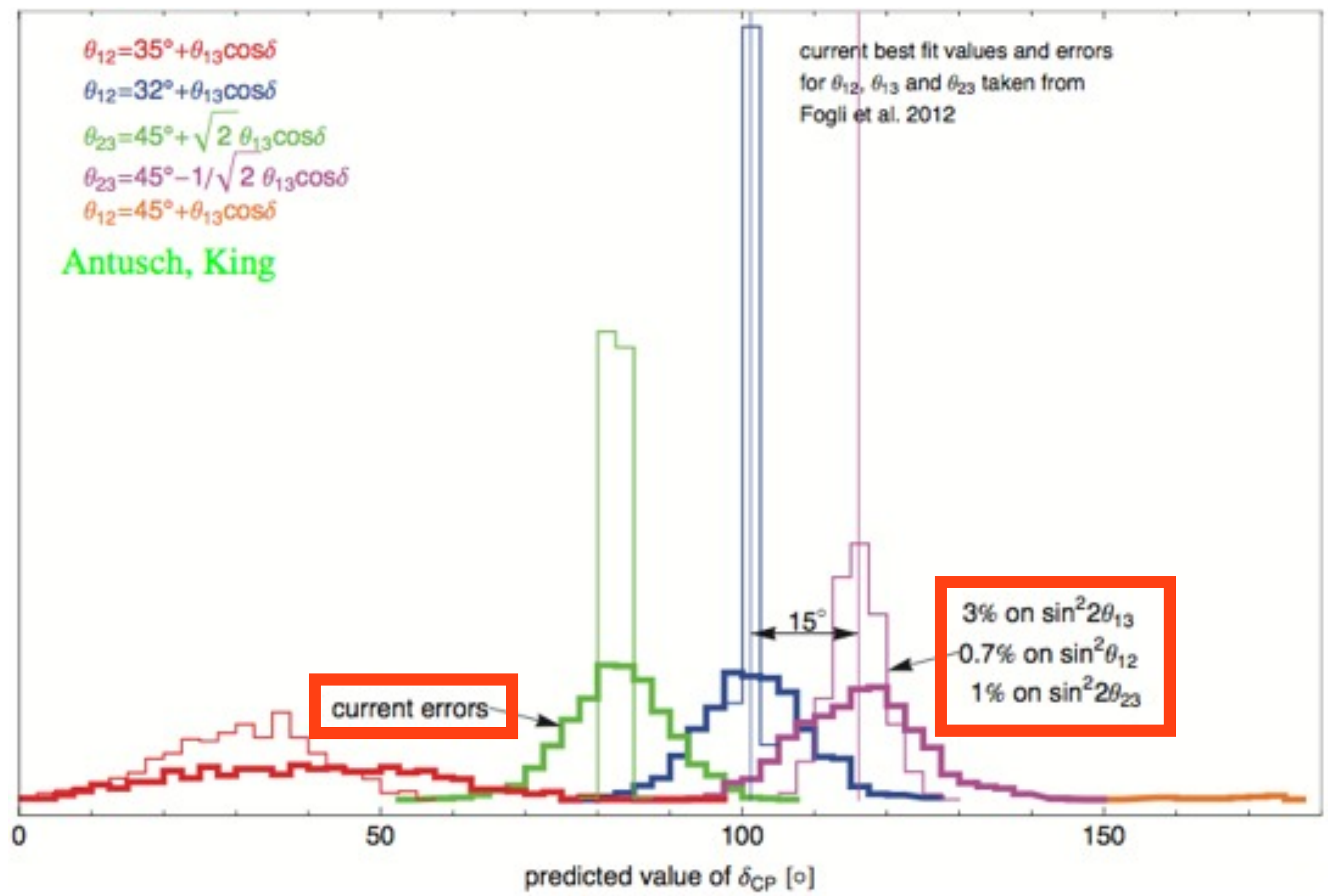

Looking Forward: Absolute Flux

- By measuring absolute flux at near site reactors, can provide some additional insight on reactor anomaly
  - Currently hammering out absolute efficiency systematics
  - Ultimate uncertainty limiter comes from nuebar per fission: ~2-3%

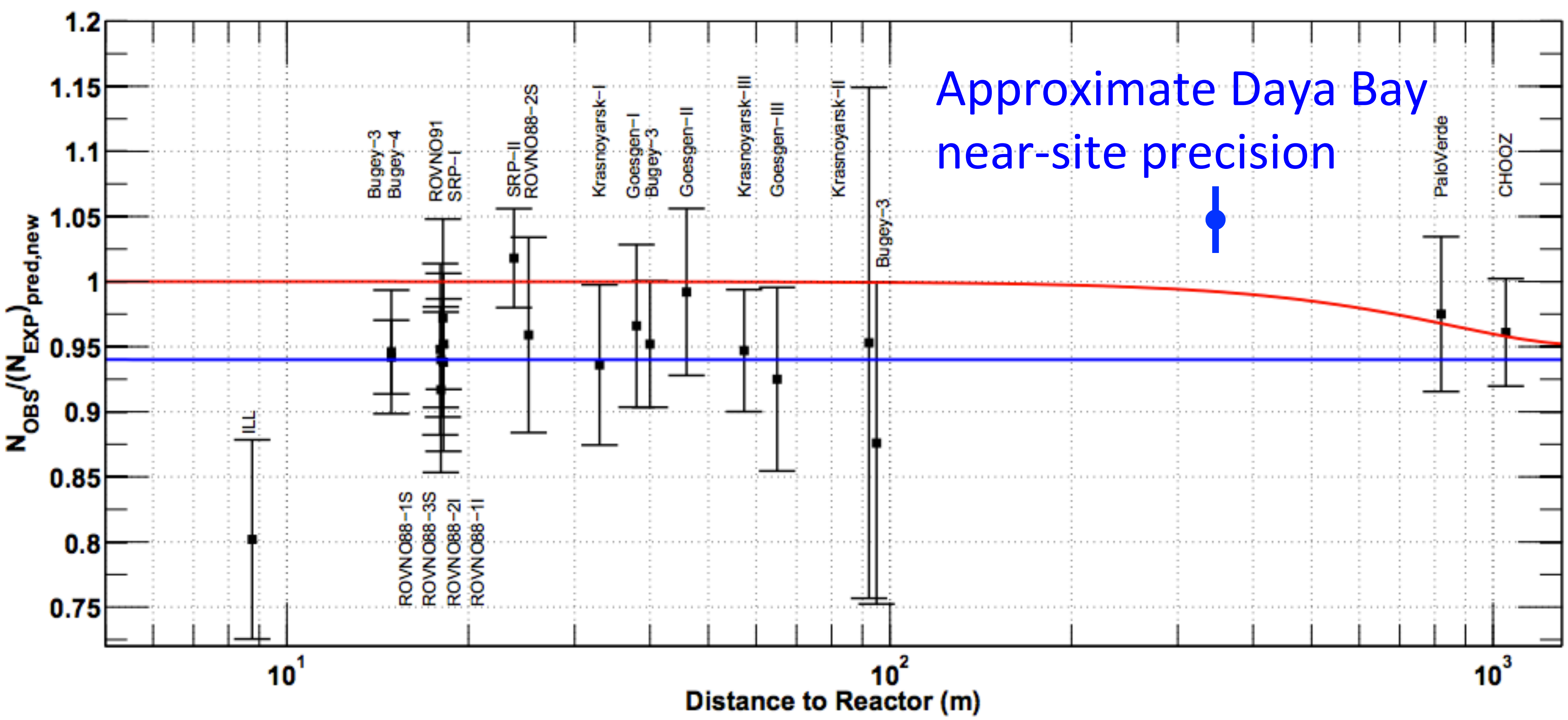

Blue line: $\theta_{13} = 0$
Norm = 0.94

Red line: best-fit θ_{13}
Norm = 1.00

Looking Forward: Absolute Spectrum

- Measurement of spectrum can test reactor flux predictions
  - Unexpected deviations could indicate improper understanding of beta branch production in reactor cores
  - Excellent (<0.5%) precision may give spectral profile of reactor anomaly
  - Need to improve energy response model further
    - Eventual measure non-linearity of readout electronics utilizing simultaneous FADC readout
    - Further stand-alone laboratory tests of scintillator non-linearity
    - Further studies of calibration and background beta, gammas, neutrons, alphas
  - Obvious R&D synergies with short- and long-baseline reactor experiments
    - Non-proliferation and reactor physics at short baselines
    - Measurement of mass hierarchy at longer baselines

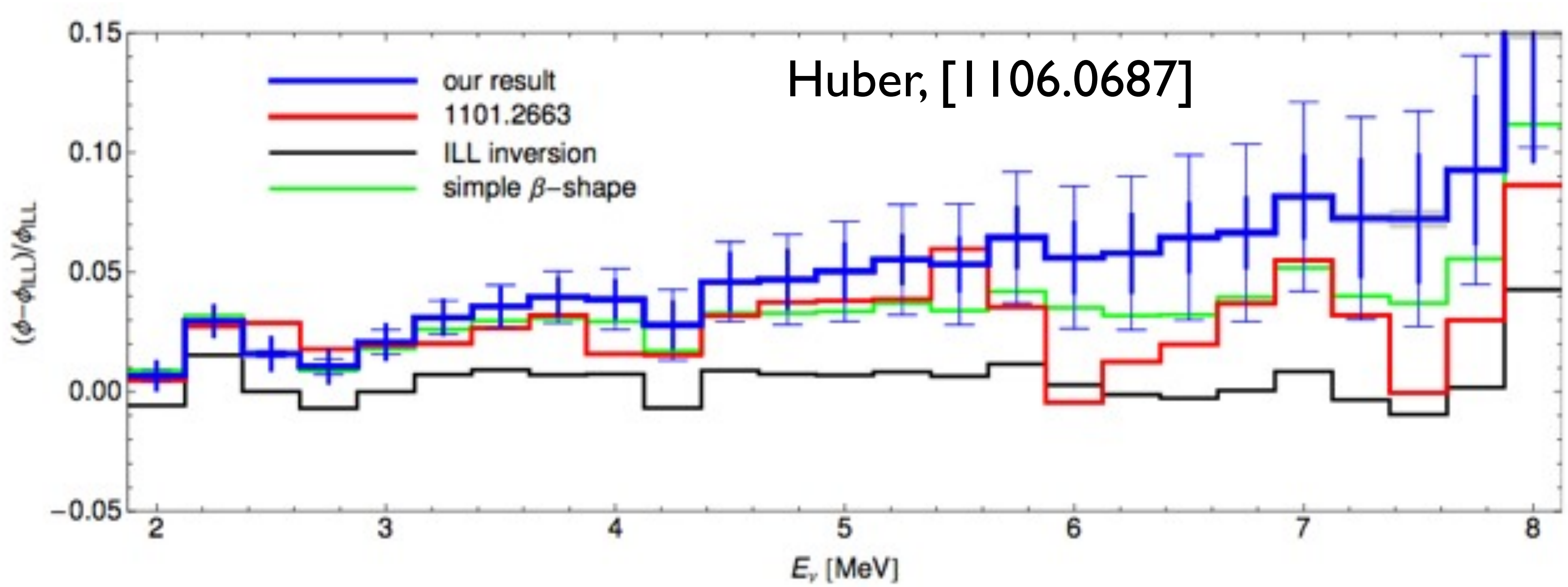

Looking Forward: Sterile Oscillations

- Apart from absolute flux, one can use relative comparisons between Daya Bay near/far sites to constrain sterile oscillations
  - Tests different mass splitting between reactor anomaly and Δm^2
  - Would be nice to know that θ_{13} measurement wasn't being biased by some other mass squared splitting
  - Spectral analysis very helpful
  - Daya Bay will be working on this analysis in the future

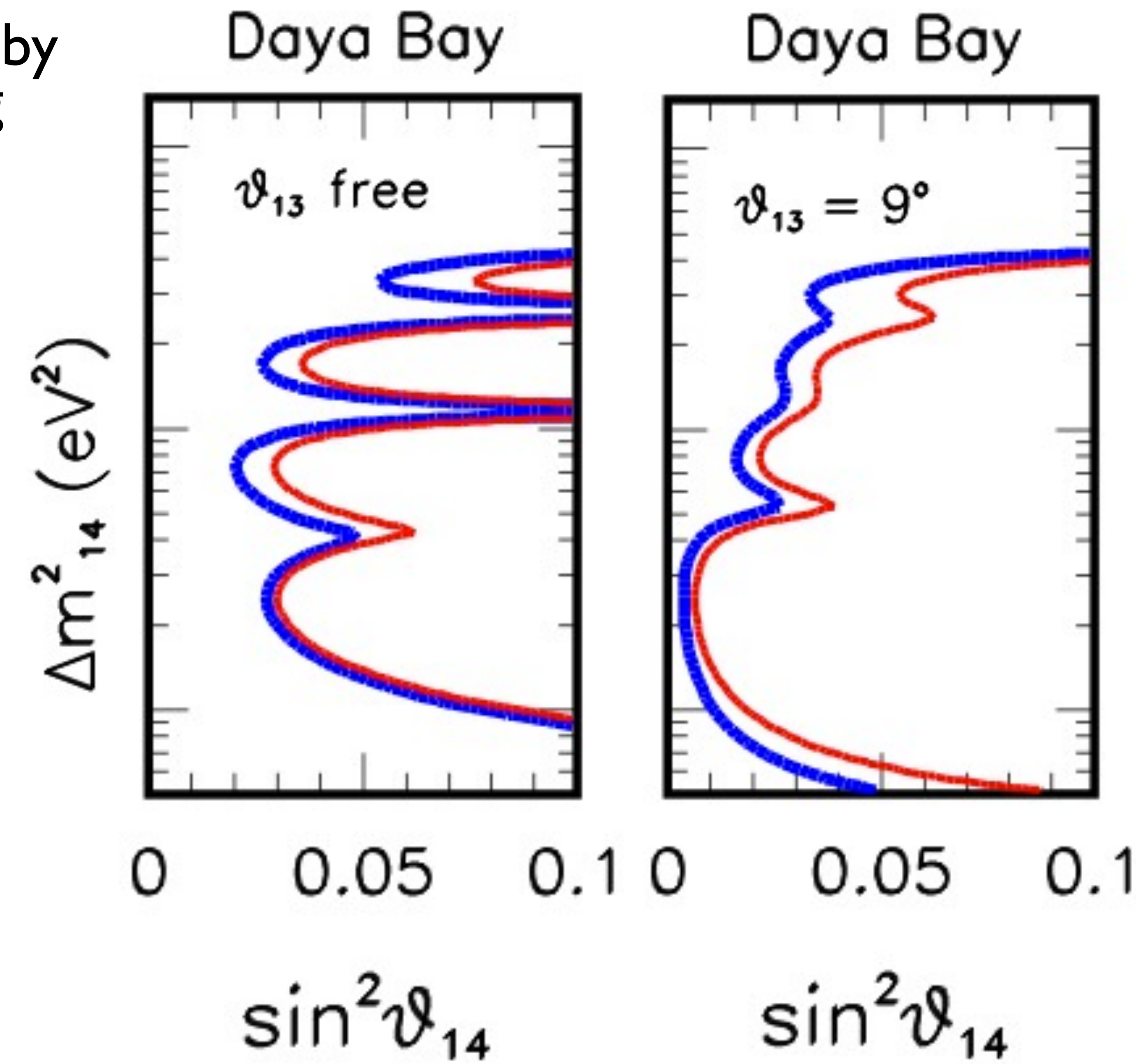

Palazzo, [1308.5880]

Kang, Kim, Ko, Siyeon, [1303.6173]

Bergevin, Grant, Svoboda, [1303.0310]

Summary

The Daya Bay Experiment has reported the first direct measurement of the oscillation short-distance electron antineutrino oscillation frequency:

$$|\Delta m^2_{ee}| = 2.59^{+0.19}_{-0.20} \times 10^{-3}\mathrm{eV}^2$$

The measurement has also produced the most precise estimate of the mixing angle:

$$\sin^2(2\theta_{13}) = 0.090^{+0.008}_{-0.009}$$

Expect more from Daya Bay:
- Measurement of the absolute reactor flux, addressing the reactor anomaly
- Constraints on non-standard neutrino models
- Significantly increased precision (all 8 detectors, >2 years of operation)

Backup

Backgrounds: Fast Neutron

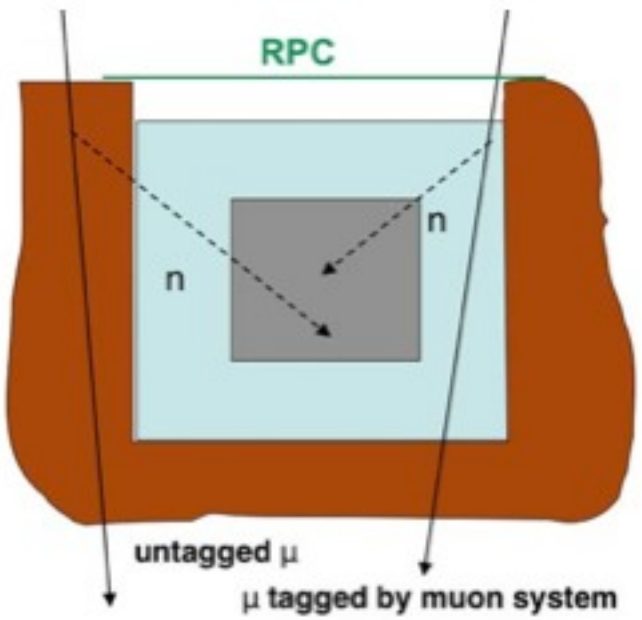

- Hard-to-shield cosmogenic products
- Produce proton recoils (prompt) and n-Gd capture (delayed)
- Muon-tagged fast neutrons: continuous prompt spectrum

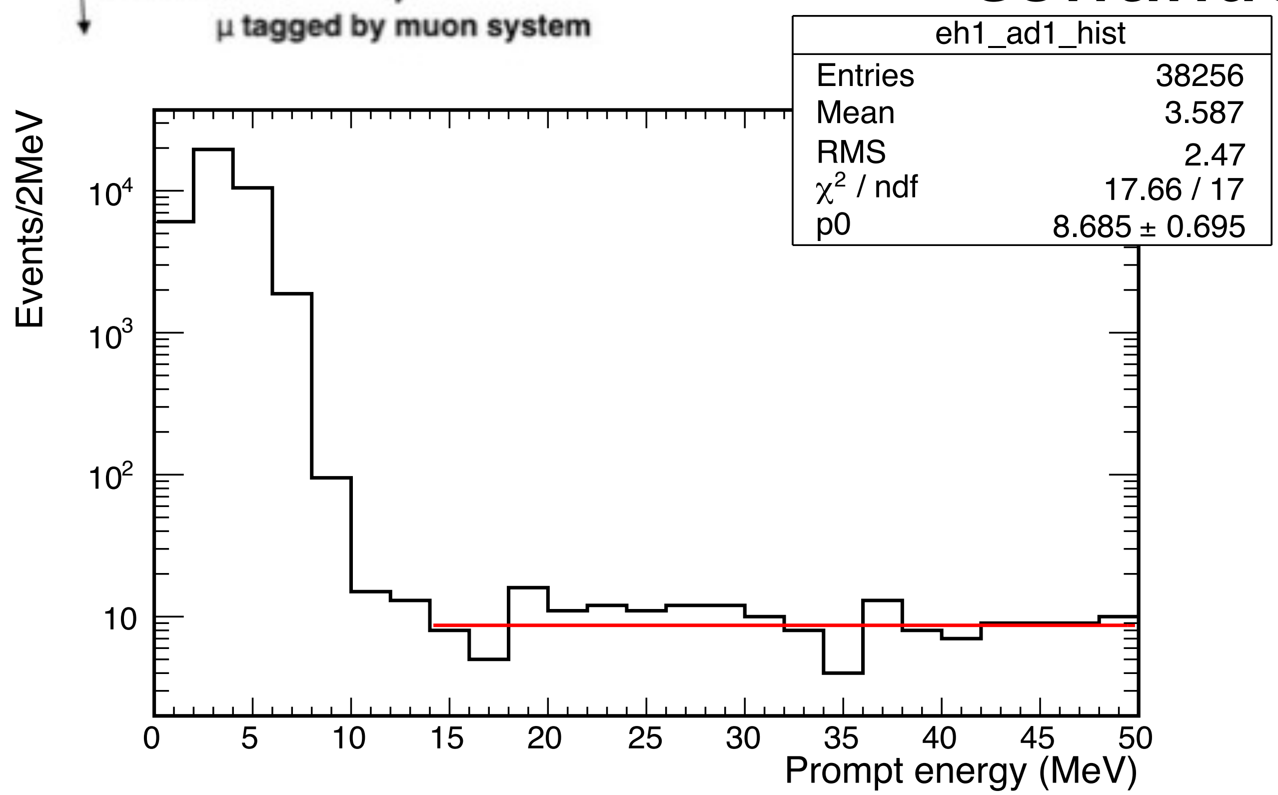

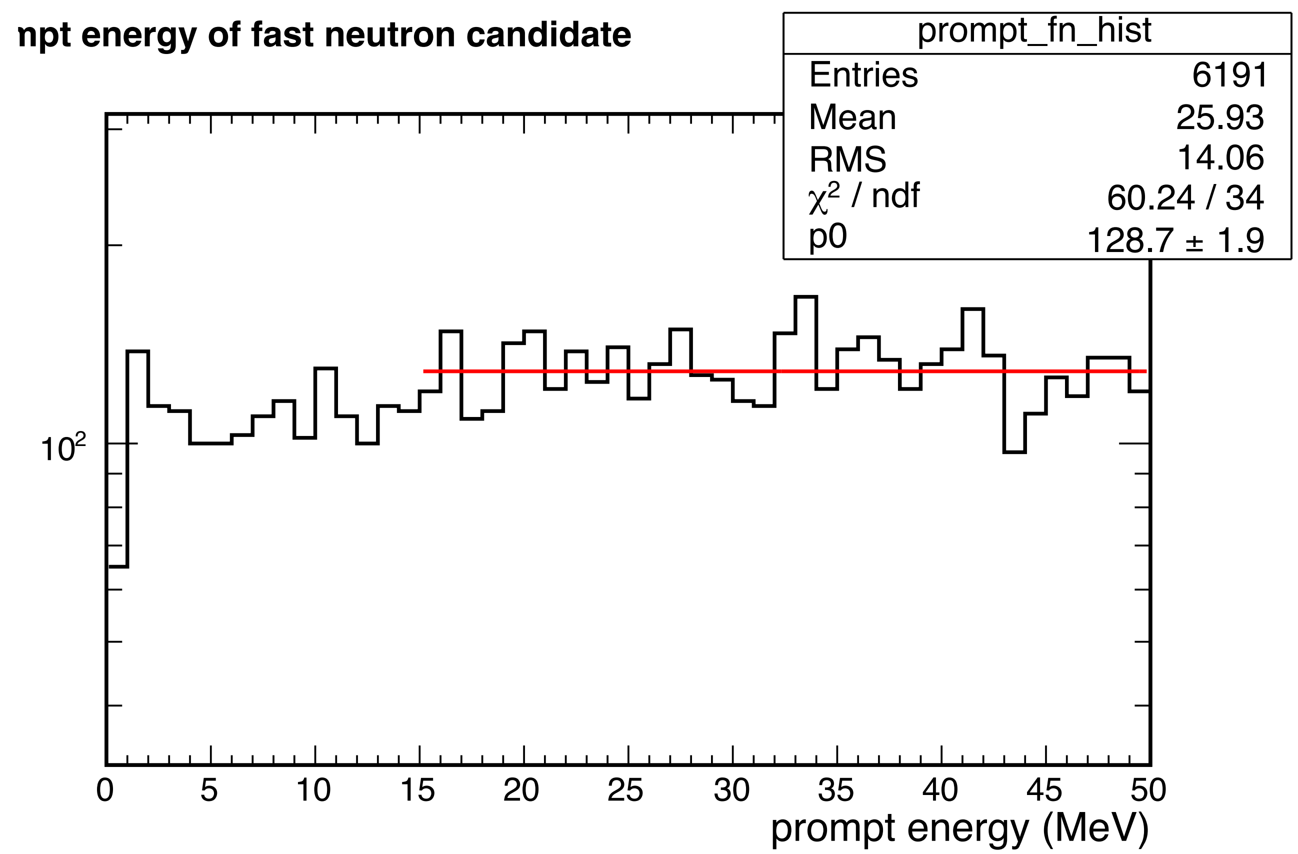

- Statistical subtraction of continuous spectrum controls B/S to 0.1% ± 0.1%

A Note on Mass Splitting

Short-baseline reactor experiments insensitive to neutrino mass hierarchy.

Cannot discriminate two frequencies contributing to oscillation: $\Delta m^2_{31}, \ \Delta m^2_{32}$

One effective oscillation frequency is measured:

$$P_{\bar{\nu_e} \rightarrow \bar{\nu_e}} = 1 - \sin^2 2\theta_{13} \sin^2 \left(\Delta m^2_{ee} \frac{L}{4E} \right) - \sin^2 2\theta_{12} \cos^4 2\theta_{13} \sin^2 \left(\Delta m^2_{21} \frac{L}{4E} \right)$$

$$\sin^2 (\Delta m^2_{ee} \tfrac{L}{4E}) \equiv \cos^2 \theta_{12} \sin^2 (\Delta m^2_{31} \tfrac{L}{4E}) + \sin^2 \theta_{12} \sin^2 (\Delta m^2_{32} \tfrac{L}{4E})$$

Result can be easily related to actual mass splitting, based on true hierarchy:

$$|\Delta m^2_{ee}| \simeq |\Delta m^2_{32}| \pm 5.21 \times 10^{-5} \mathrm{eV}^2$$

+: Normal Hierarchy
–: Inverted Hierarchy

Hierarchy discrimination requires ~2% precision on both Δm^2_{ee} and $\Delta m^2_{\mu\mu}$

A Note on Mass Splitting

arXiv: 1208.1551

Xin's formula in the previous page looks complicated,
but indeed, is equivalent to a simple formula in p2

Start from Xin's formula:

~0

$$P(\overline{\nu}_e \to \overline{\nu}_e) = 1 - 2s_{13}^2c_{13}^2 + 2s_{13}^2c_{13}^2\sqrt{1 - \boxed{4s_{12}^2c_{12}^2\sin^2\Delta_{21}}}\cos(2\Delta_{32} \pm \phi) - \boxed{c_{13}^4s_{12}^2c_{12}^2\sin^2\Delta_{21}}$$

Solar term

$$\simeq 1 - 4s_{13}^2c_{13}^2\frac{1-\cos(2\Delta_{32} \pm \phi)}{2} - (solar\ term)$$

$$= 1 - \sin^2 2\theta_{13}\sin^2(\boxed{\Delta_{32} \pm \phi/2}) - (solar\ term)$$

$$\Delta_{ee} = \Delta_{32} + \phi/2 \quad \text{(NH)}$$

Then,

$$\Delta m_\phi^2 = \phi \times \frac{L}{1.267E}$$

$$\Delta m_{ee}^2 = \Delta m_{32}^2 + \Delta m_\phi^2/2 \quad \text{(NH)}$$

If we neglect $\boxed{}$ term, it becomes to a simple expression in p2.
It should be a good estimate for Daya Bay energy and baseline length.

Calibration: PMT+Electronics Gain

Measure charge from single photons in-situ with data

Use out-of-time PMT signals hits to calibrate the PMT + electronics response to single photons.

Cross-check with weekly LED deployments.

Gain variation with time

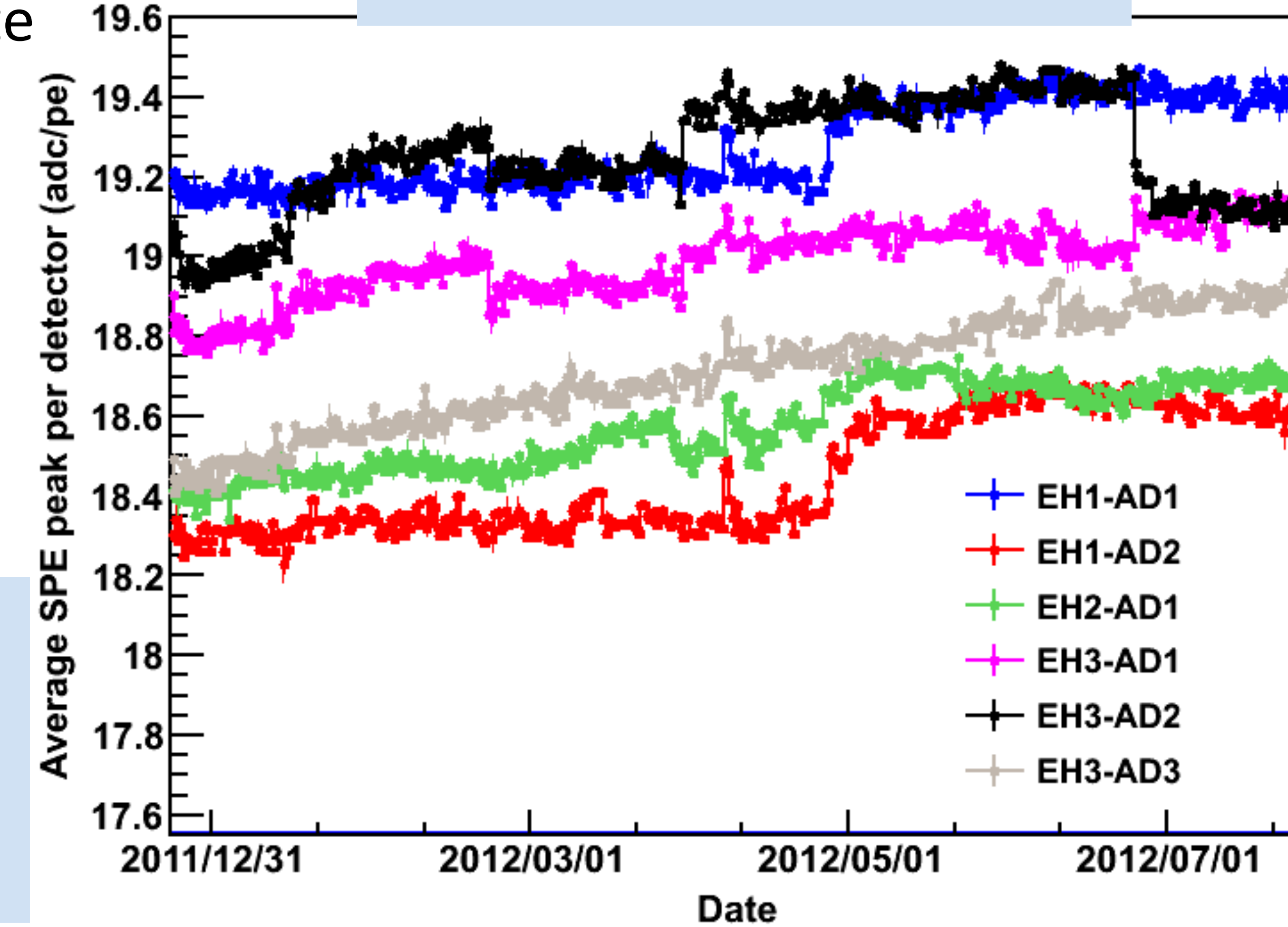

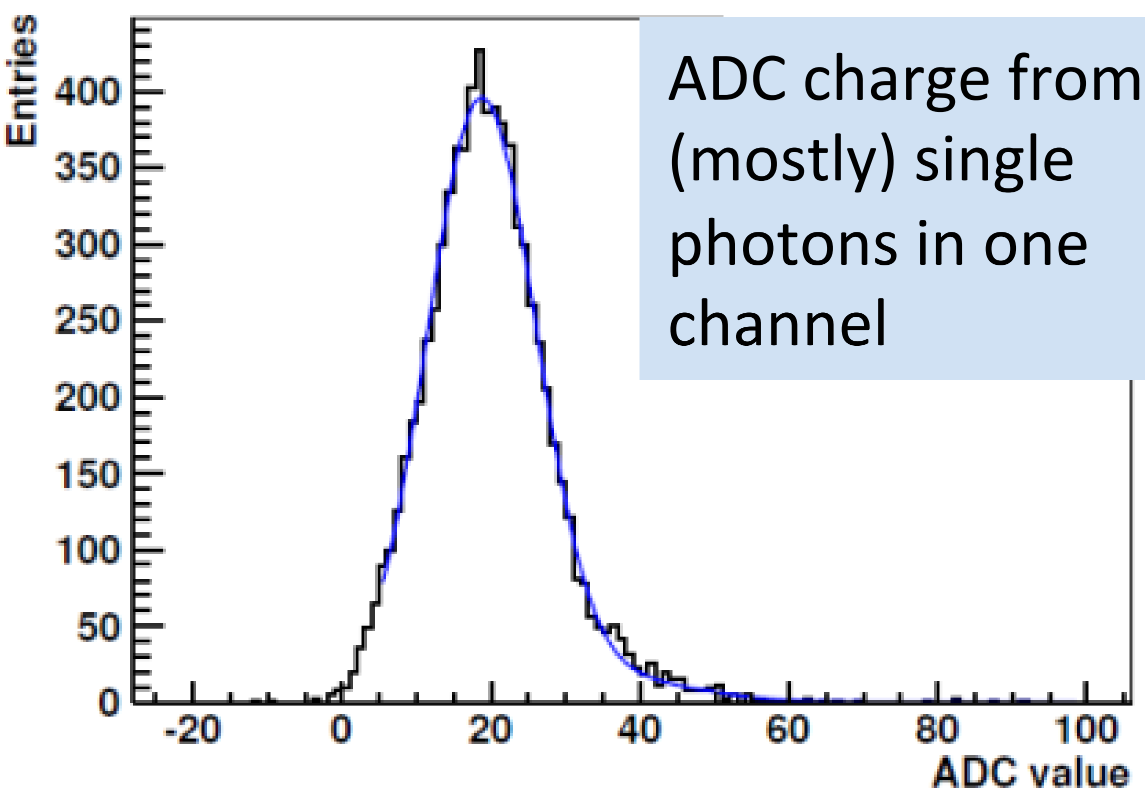

ADC charge from (mostly) single photons in one channel

Calibration driven by uncertainty in relative detector efficiency

$$\frac{N_{\mathrm{f}}}{N_{\mathrm{n}}} = \left(\frac{N_{\mathrm{p,f}}}{N_{\mathrm{p,n}}}\right)\left(\frac{L_{\mathrm{n}}}{L_{\mathrm{f}}}\right)^2\left(\frac{\epsilon_{\mathrm{f}}}{\epsilon_{\mathrm{n}}}\right)\left[\frac{P_{\mathrm{sur}}(E, L_{\mathrm{f}})}{P_{\mathrm{sur}}(E, L_{\mathrm{n}})}\right]$$

Calibration: Energy Scale

Measure energy scale in-situ with data

Calibrate charge (photoelectrons) collected per MeV in-situ using spallation nGd capture events. Also use weekly deployments of ^{60}Co source.

Spallation *n*Gd capture
(uniform throughout detector)

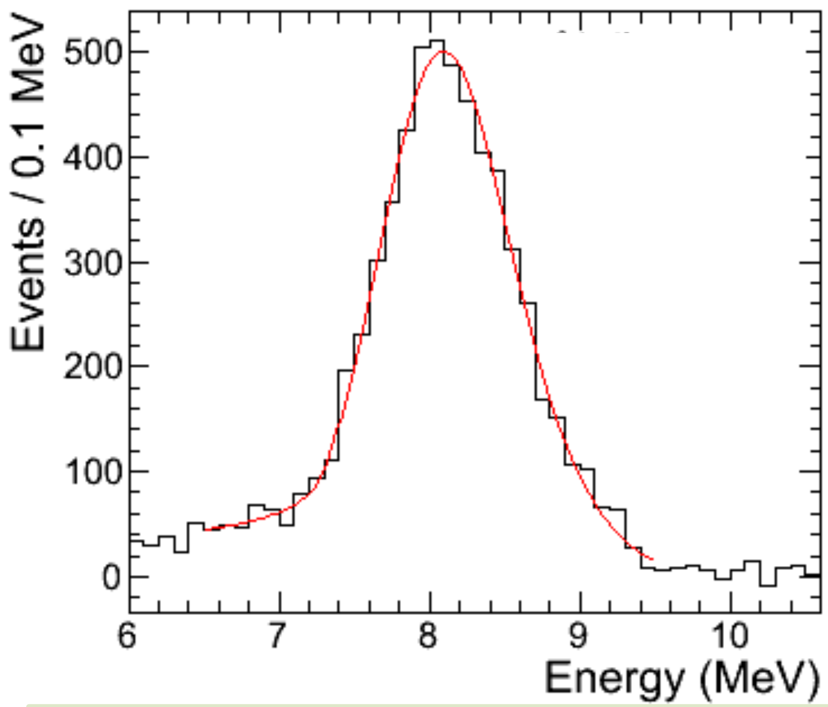

Energy Scale = Q / E

Measured charge of nGd peak

Average energy released in nGd

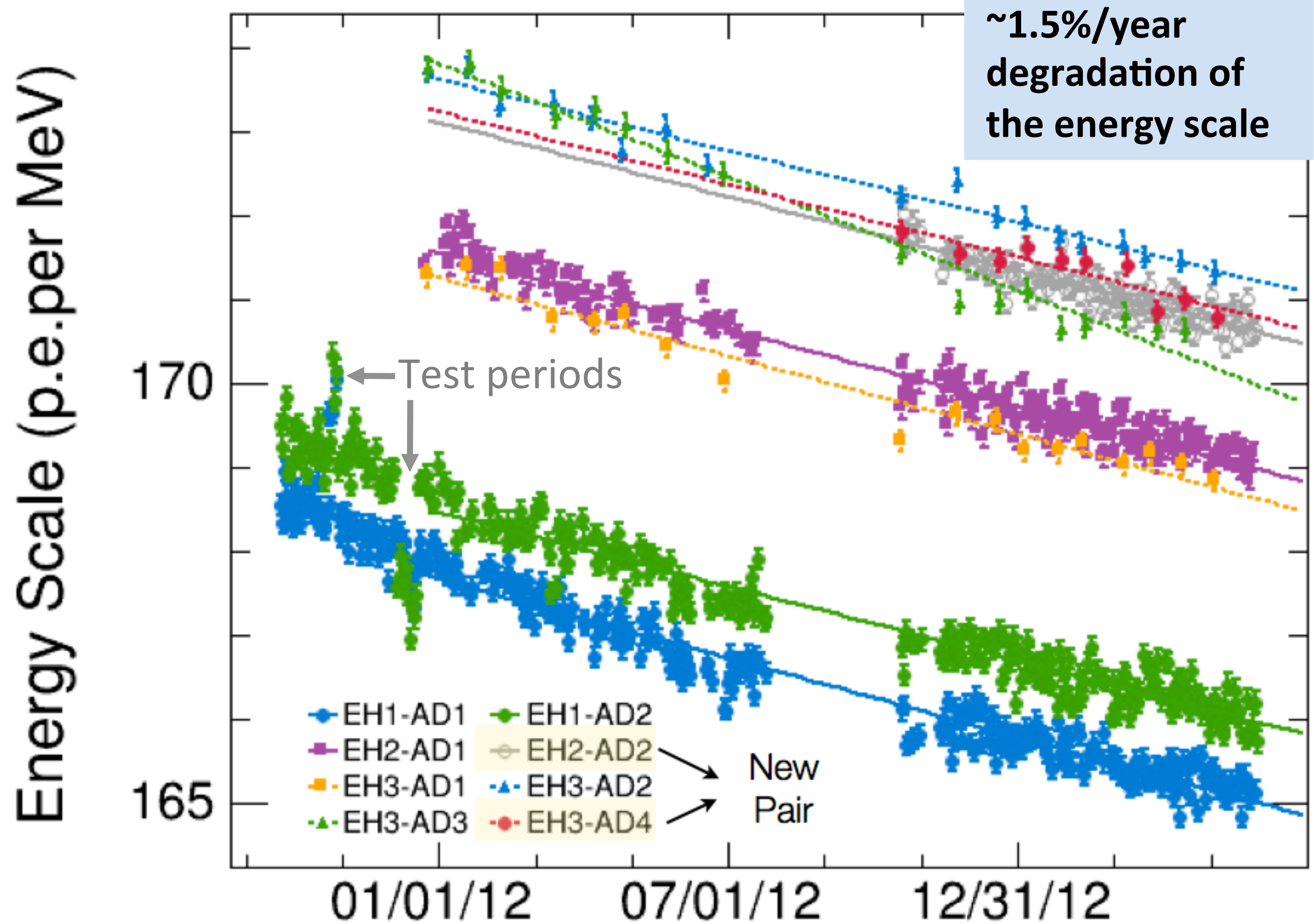

~1.5%/year degradation of the energy scale

Small degradation of energy scale is seen with nGd, ^{60}Co, and other event types. Its origin is still unknown, but do not anticipate any problems in experiment's lifetime.

Calibration and Non-Uniformity

Measure uniformity with sources placed along three axes and spallation nGd events

Example: ^{60}Co

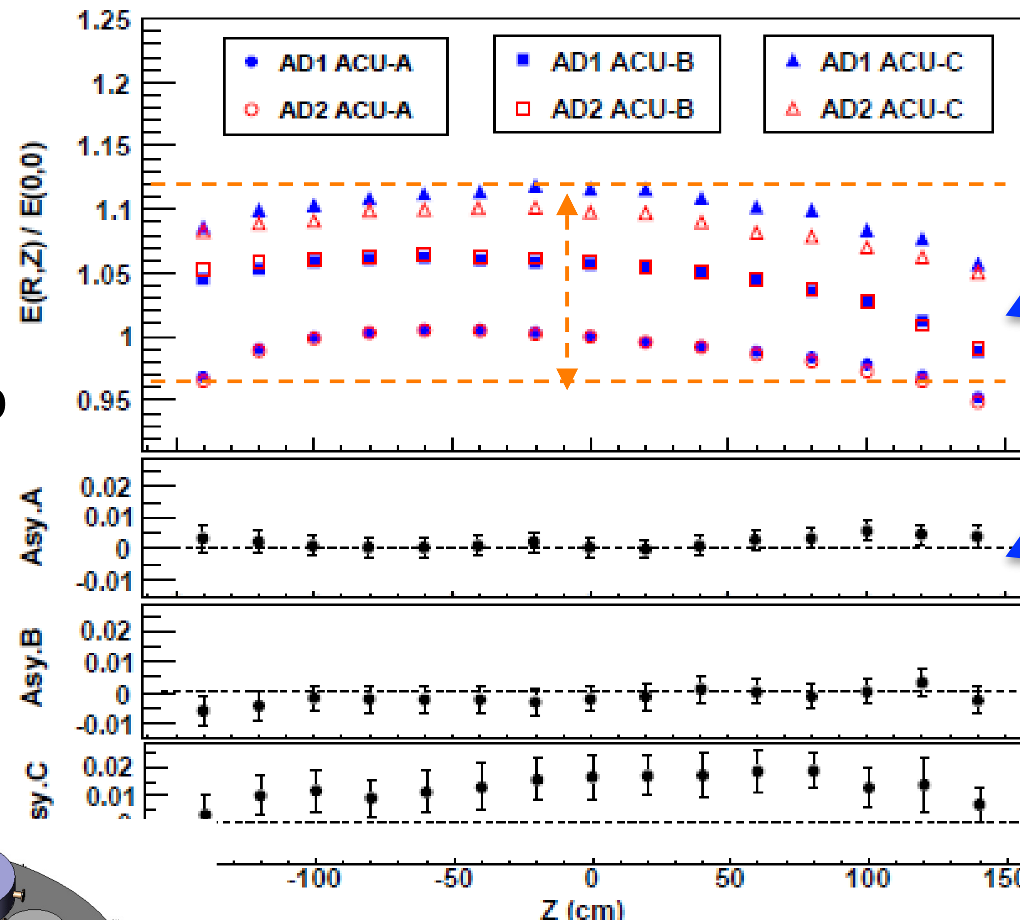

Energy response varies across detector…

…but still consistent between detectors

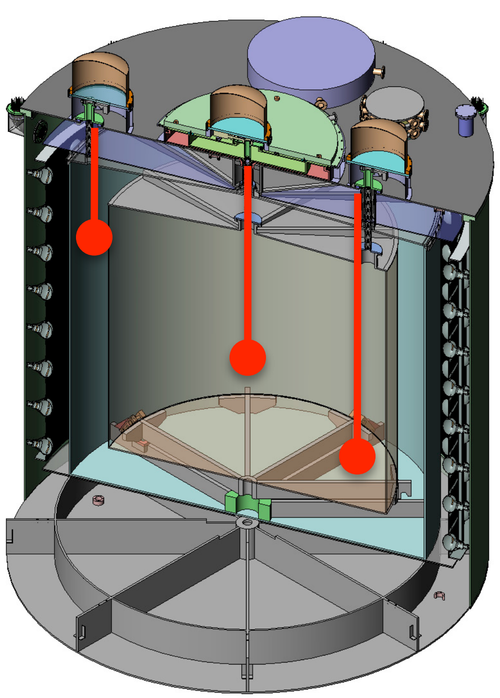

After first-order correction, energy is more uniform.

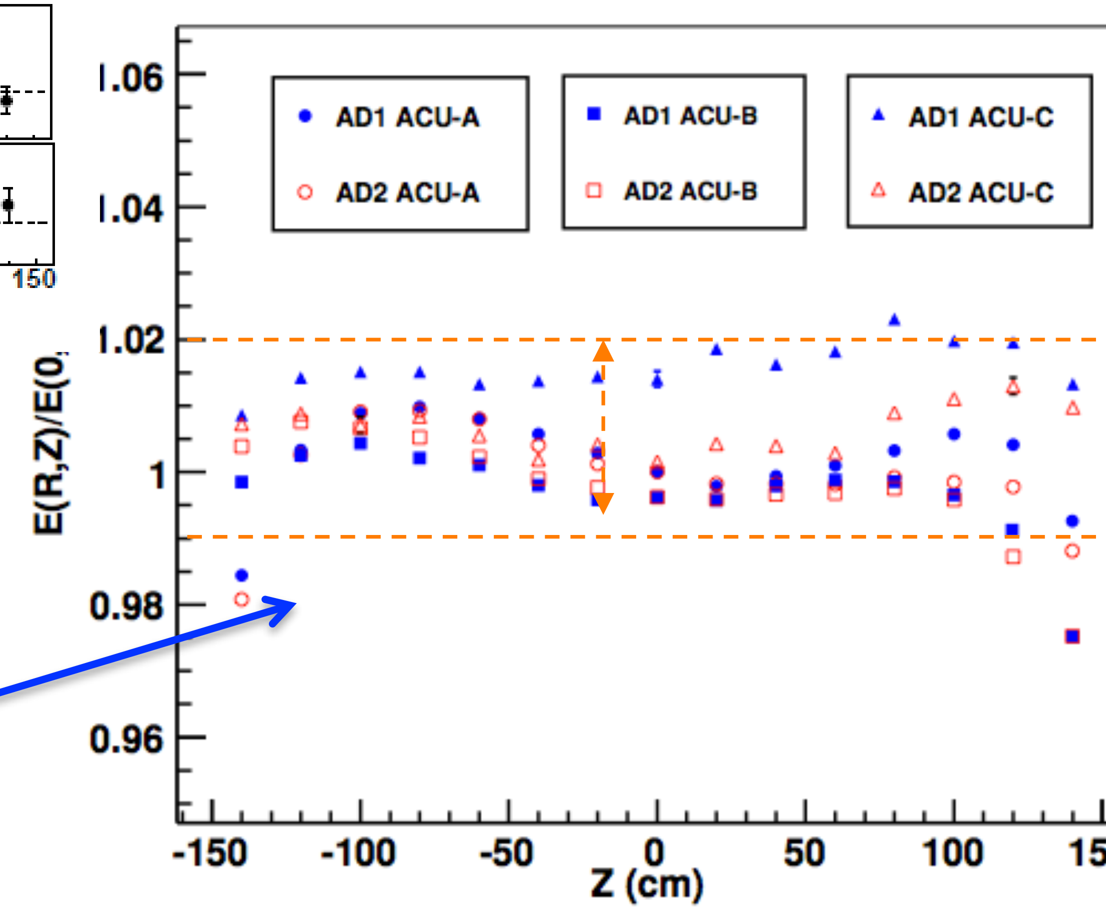

Calibration and Non-Uniformity

Predicted prompt spectrum assumes totally flat non-uniformity

We know percent-level non-uniformities in E_{rec} exist. **Does this matter?**

Will cause percent-level spectral broadening, less than from photon statistics (~7%)

Can complicate distortion from acrylic vessel, which is also position dependent.

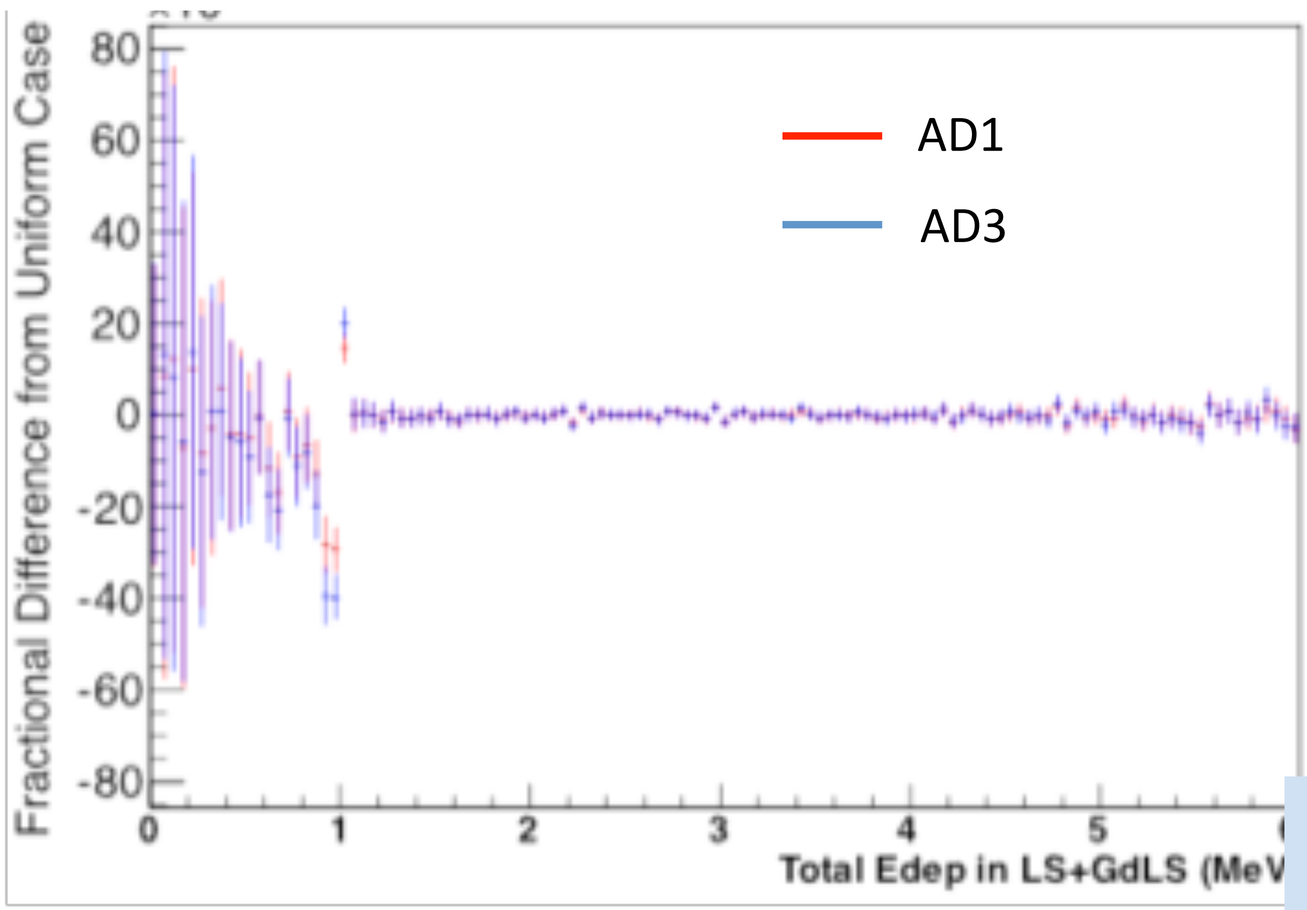

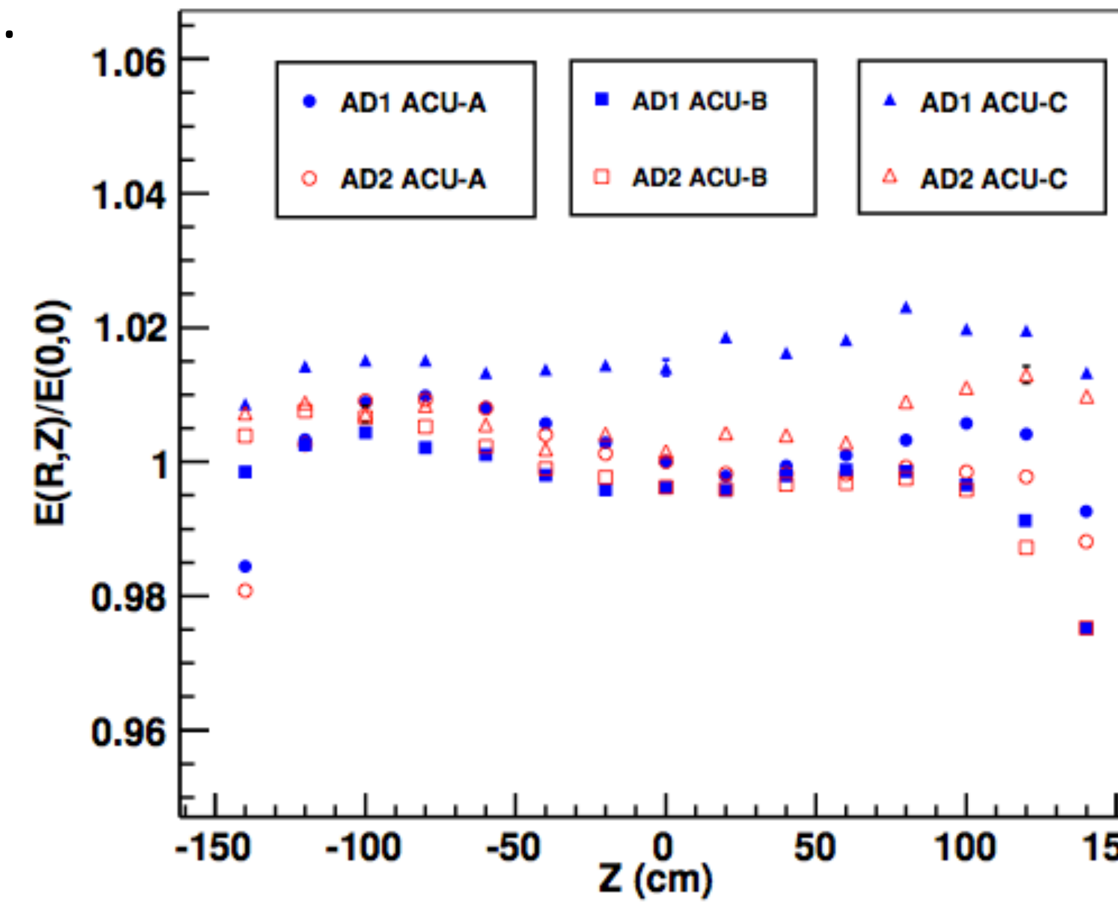

Simulate prompt spectrum for flat, AD1 and AD3 residual non-uniformities

Differences much smaller than spectral uncertainties from other sources.

All energy scale non-uniformities have a negligible effect on Daya Bay prompt spectra

PMT Light Emission (Flashing)

Flashing PMTs:

- Instrumental background from ~5% of PMTS
- 'Shines' light to opposite side of detector
- Easily discriminated from normal signals

Neutrinos ← | → Flashers

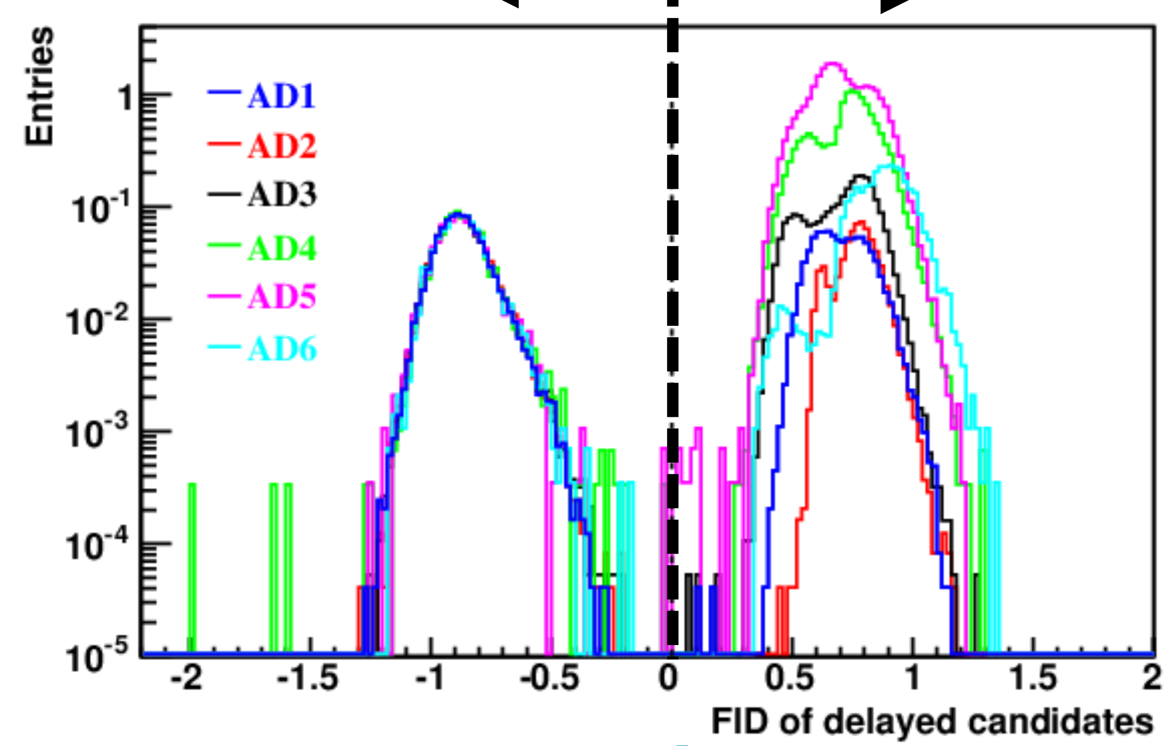

$$FID = \log_{10}((MaxQ)^2/(0.45)^2 + (Quad)^2)$$

Quadrant = Q3/(Q2+Q4)

MaxQ = maxQ/sumQ

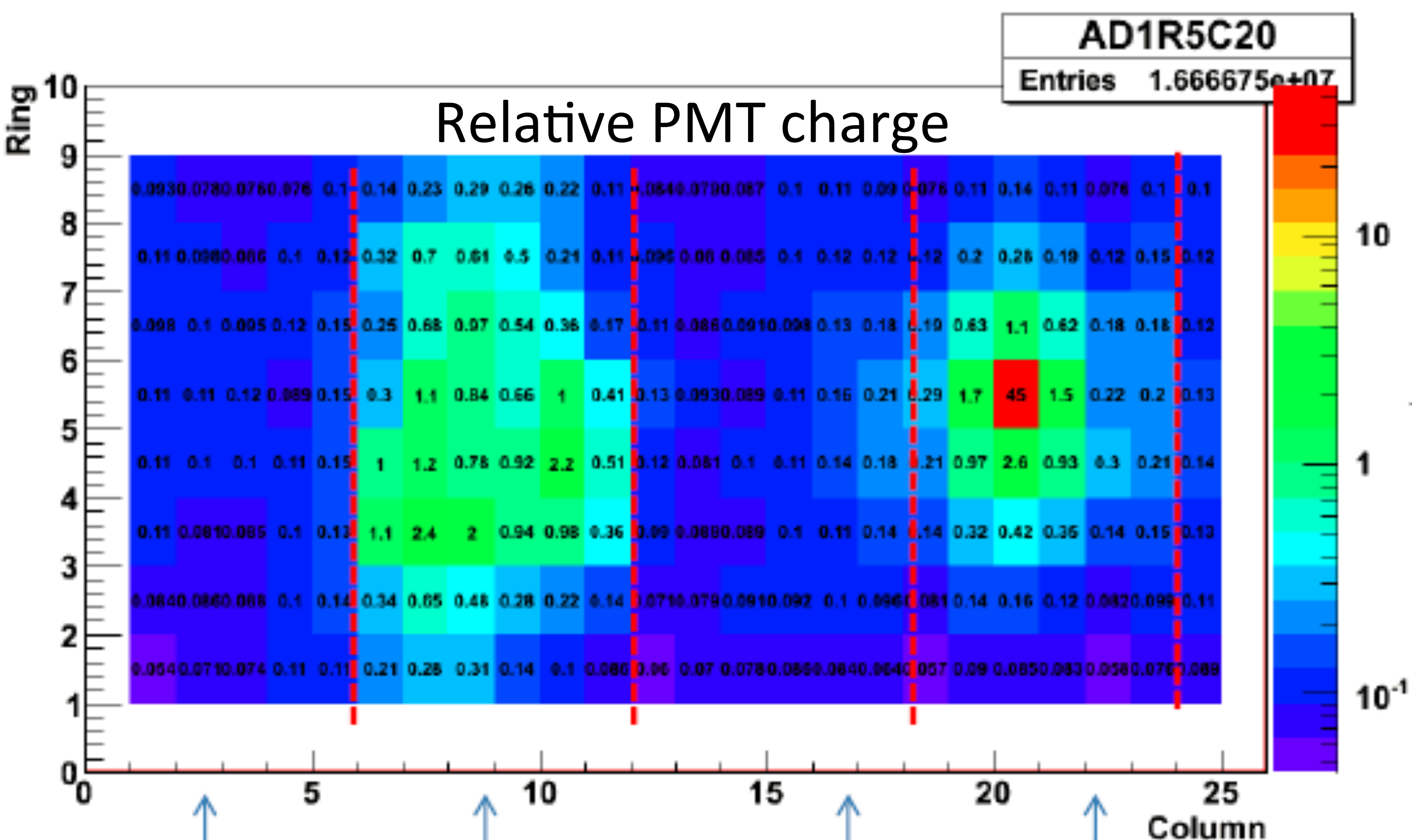

Quadrant 4 Quadrant 3 Quadrant 2 Quadrant 1

(contains 'hottest' PMT)

Inefficiency to antineutrinos signal: 0.024% ± 0.006%(stat)

Contamination: < 0.01%

Multiplicity

Ensure exactly one prompt-delayed coincidence

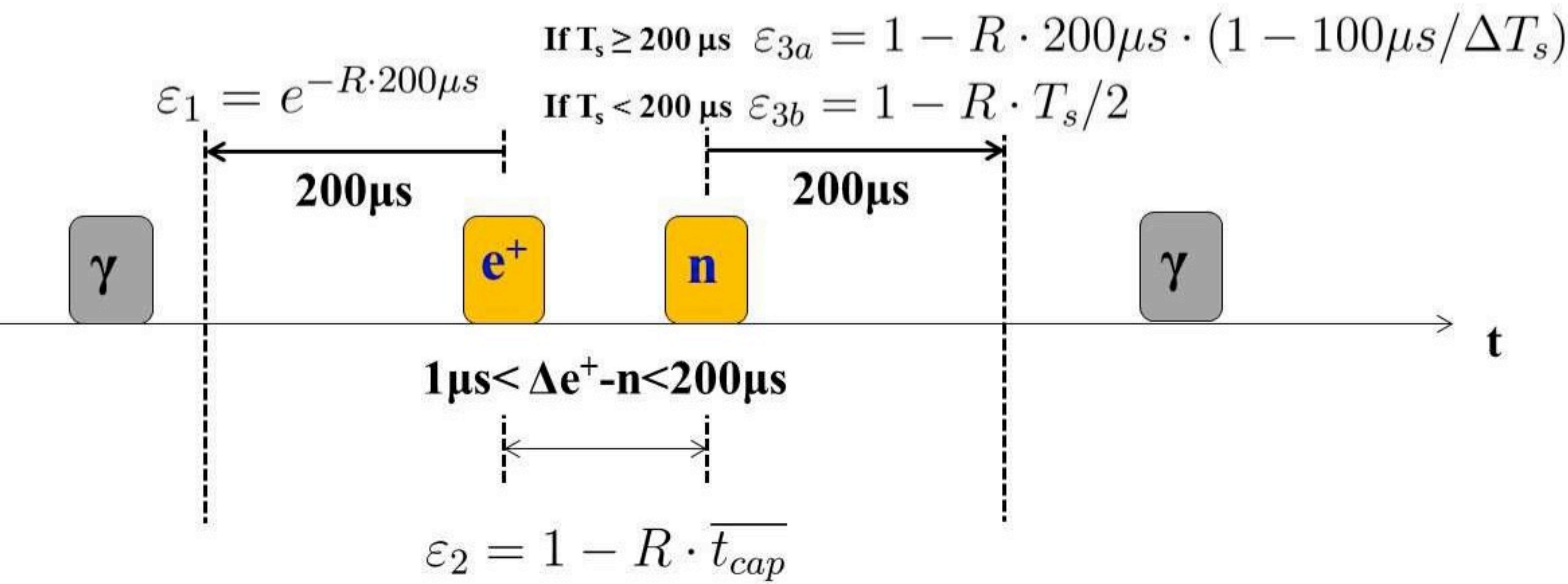

Uncorrelated background and IBD signals result in ambiguous prompt,delayed signals.

-> Reject all IBD with >2 triggers above 0.7 MeV in -200μs to +200μs.
Introduces ~2.5% IBD inefficiency, with negligible uncertainty

Capture Time

Consistent IBD neutron capture time measured in all detectors

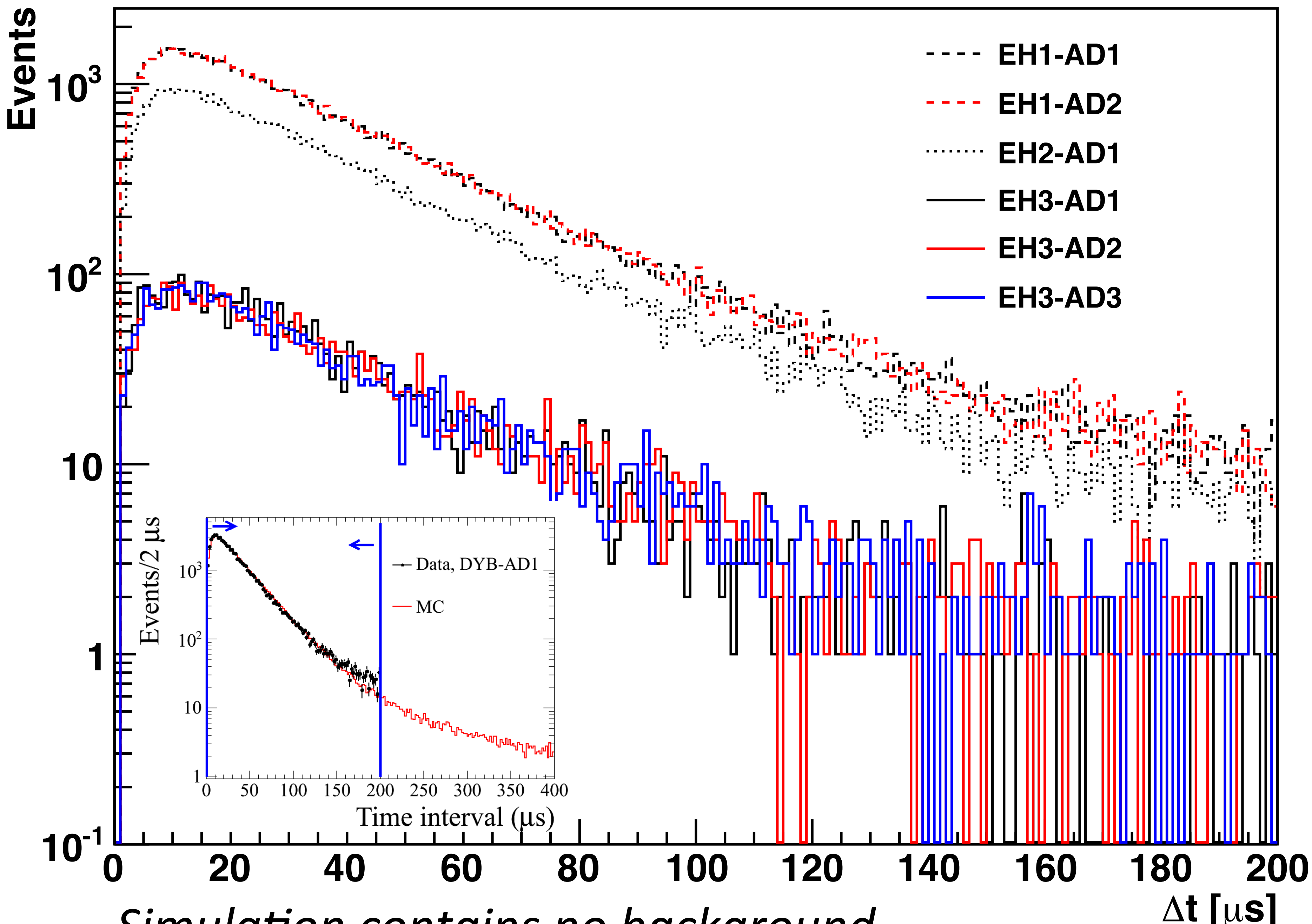

Capture time cut:
1μs to 200μs

Efficiency uncertainty within 0.01% between detectors.

Simulation contains no background (deviates from data at >150 μs)

Delayed Energy Cut

Largest uncertainty between detectors

Some *n*Gd gammas escape scintillator region, visible as tail of *n*Gd energy peak.

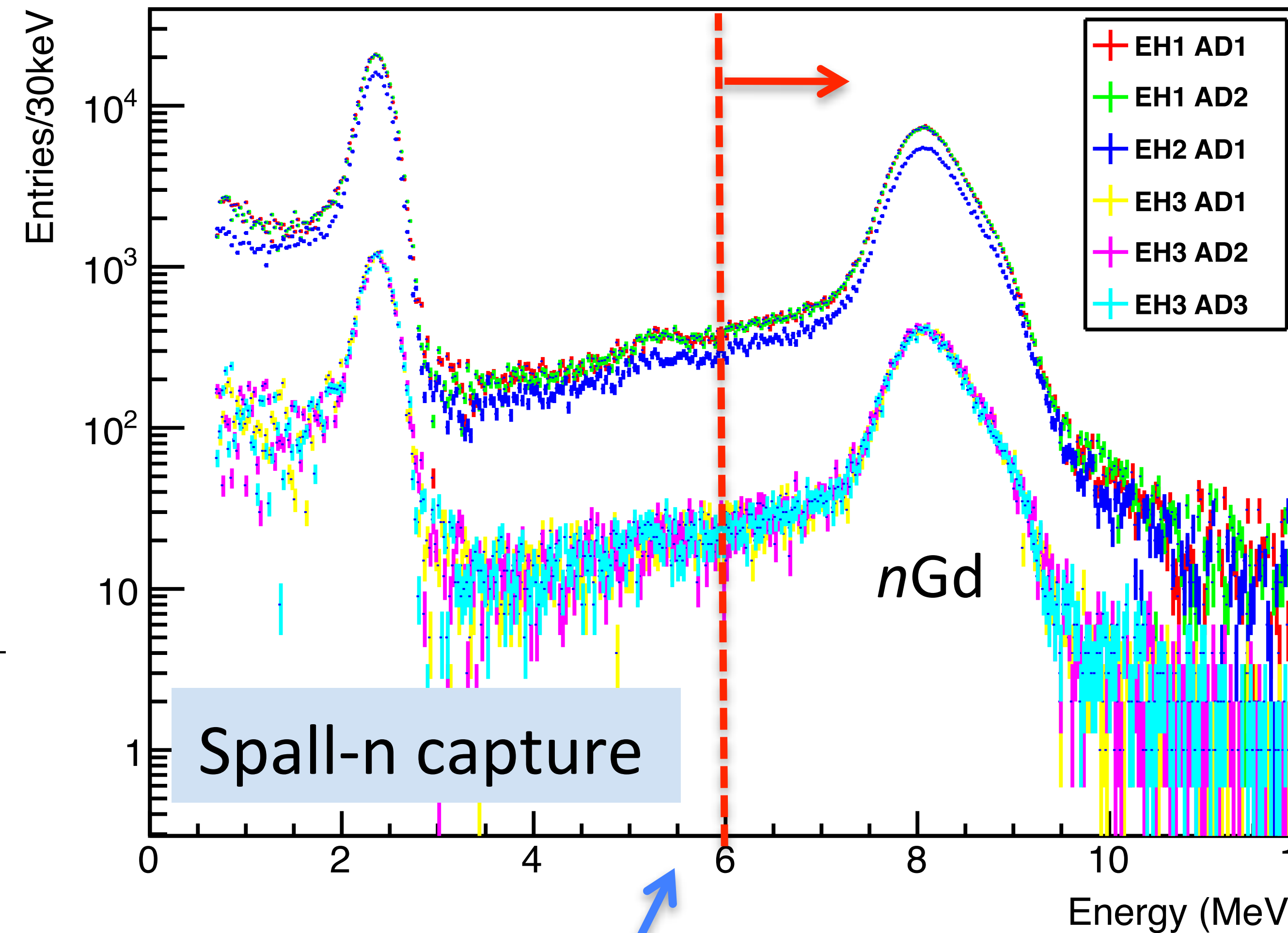

Use variations in energy peaks to constrain relative efficiency.

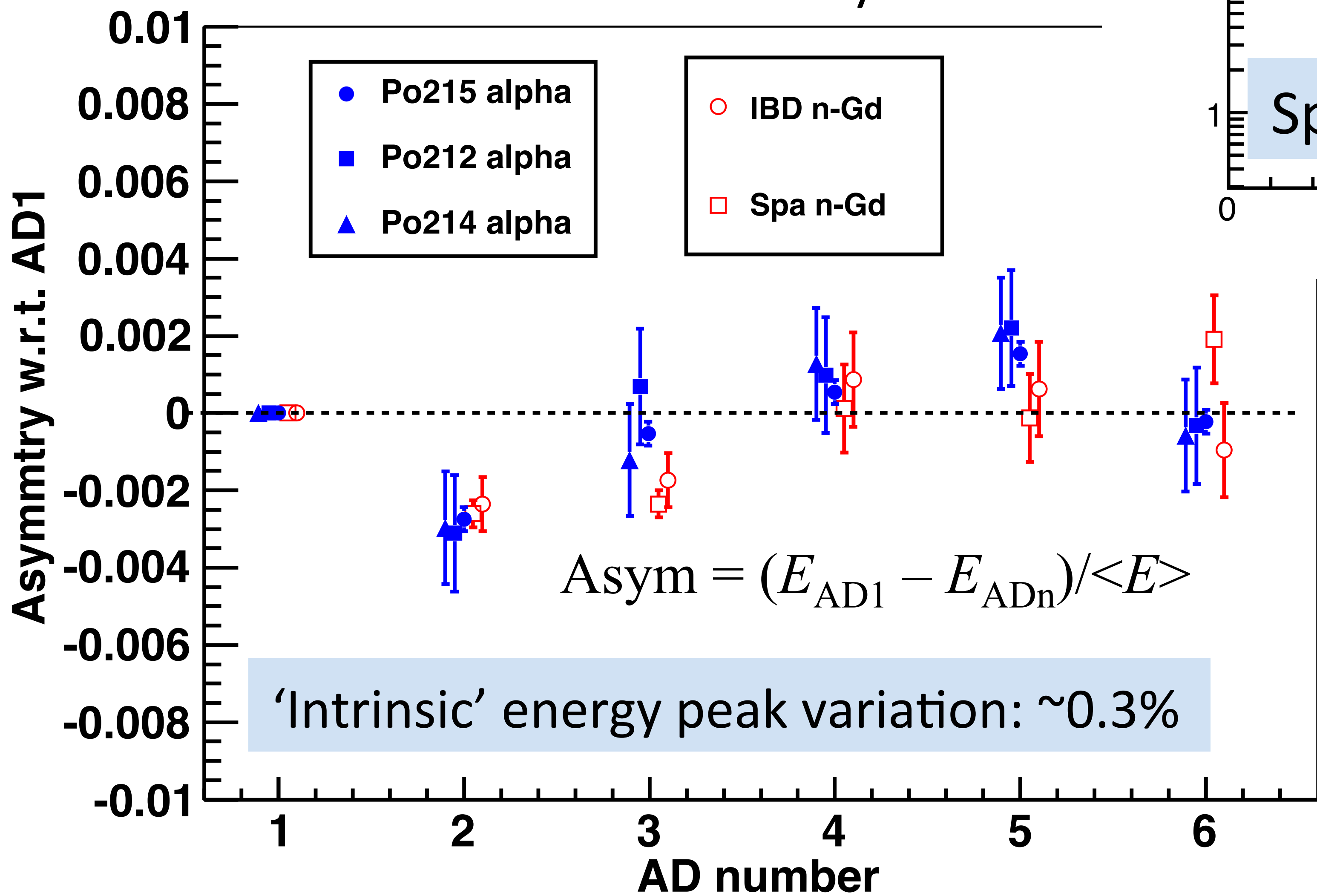

Efficiency variations estimated at 0.12%

Motivation for 3-zone design

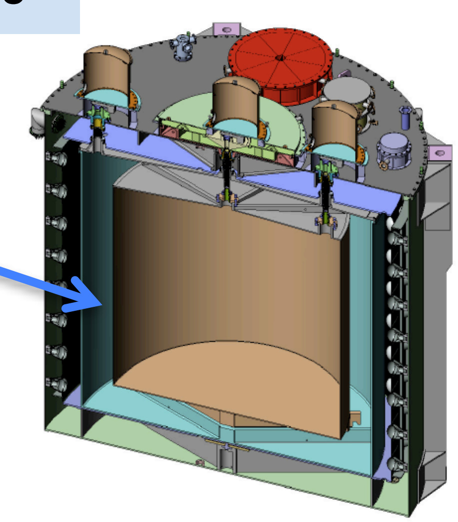

Detector Construction

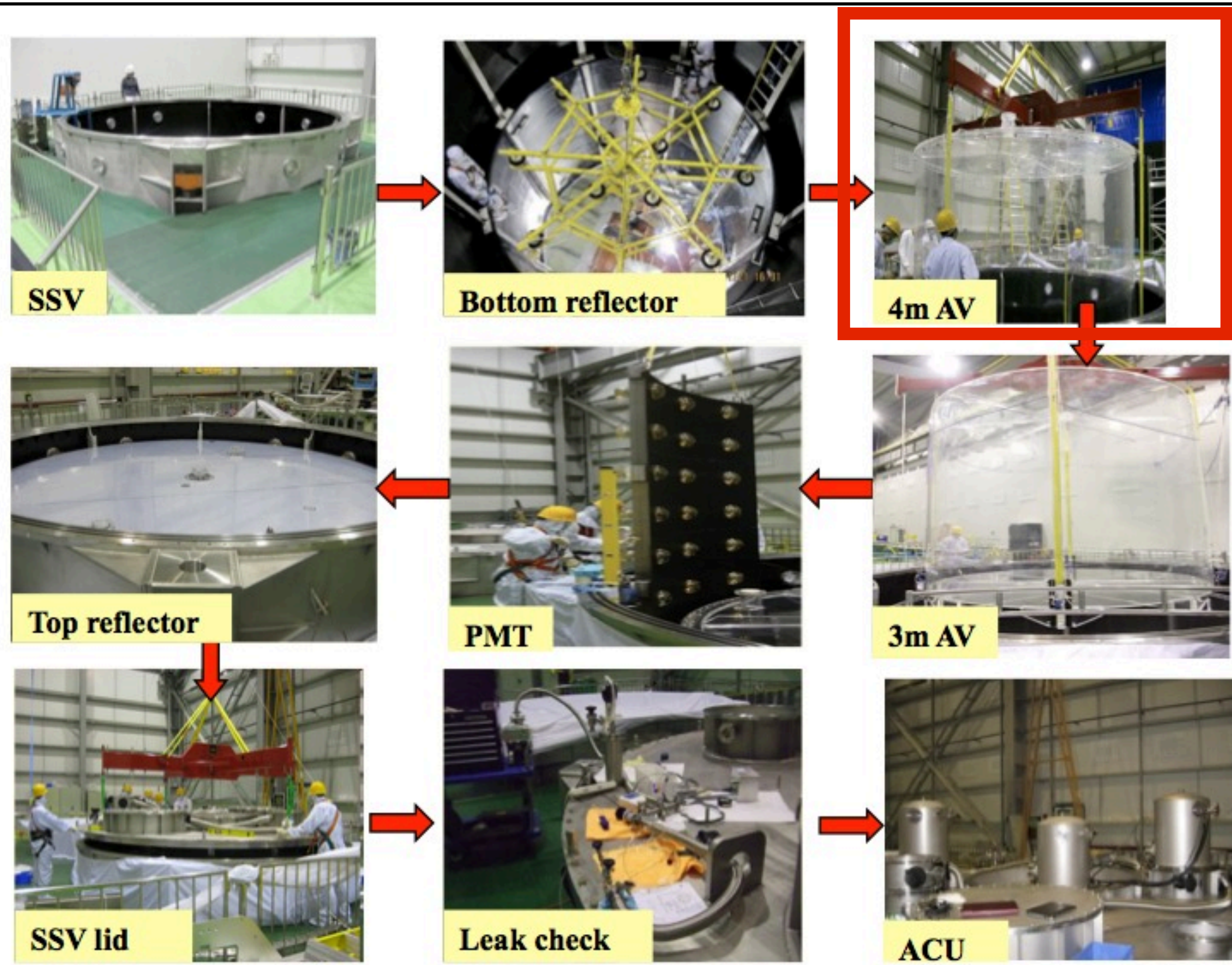

Filling and Mass Measurement

- GdLS mass measured with load cells to 0.03%, flowmeters to 0.1%

$$\frac{N_{\mathrm{f}}}{N_{\mathrm{n}}} = \left(\frac{N_{\mathrm{p,f}}}{N_{\mathrm{p,n}}}\right)\left(\frac{L_{\mathrm{n}}}{L_{\mathrm{f}}}\right)^2\left(\frac{\epsilon_{\mathrm{f}}}{\epsilon_{\mathrm{n}}}\right)\left[\frac{P_{\mathrm{sur}}(E,L_{\mathrm{f}})}{P_{\mathrm{sur}}(E,L_{\mathrm{n}})}\right]$$

- Used flowmeters to measure LS to 0.1%, MO to 0.3%
- Detectors filled equally from common batches of liquid to ensure identical ADs

View with monitoring camera inside AD

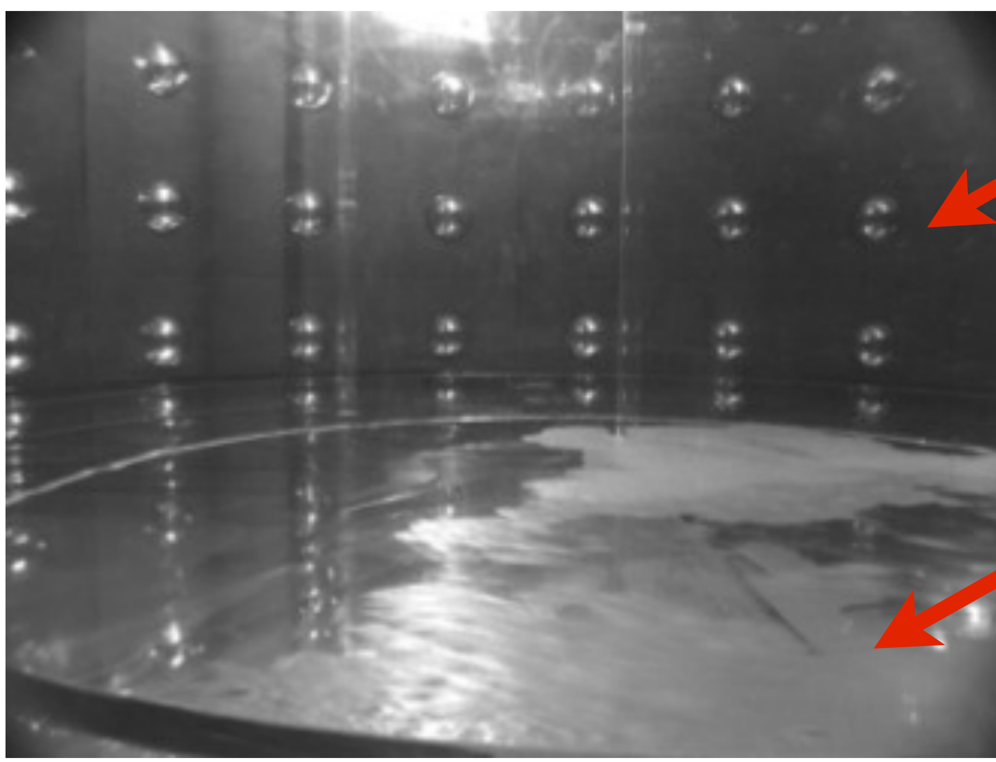

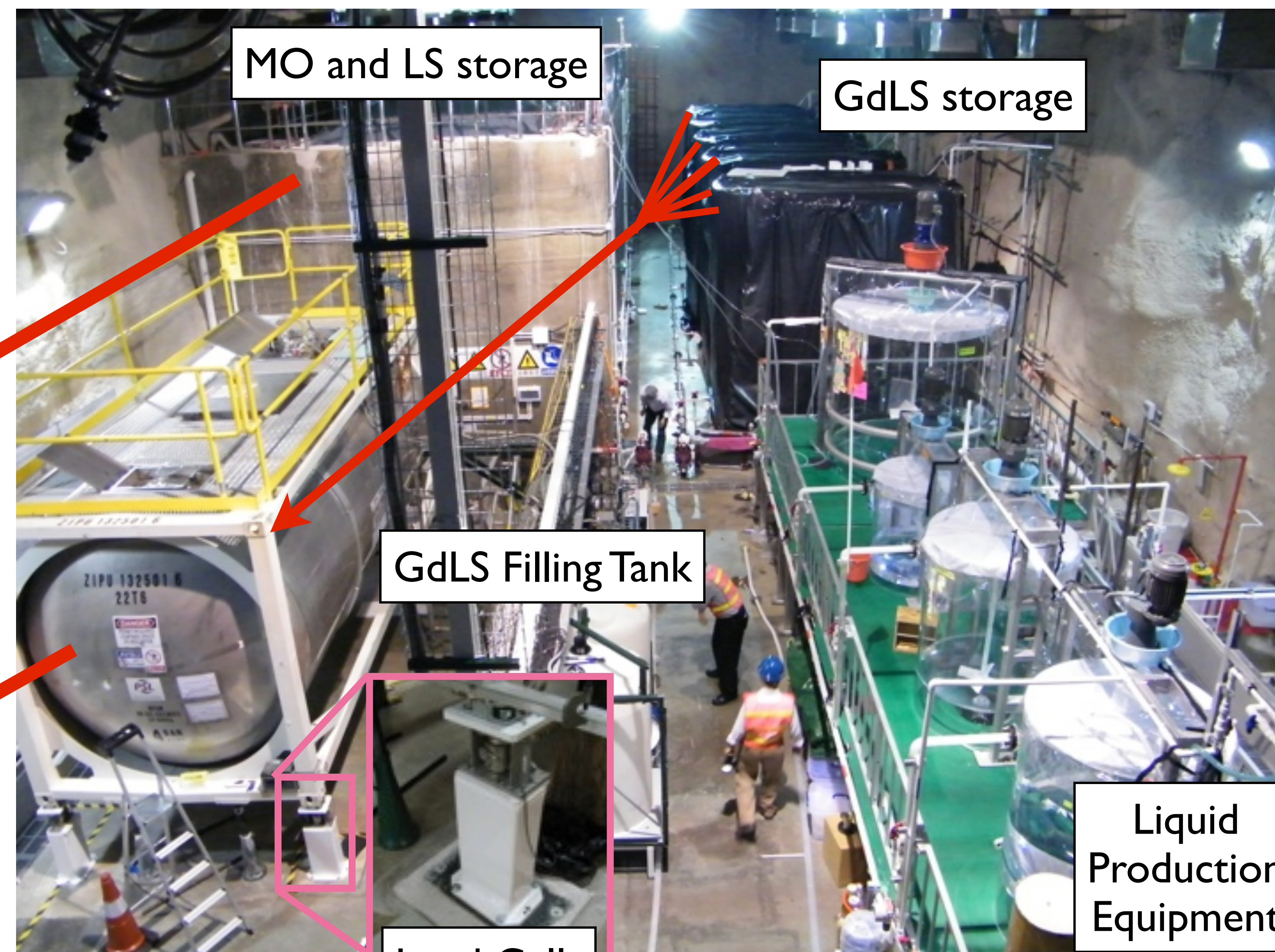

Reactor Flux Models

Antineutrino flux S(E) from each reactor used to predict IBDs at each detector

	^{235}U	^{238}U	^{239}Pu	^{241}Pu
AD 1	63.3	12.2	19.5	4.8
AD 2	63.3	12.2	19.5	4.8
AD 3	61.0	12.5	21.5	4.9
AD 4	61.5	12.4	21.1	4.9
AD 5	61.5	12.4	21.1	4.9
AD 6	61.5	12.4	21.1	4.9

Approximate percentage of IBDs from each fission isotope at each detector

New/Old flux model difference in unoscillated IBD prediction by hall

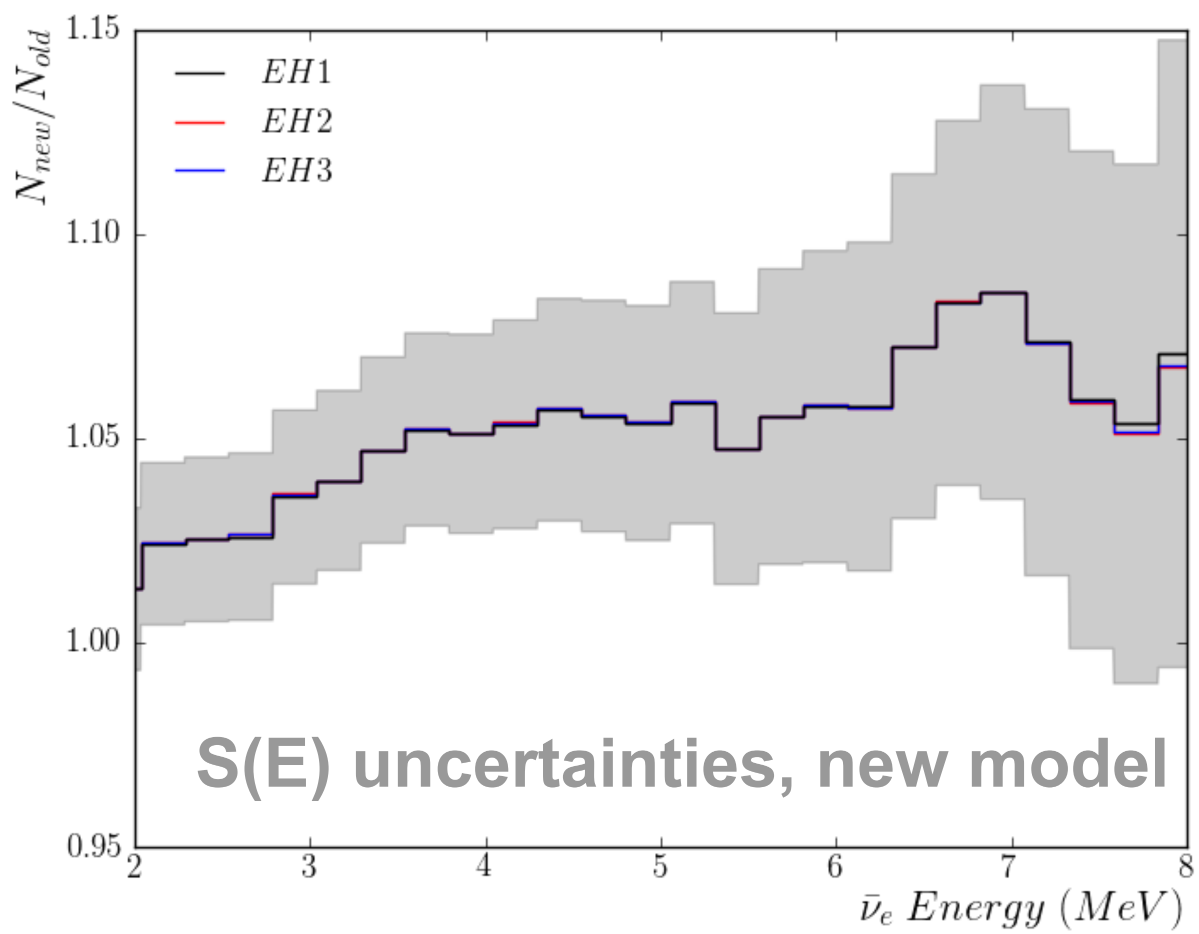

New model:

P. Huber, Phys. Rev. C84, 024617 (2011),
T. Mueller et al., Phys. Rev. C83, 054615 (2011)

Old model:

K. Schreckenbach et al., Phys. Lett. B160, 325 (1985)
A. A. Hahn et al., Phys Rev Lett. B218, 365 (1989)
P. Vogel et al. Phys. Rev. C24, 1543 (1981)

Flux model has negligible impact on far vs. near oscillation measurement

Reactor Antineutrino Flux Predictions

Reactor flux uncertainty ALMOST completely cancels.
Must estimate antineutrino flux from each reactor.

$$N_{det} = \frac{N_p}{4\pi L^2} \int \epsilon \sigma P_{sur} S \, dE$$

- **Inputs:**
- Reactor operators provide:
  - Thermal power: W_{th}
  - Fission fractions f_i
- Energy per fission: e_i
  - V. Kopekin et al., Phys. Atom. Nucl. 67, 1892 (2004)
- Antineutrino spectra per fission: $S_i(E_{nu})$
  - Many varied models have negligible effect on near-far relative measurement

Isotope fission rates vs. reactor burnup

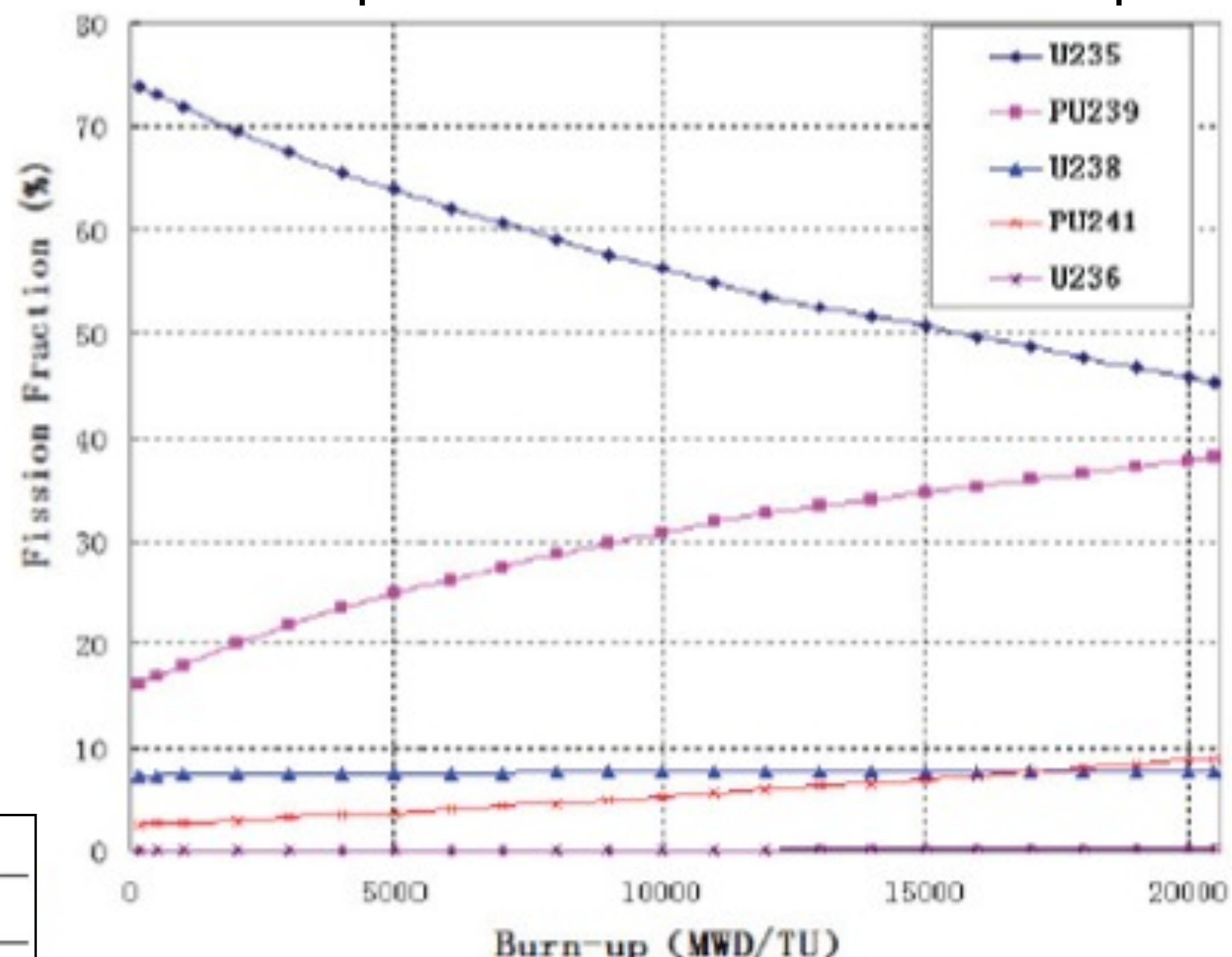

Reactor			
Correlated		Uncorrelated	
Energy/fission	0.2%	Power	0.5%
$\overline{\nu}_e$/fission	3%	Fission fraction	0.6%
		Spent fuel	0.3%
Combined	3%	Combined	0.8%

TABLE III. Summary of systematic uncertainties.

Uncorrelated uncertainties are further reduced by ~1/20 for near/far measurement

65

Reactor Antineutrino Flux Predictions

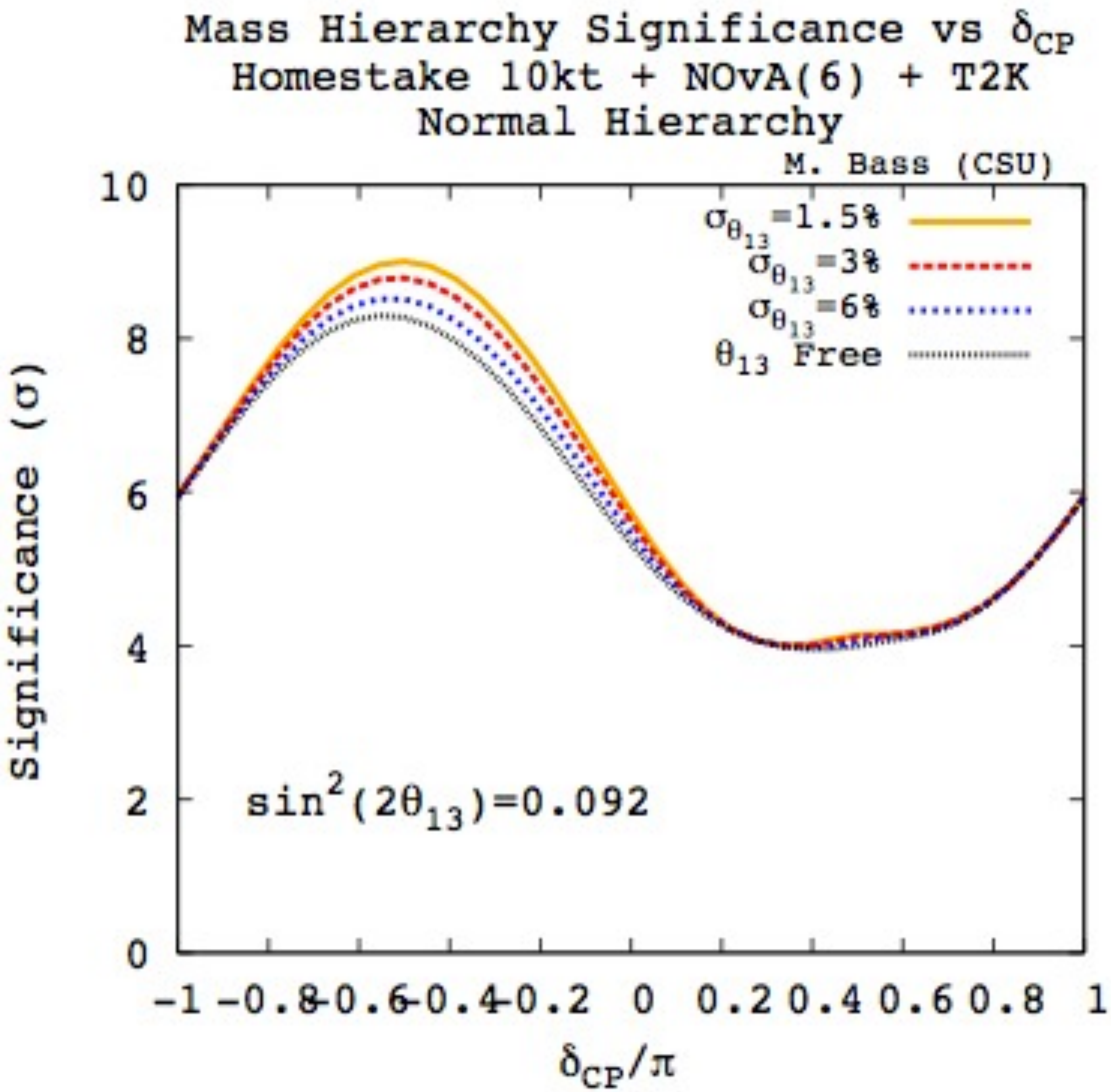

After θ_{13}: A Sterile Neutrino Search

- D. Dwyer, K. Heeger, B. Littlejohn, P. Vogel; arXiv:1109.6036
- 18 PBq ^{144}Ce source at the Daya Bay far site
  - Look for very short baseline oscillation from large Δm_{new}^2
  - 35 cm thick Tungsten source shield, water pool reduce gamma backgrounds
  - Many possible source locations

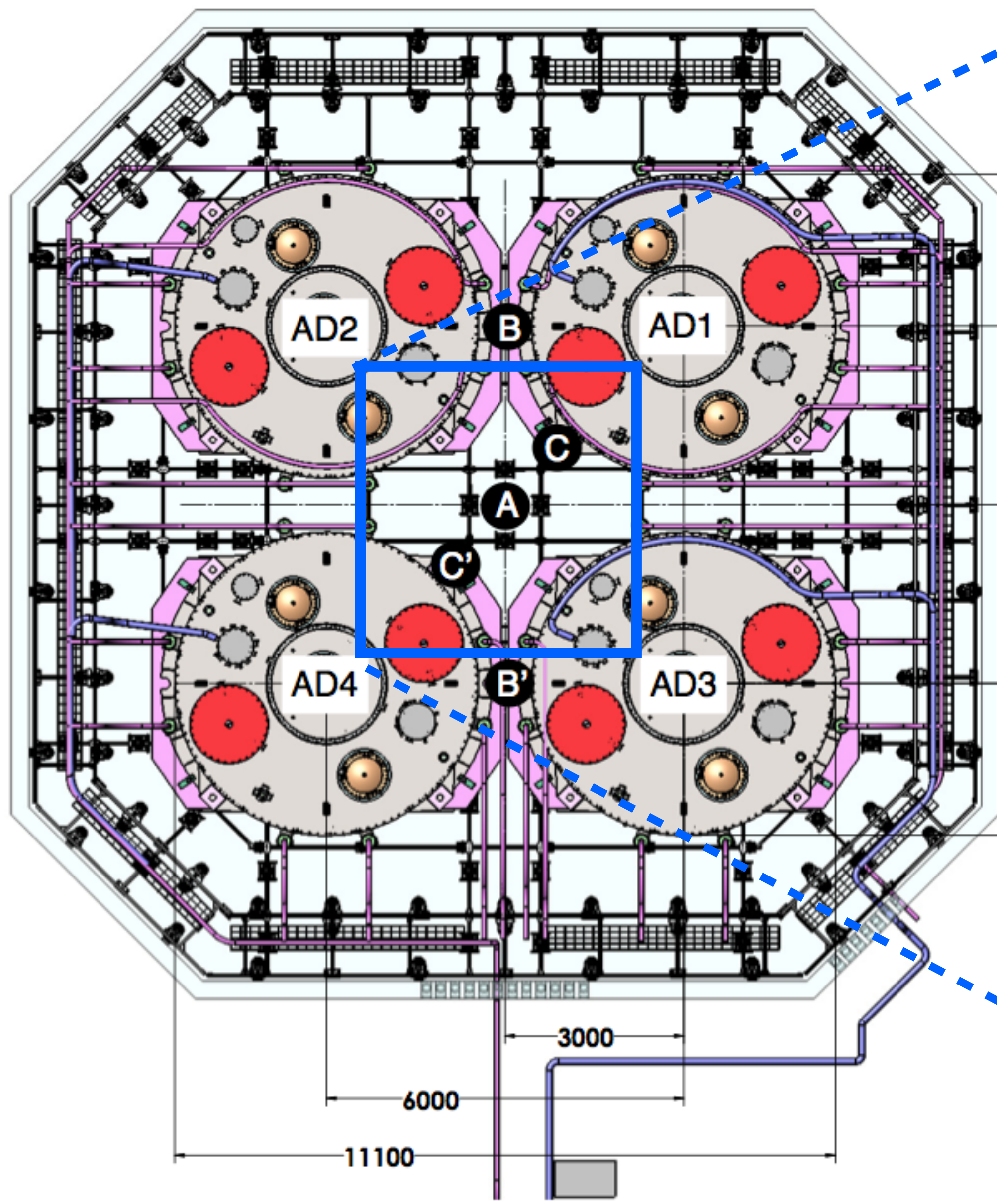

Position A and C: Source and Support Structure

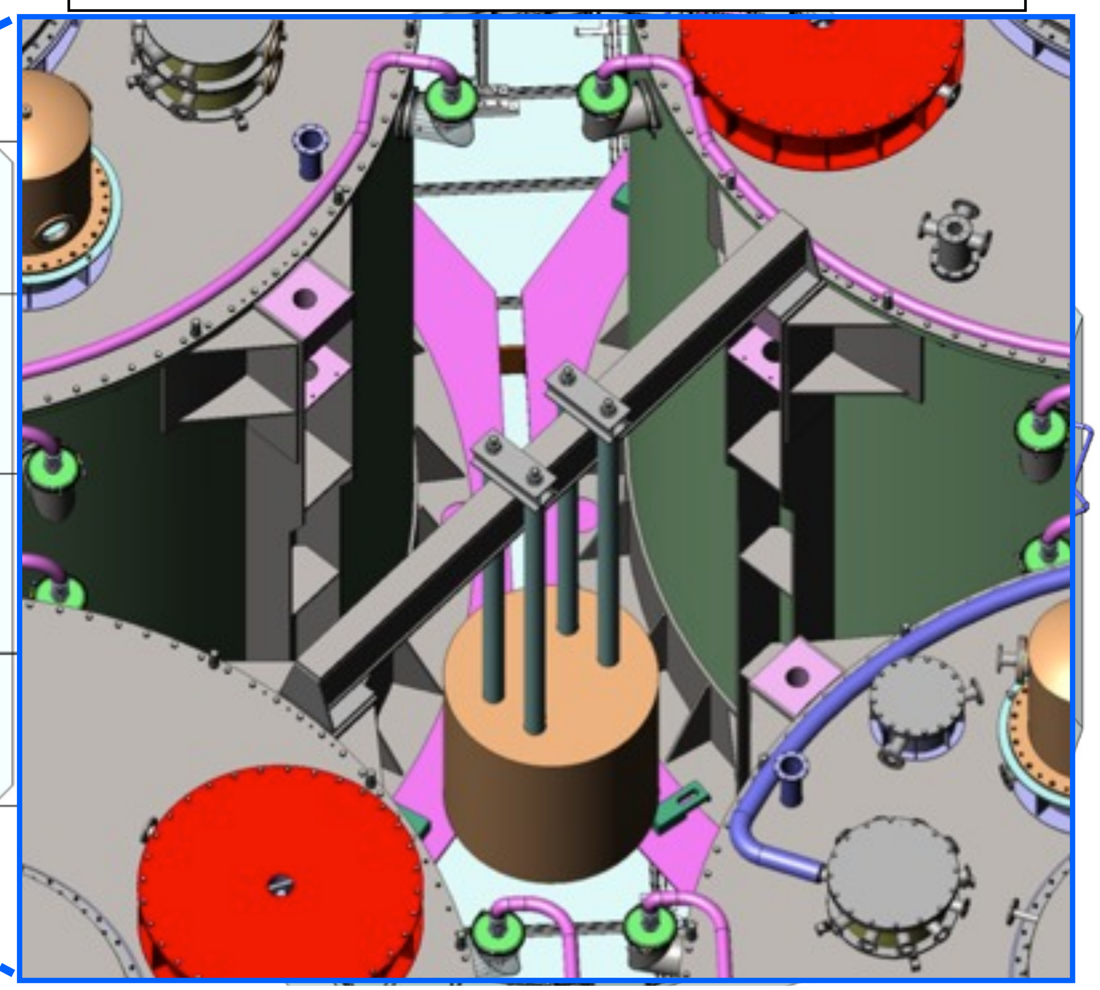

courtesy of the Daya Bay Collaboration

44

After θ13: A Sterile Neutrino Search

- With 1 year of running, 30k-40k IBD detections
- Backgrounds:
  ~0.5 m thick shielding, water pool, shield gammas
  Reactor neutrino flux well-known to <1% from near halls
- Detector systematics:
  - Well-understood from Daya Bay θ_{13} measurement
- Sensitivity:
  - Shape+rate analysis can rule out large majority of reactor anomaly, 3+1 global fits to 95% CL with one year of data.